MODERN SEDIMENTARY ENVIRONMENTS ON THE INNER SHELF, EASTERN SHORE, NOVA SCOTIA

by

ANTHONY B. LaPIERRE

Submitted in partial fulfillment of the requirements for the Degree of Bachelor of Science (Honours)

DALHOUSIE UNIVERSITY

HALIFAX, NOVA SCOTIA

1985

DALHOUSIE UNIVERSITY
Department of Geology
Halifax, N.S. Canada B3H 3J5 Telephone (902) 424-2358 Telex: 019-21863

DALHOUSIE UNIVERSITY, DEPARTMENT OF GEOLOGY

B.Sc. HONOURS THESIS

Author:

Title:

Permission is herewith granted to the Department of Geology, Dalhousie University to circulate and have copied for non-commerical purposes, at its discretion, the above title at the request of individuals or institutions. The quotation of data or conclusions in this thesis within 5 years of the date of completion is prohibited without permission of the Department of Geology, Dalhousie University, or the author.

The author reserves other publication rights, and neither the thesis nor extensive extracts from it may be printed or otherwise reproduced without the authors written permission.

Date: April 4, 1985

COPYRIGHT

Distribution License

DalSpace requires agreement to this non-exclusive distribution license before your item can appear on DalSpace.

NON-EXCLUSIVE DISTRIBUTION LICENSE

You (the author(s) or copyright owner) grant to Dalhousie University the non-exclusive right to reproduce and distribute your submission worldwide in any medium.

You agree that Dalhousie University may, without changing the content, reformat the submission for the purpose of preservation.

You also agree that Dalhousie University may keep more than one copy of this submission for purposes of security, back-up and preservation.

You agree that the submission is your original work, and that you have the right to grant the rights contained in this license. You also agree that your submission does not, to the best of your knowledge, infringe upon anyone's copyright.

If the submission contains material for which you do not hold copyright, you agree that you have obtained the unrestricted permission of the copyright owner to grant Dalhousie University the rights required by this license, and that such third-party owned material is clearly identified and acknowledged within the text or content of the submission.

If the submission is based upon work that has been sponsored or supported by an agency or organization other than Dalhousie University, you assert that you have fulfilled any right of review or other obligations required by such contract or agreement.

Dalhousie University will clearly identify your name(s) as the author(s) or owner(s) of the submission, and will not make any alteration to the content of the files that you have submitted.

If you have questions regarding this license please contact the repository manager at dalspace@dal.ca.

Grant the distribution license by signing and dating below.

_____ _____

Name of signatory Date

CHAPTER 1

1.1 Introduction

The Eastern Shore of Nova Scotia has been the site of extensive research into coastal and inner shelf processes and sedimentology. Work by Boyd and Bowen (1983) on modelling the coastal evolution of the Eastern Shore, based on present-day coastal processes, has provided a framework for understanding this transgressive marine environment. Follow-up studies include investigation of: (1) beach ridge development (Hoskin, 1983), sediment budgeting (Sonnichson, 1984), beach stability and sedimentology (Nair, unpublished data, 1984) and estuarine sedimentation (Honig, unpublished data, 1984). Hall (unpublished data, 1984) investigated surficial sediment distribution and seismic stratigraphy in the inner shelf. As a follow-up to work initiated by Hall (1984) this current study uses higher quality seismic and side scan data, along with surface grab sample collections by Hall, and BRUTIV imagery collected during this study, to establish more precisely the sedimentary environments on the inner continental shelf of Eastern Shore, Nova Scotia. The morphology, distribution, scale orientation and possible mechanisms responsible for the generation of coarse-grained megaripples are also addressed in this study.

All of these studies are intended to provide a better understanding of this environment so that facies modelling for the nearshore can be better constrained.

Study Area

The study area is located along the Eastern Shore of Nova Scotia between Osborne Head and Jeddore Cape, approximately 30 km along the east-northeast trending coastline. Bounded nearshore by the 15 m isobath and offshore by the 60 m isobath, the total study area is approximately 300 km^2 (Figure 1.1).

1.1.1 Coastal Morphology

The Eastern Shore is indented by numerous north-south trending estuaries, perpendicular to the coastline (Figure 1.1). These features are thought to be structurally controlled (Keppie, 1979). The estuaries along the Eastern Shore are former valleys submerged by rising sea level. Excavation by glacial ice flowing in the north-south direction scoured out structurally weak areas in the bedrock forming glacial valleys (Boyd *et al*, in press). Valleys are found in regional bedrock depressions and probably relate to pre-ice drainage patterns (Piper *et al*., in press). The depth of some of the valleys suggests repeated flushing and filling by sediment in successive glaciations (Piper *et al*., in press).

1.2 Background

Detailed bathymetry of the inner shelf between Osborne Head and Jeddore Cape was constructed by contouring CHS chart 4347 at 10 m contour intervals (Figure 1.1). The irregular topography seen offshore mimics that seen on land. Topographic highs that form coastal headlands such as Osborne Head, Half Island Point and Jeddore Cape also

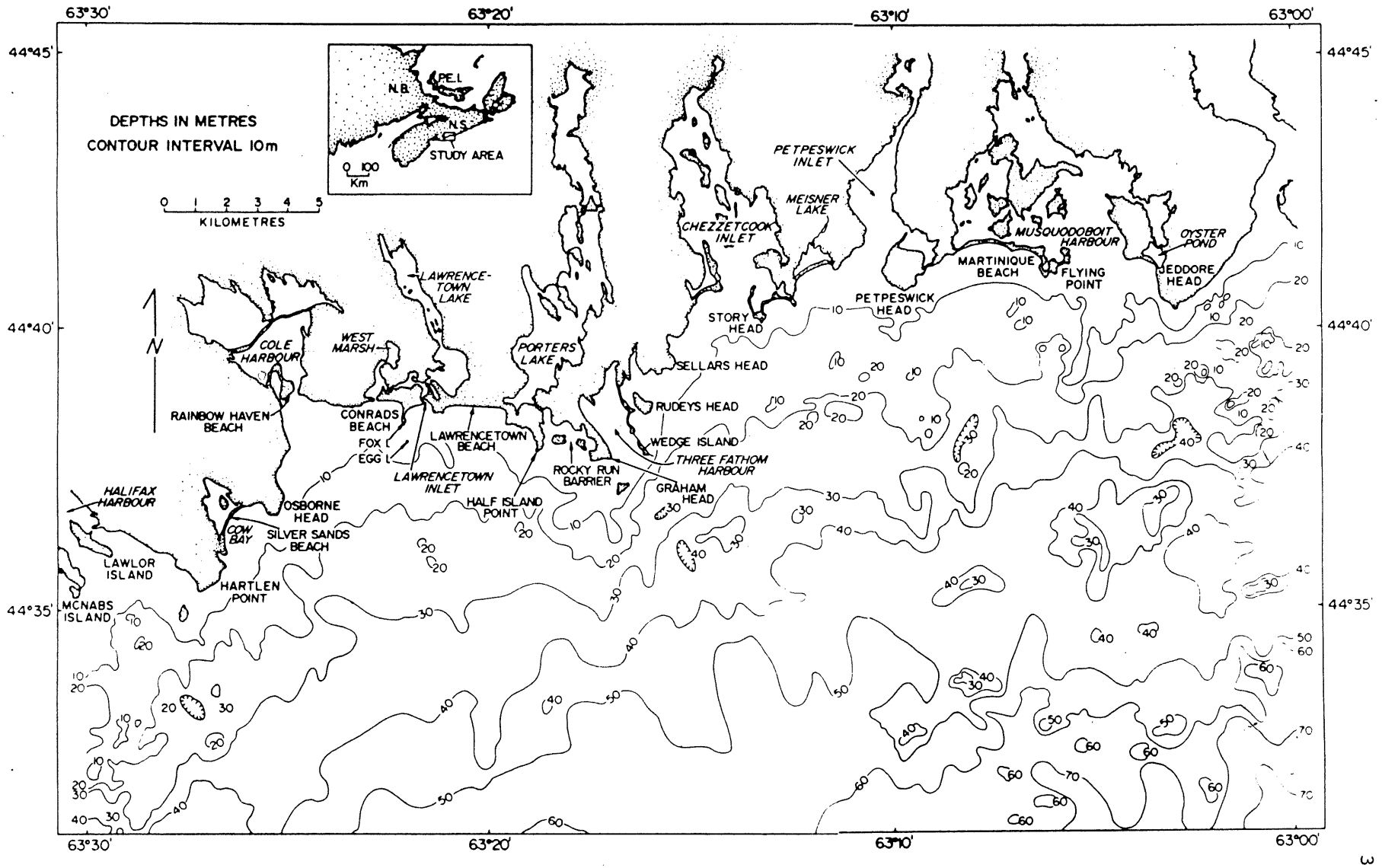

Figure 1.1. Location of the study area and bathymetry of the inner shelf.

extend offshore to form bedrock shoals. The topographic lows, which are seen as estuaries on land, also extend offshore Cole Harbour, Chezzetcook Inlet, Petpeswick Inlet, Martinique beach and Musquodoboit Harbour.

On the basis of offshore bathymetry, the study area can be divided into two main regions. The western region is bounded by bedrock shoals extending seaward of Osborne Head and Graham's Head, with a large central valley extending seaward of Cole Harbour. The eastern region can be subdivided into smaller bedrock shoals and valley systems. Smaller bedrock shoals extend out from Story Head, Petpeswick Head and Flying Point with valleys forming Chezzetcook Inlet, Petpeswick Inlet, and Musquodoboit Harbour (Hall, unpublished data).

1.2.2 Bedrock Geology

Cambro-Ordovican rocks of the Meguma Group form the bedrock along the Eastern Shore. The Meguma Group is divided into quartzites of the Goldenville Formation, and stratigraphically higher slates of the Halifax Formation. Regionally the bedding of the Meguma Group rocks strikes east-northeast. Folds in the Meguma Group are en echelon and commonly cylindrical; they range from open to tight and may be upright to low plunging (Harris and Schenk, 1975). Fold axes are parallel to the regional strike. Halifax Formation slates occur in the core of synclines; elsewhere the slates may be completely eroded. Goldenville Formation quartzites are more resistant to erosion than the Halifax slates and are the most abundant rock type along the Eastern Shore.

From projection of lithologic and structural boundaries from the coastline onto the inner shelf, the distribution of bedrock shoals and valley systems in the inner shelf seem to be unrelated to bedrock lithology and structure.

1.2.3 Glacial Sediments on the Eastern Shore

A loose oligomictic sandy till sheet is the most extensive unit of glacial sediments on the Eastern Shore (Grant, 1963). This is termed the quartzite till and is locally derived from the underlying quartzite (Stea and Fowler, 1979). Inland of the coastline, the slate till is found overlying the Halifax Formation. The slate till ranges in thickness from 2 m to 4 m and is generally thinner than the quartzite till which ranges in thickness from 3 m to 10 m (Stea and Fowler, 1979). Both of these tills are autochthonous. The allochthonous Lawrencetown till is a compact boulder clay till which has formed into drumlins (Stea and Fowler, 1979). The drumlins occur in fields which may contain up to several hundred randomly spaced individuals (Boyd and Bowen, 1983). Figure 1.2 shows the abundance of drumlins along the Eastern Shore coastline. Individual drumlins are composed of an average of 7.5×10^6 m^3 of sediment (Boyd and Bowen, 1983).

1.2.4 Glacial History and Relative Sea Level Rise

A submarine wave cut platform situated 120 meters below present sea level (b.p.s.l.) on the Scotian Shelf is considered by King (1980) and King and Fader (1984) to represent a low stand of late Wisconsinan

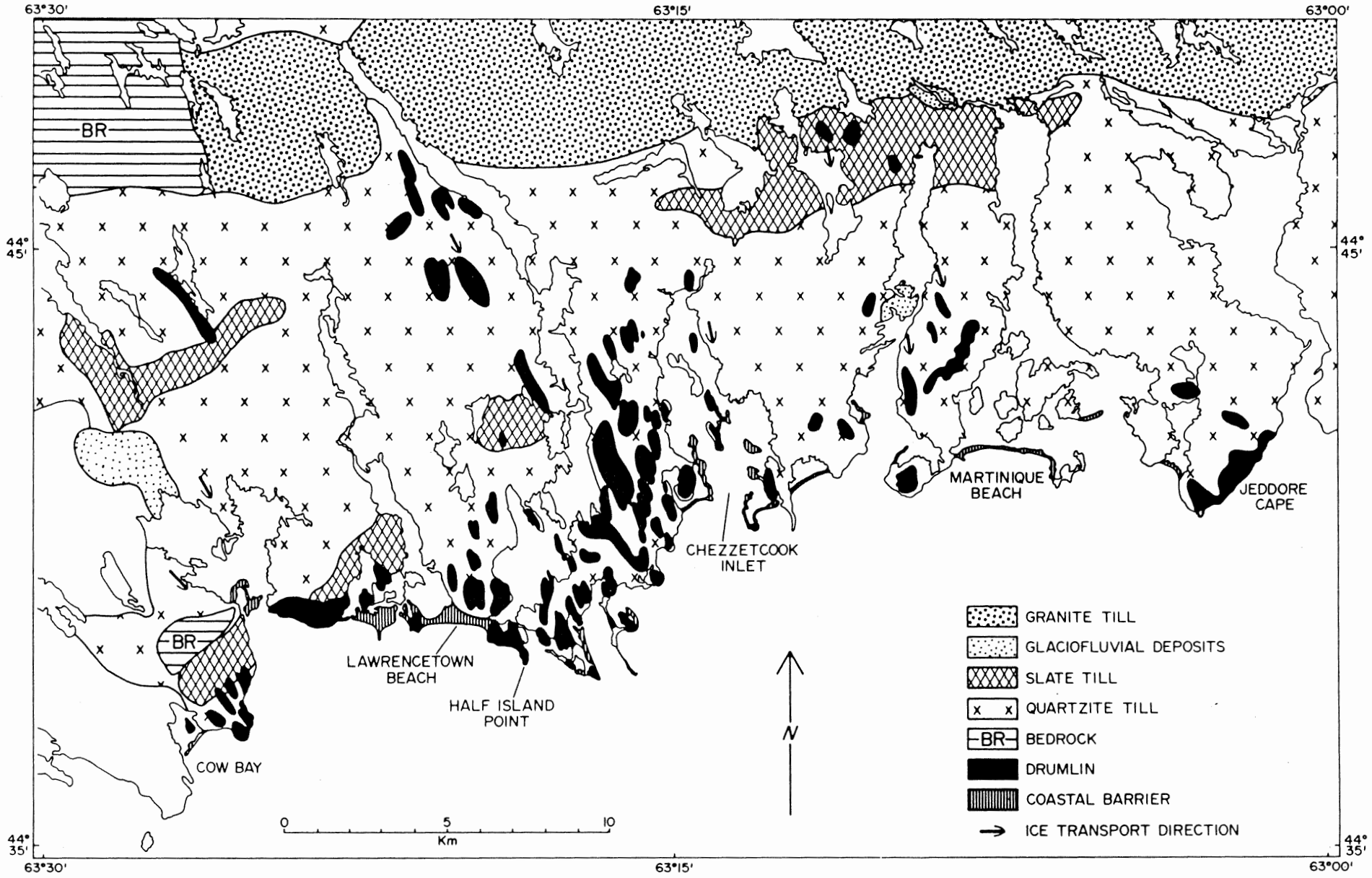

Figure 1.2. Distribution of drumlins along the Eastern Shore coastline.

sea level. Due to the lack of datable organic material, the age of this terrace has not been established. Therefore, the timing of the sea level low stand which this terrace marks is only speculative. In contrast, Scott and Medioli (1982) employed micropaleontological analysis of saltmarsh core from Lunenburg Bay to derive a minimum relative sea level of -27 m (b.p.s.l.) with a carbon 14 date of 7070+/--27 m (b.p.s.l.) 300 y.b.p. Quinlan and Beaumont (1981) suggested minimum sea level of 80 m (b.p.s.l.) based upon the migrating forebulge concept. Quinlan and Beaumont's (1981) model estimates that the ice sheet thickness was 500 m and that it extended offshore as far as the outer Scotian Shelf.

The isostatic response to deglaciation of the Eastern Shore coastline has been emergence followed by submergence, since the Eastern Shore was located, at the time when the ice reached its maximum seaward extent, on the landward side of the peripheral bulge (Quinlan and Beaumont, 1981). Figure 1.3 illustrates the concept of landward migration of the peripheral bulge as the mantle and crust re-equilibrates to deglaciation. According to Quinlan and Beaumont (1981) the Eastern Shore is located in Stage C. According to this model, response of the Eastern Shore sea level to deglaciation has been dominated by RSL rise due to coastal submergence since about 18 k.y.b.p.

Approximately 18 k.y.b.p. the ice began to retreat (Bowen et al., 1975). Relative sea level rose corresponding as a function of eustatic and isostatic response to diminishing ice cover. According to the model proposed by Scott and Medioli (1982), sea level rose from -27 m at 7000 (y.b.p.) at a rate of 38 cm/100 y for the first 5000

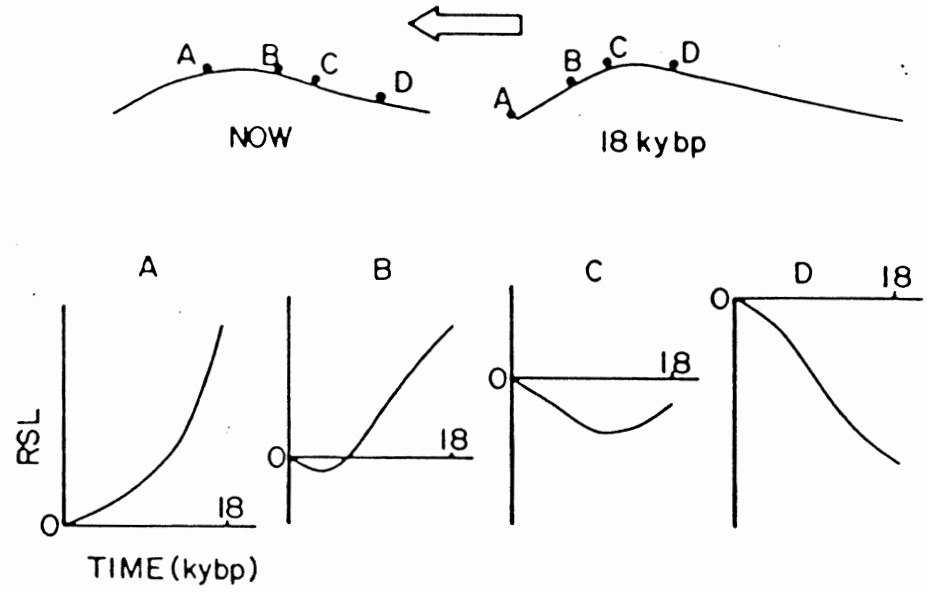

Figure 1.3. The top diagram illustrates the peripheral bulge at two points in time 18 (k.y.b.p.) and now. The Eastern Shore is located at point C. Passage of the peripheral bulge has lead to submergence of point C and RSL rise. RSL rise for the Eastern Shore is illustrated in the bottom diagram, second from right.

From Quillin and Beaumont (1981)

years and 32 cm/100 y for the last 2000 years.

1.2.5 Holocene Transgression

Relative sea level rise along the Eastern Shore has resulted in an onshore migration of the coastline, through erosion and submergence. Since sea level began to rise, the Eastern Shore has transgressed at least 5.8 km as evidenced by the position of the -27 m isobath (Sonnichson, 1984). Boyd et al. (in press) proposed a conceptual model for the evolution of the Eastern Shore in response to the Holocene transgression. Figure 1.4, stages 1 to 6, illustrate the cyclic model. Each stage is summarized below:

Stage 1: Continental Glacier and Ice Shelf

Stage 1 begins with the advance and retreat of the last major ice sheet. During Stage 1, the Scotian Drift was deposited as till in glacially scoured bedrock valleys, as drumlins on bedrock highs and as sand and gravel ground moraine.

Stage 2: Relative Rise in Sea Level and Estuary Formation

This second stage represents a transition phase between the glacial cover of Stage 1 and the active coastal erosion and sediment reworking in Stage 3. Initially in Stage 2, relative sea level (RSL) fell to at least -27 m. By the end of Stage 2, RSL rise had commenced, submerging bedrock valleys and turning the most seaward valleys into marine or brackish estuary systems influenced by tidal processes.

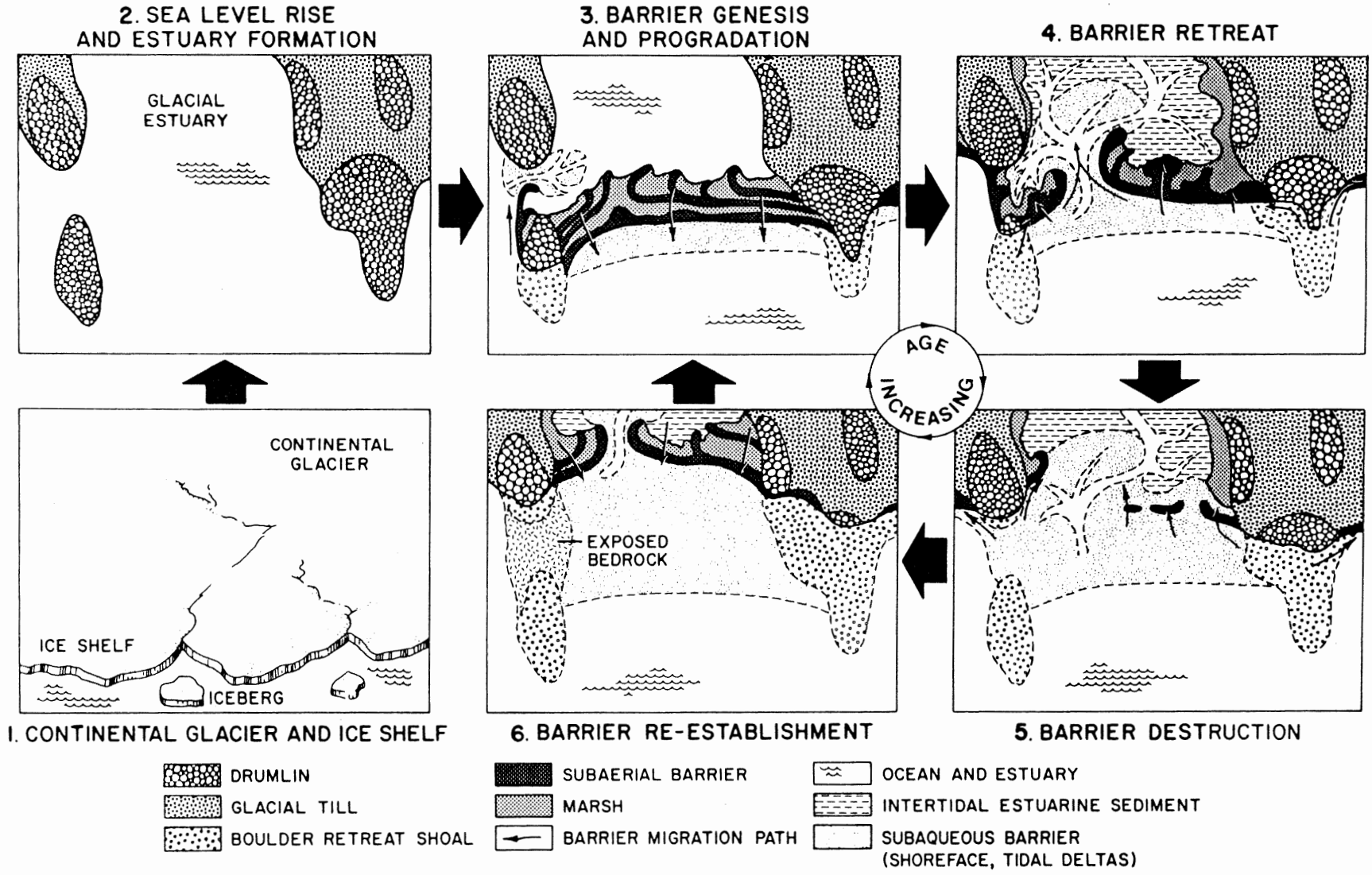

Figure 1.4. A conceptual model for the genesis and evolution of barrier-estuary systems along the Eastern Shore, Nova Scotia.

Stage 3: Barrier Genesis and Progradation

This stage is initiated with sediment erosion from drumlin headlands and ground moraine by a combination of RSL rise and ocean waves. Sand and fine gravels are transported longshore to form estuary mouth spits or beaches adjacent to drumlin headlands. Silty sediments reworked from the drumlin headlands and ground moraines are carried in suspension into mid-shelf basins. Sediments too coarse to be transported form boulder retreat shoals seaward of eroded drumlins.

Stage 4: Barrier Retreat

Barrier sediment supply slows in this stage as drumlin sediment sources are depleted. Barrier beaches retreat into the estuary through washover events and tidal inlet development.

Stage 5: Barrier Destruction

Once washovers and tidal inlets are initiated in Stage 4, the beach becomes very unstable. Complete barrier destruction occurs in Stage 5 with continuing washover events and establishment of the tidal inlet. The sand and gravels which formed the barrier are reworked into spits and intertidal shoals in the tidal estuary or form deposits in the backshore marshes.

Stage 6: Barrier Re-establishment

Stage 6 is a repetition of Stage 3 but with an important difference. Sediments from previous beach systems are available for establishment of a new barrier farther back in the estuary. New drumlin sediment sources and bedrock outcrops act as anchors for

redeveloped prograding barrier beach systems.

1.3 Objectives

The model summarized above is based on processes observed, at present, along the Easten Shore coastline. Testing the adequacy of this model as an explanation for the distribution of sedimentary environments on the inner shelf was one of the key objectives which prompted this research. To help answer this question, the sedimentary environments on the Eastern Shore inner shelf were investigated.

Environmental investigation requires mapping the surficial sediment distribution and relating this to the seismic stratigraphy. Mapping the surficial sediment distribution on the Eastern Shore is done by interpreting acoustic signatures on side scan sonographs and high resolution seismic reflection profiles and comparing them to the actual sediment types observed by ground truthing with underwater video still-frame photography and bottom grab samples. Seismic stratigraphy is established by relating the sediment types on the surface to those in the subsurface. This is achieved by simultaneous analysis of seismic reflection profiles and side scan sonographs.

The applicability and limitation of the coastal model proposed by Boyd and Bowen (1983) in explaining the distribution of environments on the inner shelf are addressed in this study. An evolutionary model which takes into consideration surficial and subsurface sediment distribution, glacial history, bedrock topography, glaciofluvial, tidal and wave processes, relative sea level rise, sediment availability, preferential deposition, and preservation potential of glacial till is

proposed in this study as an extension of the coastal model of Boyd and Bowen (1983).

As a secondary objective, the distribution, crest morphology, plan shape, orientation, texture and possible mode of generation of coarse-grained megaripples (CGM) observed in the study area were investigated.

1.4 Applications

An understanding of the various sedimentary environments on the inner shelf has at least six practical applications. Firstly, it provides a guide to future utilization of the seabed in this area. Future seabed activities may include burial of oil and gas pipelines, disposal of dredged spoils and mining of offshore sand, gravel and placer mineral deposits (Pasho, pers. comm.). Second, insight may be gained into the distribution and ultimate deposition of man-made pollutants that might be introduced over the inner shelf. Such pollutants could come from oil and gas or chemical spills or disposal of human waste. Modern sediment accumulation, reworking and winnowing influence not only the vertical and lateral dispersal of pollutants but also their residence time at a particular location (Knebel et al., 1982). Third, quantitative studies of CGM in this modern environment may aid in interpretation of ancient siliclastic sequences such as the oil and gas bearing Cretaceous seaway siliclastics in Western Canada (Leckie, pers. comm.). Fourth, knowledge of sedimentary environments is a major aid to generation of facies models (Walker, 1984). Fifth, the geometry, distribution, and origin of thick inner-shelf sandbodies

mapped in this study may provide aid in exploration strategies for oil and gas bearing shelf sandstones such as the Cardium Formation in Western Canada. Finally, the surficial sediment distribution outlined in this study may be an important controlling parameter in an upcoming (1985-86) joint Canadian/American inner shelf oceanographic study to take place within the Eastern Shore field area (Forbes, pers. comm.).

CHAPTER 2

Methods

2.1 Data Collection

Data used for this project were collected during a two day cruise aboard the CSS Dawson. The total survey area consisted of approximately 300 km^2 of inner continental shelf. Approximately 240 line km of high resolution seismic reflection profiles, side scan sonographs, fathometer records and approximately 50 line km of continuous underwater video and still-frame photographs were collected simultaneously. Figure 2.1 is a simplified track plot illustrating the north-south/east-west survey grid. Line spacing varied but was generally between 1 and 3 km on shore-parallel lines and 2 to 6 km on shore-perpendicular lines. Dashed lines indicate the ship's track when complete survey capacity was maintained including seismic, side scan, and photographic and video equipment. Solid lines indicate the ship's track during periods when all equipment, except for the photographic and video unit was deployed.

2.2 Survey and Navigation Instruments

A description of the survey including instrumentation, navigation and the applicability of each type of data to this study is given below.

2.2.1 Side Scan Sonar

Side scan sonar systems utilize two high frequency transducers

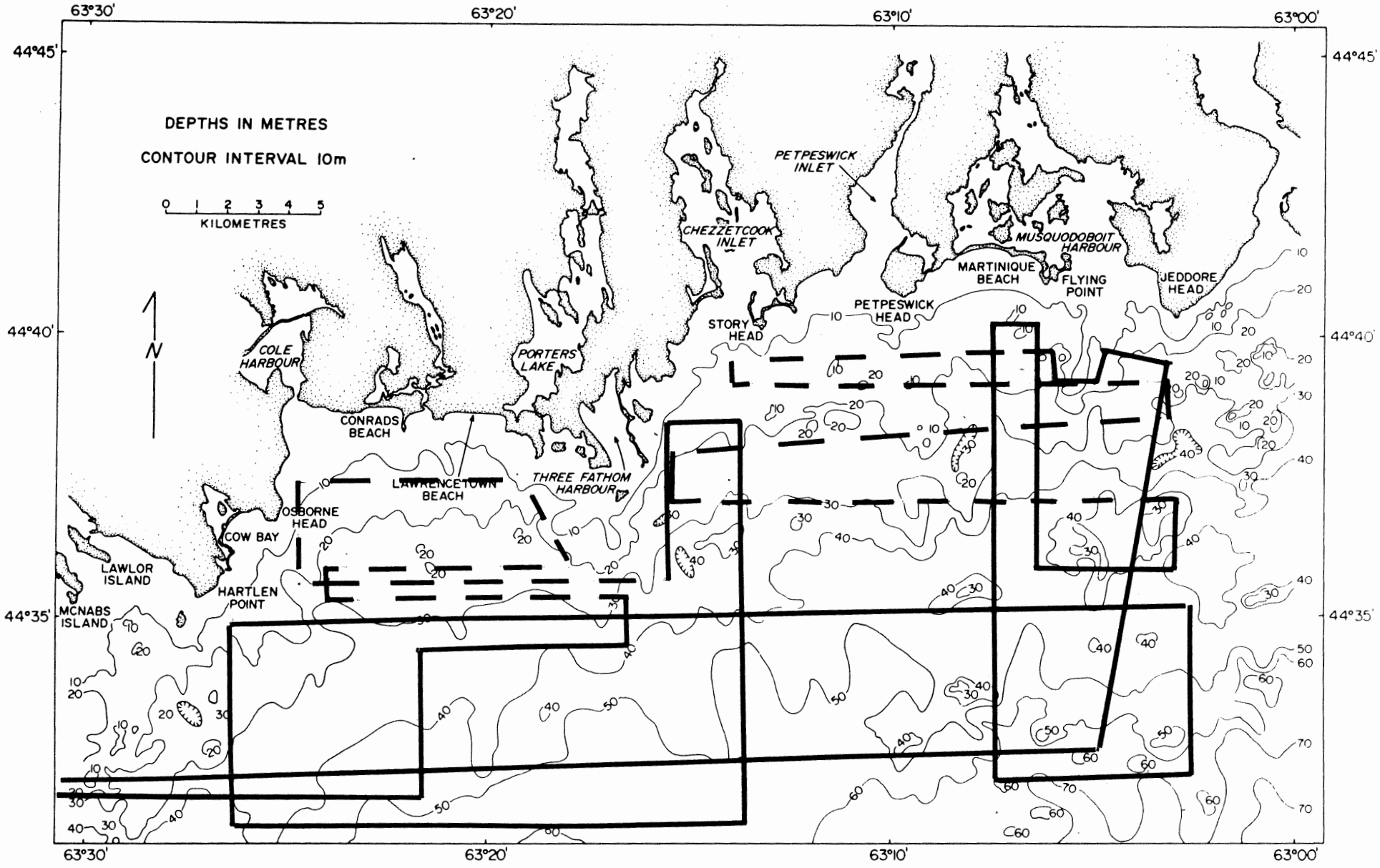

Figure 2.1. Simplified track plot of data collection cruise. Dash lines indicate full survey capacity, solid lines indicate only seismic, side scan and fathometer operative (see text)

which have a horizontal beam of 2° and a vertical beam of more than 20°. Transducers and receivers are located on opposite sides of the towfish (McQuillen and Ardus, 1977; Flemming et al., 1982). The instrument used was Atlantic Geoscience Center's Klein 421-T side scan supplied by AGC. A hydraulic winch, attached to Dawson's quarter deck, was used to maintain the fish at a height above the seabed between 10 m and 15 m and a distance of approximately 50 m behind the ship. The paper feed rate varied from 24 cm/5 min to 33 cm/5 min, with most of the survey at 33 cm/5 min. Swath width varied from 200 m to 400 m with most of the survey at 300 m swath width. This resulted in a 1:1.5 compression ratio of width to length. Five minute navigation fixes were synchronized with fix marks on side scan sonographs, seismic profiles and fathometer records. All of these instruments were run concurrently. Side scan sonographs have been used in this study to distinguish the textural variation of the surficial sediments, for a delineating wavelength, orientation, morphology and distribution of coarse-grained megaripples (CGM), for establishing the orientation and distribution of till ridges and for mapping bedrock structure exposed at the seabed.

2.2.2 Seismic Profiling System

In high resolution seismic reflection profiling, acoustic pulses emitted from a source at discrete time intervals are reflected from the boundaries of layers with contrasting acoustic properties (acoustic impedence). The depth of penetration is determined by the energy of the source and the resolution is determined by the

frequency of the acoustic pulse. Higher frequency pulses resolve thinner layers than lower frequency pulses. Higher frequency pulses are maintained by lower energy systems which have a lower limit of penetration than higher frequency systems. Since this study was concerned with the surface sediment, the high frequency, low energy (100 joule), surface-towed minisparker source from NSRF was used. The minisparker produces an acoustic pulse by rapidly heating the surface water to the point of vapourization at the sparker electrodes, thus creating a steam bubble (McQuillen and Ardus, 1977). The sparker used for this study was a line-towed array, towed 25 m behind the ship.

After the acoustic pulse is reflected it is received by a hydrophone array. The hydrophone array converts the acoustic pulse into an electric signal which is amplified and selectively filtered by the acoustic receiver.

A variable density recorder graphically plots and displays the two-way travel time of the acoustic pulse (McQuillin and Ardus, 1977; Sengbush, 1983).

The hydrophone consists of several crystal elements wired together in series to act as a receiver. Both 21 element and 9 element hydrophones were used throughout the survey. Because the hydrophone does not distinguish the source of sound, a seismic signal processer must be used to unmask the faint acoustic signal by filtering out the ship noise, tow cable noise and water reverberation (McQuillin and Ardus, 1977; Sengbush, 1983). Filter settings varied throughout the survey to compensate for water depth, but were

generally in the range of 0.3 kHz to 3.5 kHz.

An EPC variable density recorder was used throughout the survey. The seismic recorder triggers the acoustic sound source at a specific time. For this study a 0.250 sec firing rate was used. The strength of the incoming signal determines the intensity of the mark; the recorder stylus burns into the recorder paper. Line intensity is referred to as "grey level" (Parrott et al., 1980) and is one criterion used to distinguish surficial sediment type in this study. The degree of coherence of the seismic signal is used to distinguish sediment type at the seabed as well as at depth.

2.2.3 Fathometer

The fathometer is a high frequency (12 kHz) reflection profiling system which provides a profile of seabed elevation (McQuillin and Ardus, 1977). The fathometer records are used to obtain accurate bathymetric data, important, for example, in modelling the generation of CGM.

2.2.4 BRUTIV

BRUTIV is a towed subsurface video and still-frame photography sled. The camera altitude above seabed was maintained by a sonar within the sled. Altitude varied from 3 m to 5 m, and averaged 4 m. A total of 6 dives were completed during the cruise with six two-hour video tapes and six 30.5 m rolls of Ektachrome 200 colour slide film being shot. Still shots were taken approximately 12 seconds apart while the video ran continuously for each dive. Video and still photography

quality were good.

2.2.5 Navigation Equipment

A Motorola miniranger system was employed for navigation. Miniranger is a high frequency device operating in a range/range mode (McQuillin and Ardus, 1977). Distance is measured by knowing the signal speed of propagation and the time it takes the signal to travel from the master unit (located atop the Dawson's bridge) to the slave station and back to the master unit (McQuillin and Ardus, 1977). Slave stations were located along the coast at Osborne Head, Grahams Head and Gaetz Head (Figure 1.1). Ship positioning is accomplished by translating two or more measurements from slave stations; the intersection point of the measurments is the location point of the master unit (McQuillin and Ardus, 1977). Miniranger provides accuracy to within a few metres but is limited to the line of sight between the master unit and slave station (McQuillin and Ardus, 1977). Accuracy is maximum when the acute angle between the master unit and the slave stations is between 60^{o} amd 120^{o} (Dearnley-Davidson, pers. comm.). Loran-C, a medium range radio - navigation system with accuracy of 100 m (McQuillin and Ardus, 1977) was used as a backup navigation system. Loran-C was required for less than 1% of the survey.

2.3 Processing the Data

2.3.1 Base Map Production

A track line plot was drafted with 444 fix points using a beam compass arc intercept methods. Intercepts define known locations

obtained every five minutes along the track line and were generally 600 m to 800 m apart. Individual slave/master distances were converted from metres in which they were recorded to nautical miles so that they could be scaled from the latitude bar on the margin of the base map. The initial track plot was drafted on Canadian Hydrographic Service Chart 4347 at a scale of 1:58, 500. This map, with the track line plot, was photographically enlarged 200%. Enlargement allowed more space for detail on the side scan mosaic.

2.3.2 Video and Still-Frame Photographs

Six 2-hour videos and six 30.5 m long rolls of Ektachrome color bottom photographs were logged in detail in order to establish a framework for comparison of sediment types of acoustic properties.

2.3.3 Side Scan Sonar Sonographs

Five, approximately 50 m long, rolls of sonographs were described by mapping acoustic properties, adjacent to the corresponding track line on a working copy base map. Coarse-grained megaripples, till ridges and bedrock structures were mapped. Distinct acoustic properties were found to correspond to specific sediment types observed on video, and to photographs and distinct acoustic properties observed on seismic reflection profiles. From these correlations, four distinct environments were recognized within the study area. The characteristics of each of these environments are detailed in Chapter 3, along with type sections. A side scan mosaic for the entire study area is presented in Map 1 in the rear cover jacket.

Because side scan produces a distorted image of the seabed,

corrections for distortion had to be employed before a systematic evaluation of coarse-grained megaripples could be attempted. Variable ship speed in combination with variable paper speed, and variable fish height above the seabed in relation to slant range calibrations are the two main sources of distortion observed in side scan techniques and the only two which can be meaningfully corrected (Flemming et al., 1982). Angular measurements, such as those made for orientation of gravel megaripples and till ridges, are significantly distorted due to progressive compression of the angle between these features and the ships track line.

Angular distortion corrections were made by using distortion ellipses dependent on the on-line compression ratio. On-line compression is the ratio of the record length between two corresponding event marks and record length which represents the same distance covered by the corrected slant range. Variations in twofish altitude above the seabed did not produce distortions perpendicular to the ships track line of sufficient magnitude to merit correction. This meant that the megaripple wavelengths could be scaled directly from the swath width of the sonograph when megaripple crests were parallel or subparallel to the ships track line.

CHAPTER 3

ENVIRONMENTS ON THE INNER SHELF

3.1 Introduction

Krank (1972), studying the Northumberland Strait Shelf and Loring (1969), studying the Magdalen Shelf, described the sediment distribution for a glaciated shelf as consisting of numerous bedrock outcrops, with a thin veneer of sand and gravel overlying much of the inner shelf. These authors reported that sand tended to become thicker nearshore. The Eastern Shore inner shelf was surveyed using high resolution seismic reflection profiling, side scan sonar, underwater video and photography and bottom grab samples. From these data surficial sediment distribution within the study area was divided into four main environments: 1) sand, 2) sand and fine-grained gravel (SFGG), 3) till, and 4) bedrock. The characteristics of each of these environments are given below.

3.2 Environmental Characteristics

3.2.1 Bedrock

Side Scan

Bedrock is characterized by high acoustic reflectivity and hence appears dark on sonographs. Outcrops are blocky and yield a striped shadowing pattern due to bedding and jointing surfaces. Figure shows an example of bedrock outcrop. Bedding is consistently striking from left central to upper right in this figure. Here the deep cracks

within the bedrock are floored by sand and gravel and occasional gravel ripples within the bedrock cracks. Bedrock outcrops appear as positive bathymetric features on sonographs. This can be seen in Figure 3.1 to the left of fix mark 321.

Bedding mapped from sonographs parallels the regional trend mapped on land by Faribault (1906). Bedding occasionally exhibits tight to gentle folds on sonographs. The axis of these folds strike parallel to the axis of folds mapped on land by Faribault (1906). Figure 3.2 shows an example of tight folding observed at the seabed. Note the possible axial planar fault striking from right of fix mark 0720 to the upper right hand corner.

Seismic

High acoustic impedence between overlying unconsolidated sediment (or water) and bedrock produces a strong, coherent and serrated initial reflection. Cross hyperbolics, point hyperbolics, abundant first-order surface multiples and lack of penetration characterize bedrock on the seismic profiles. Figure 3.3 shows most of the features which characterize bedrock including point hyperbolics below fix mark 321, cross hyperbolics at midway between fix 321 and 322, a first-order surface multiples below fix 319 in the bottom left of the photo and the strong, coherent, serrated initial arrival. A possible fault was identified to the left of fix 321. This corresponds to the large crack midway across Figure 3.2 . This feature can be traced along strike to the coastline where it has been mapped by Faribault (1906), who called it a fault.

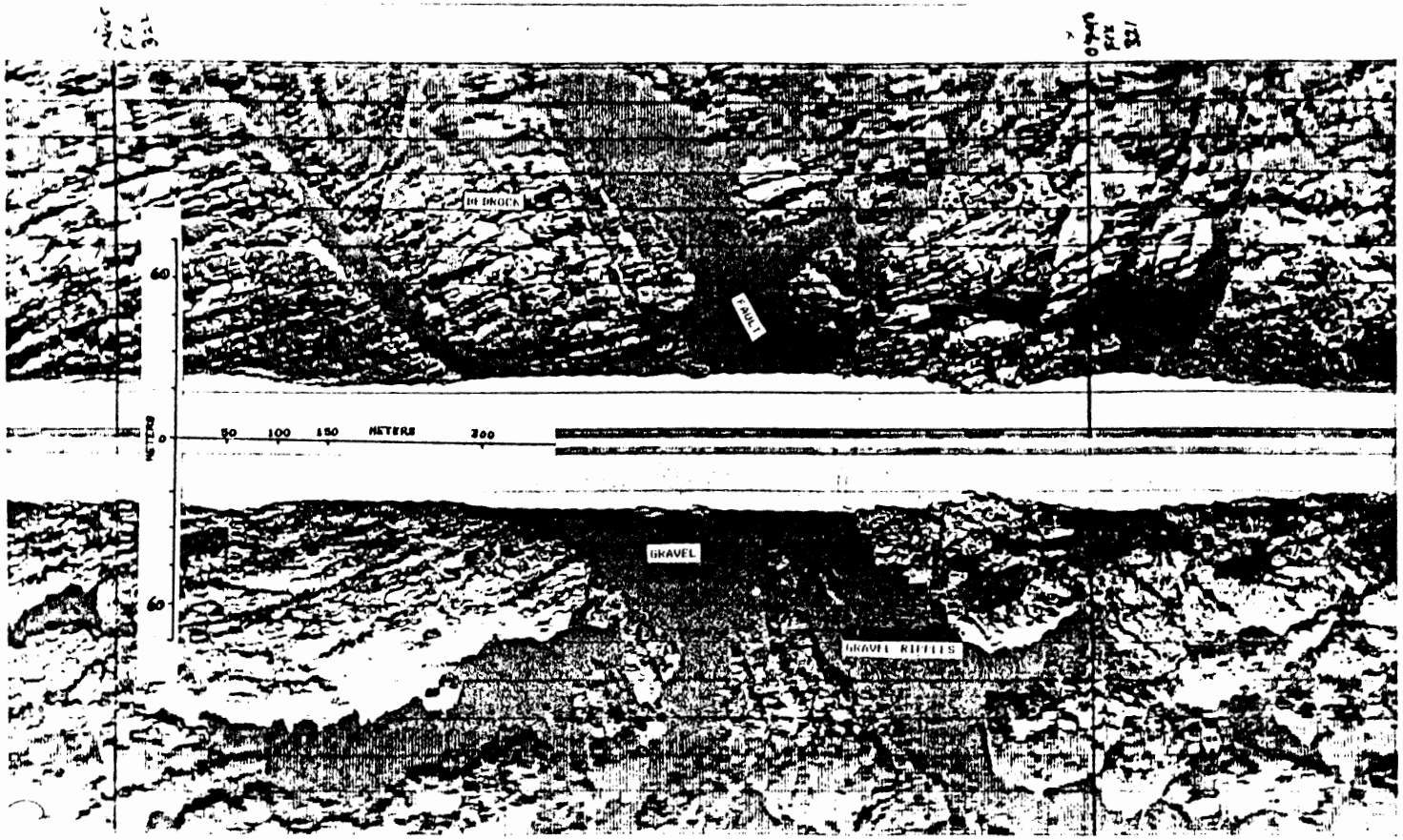

Figure 3.1: Bedrock outcrop with well exposed bedding and crack infilled with SFGG.

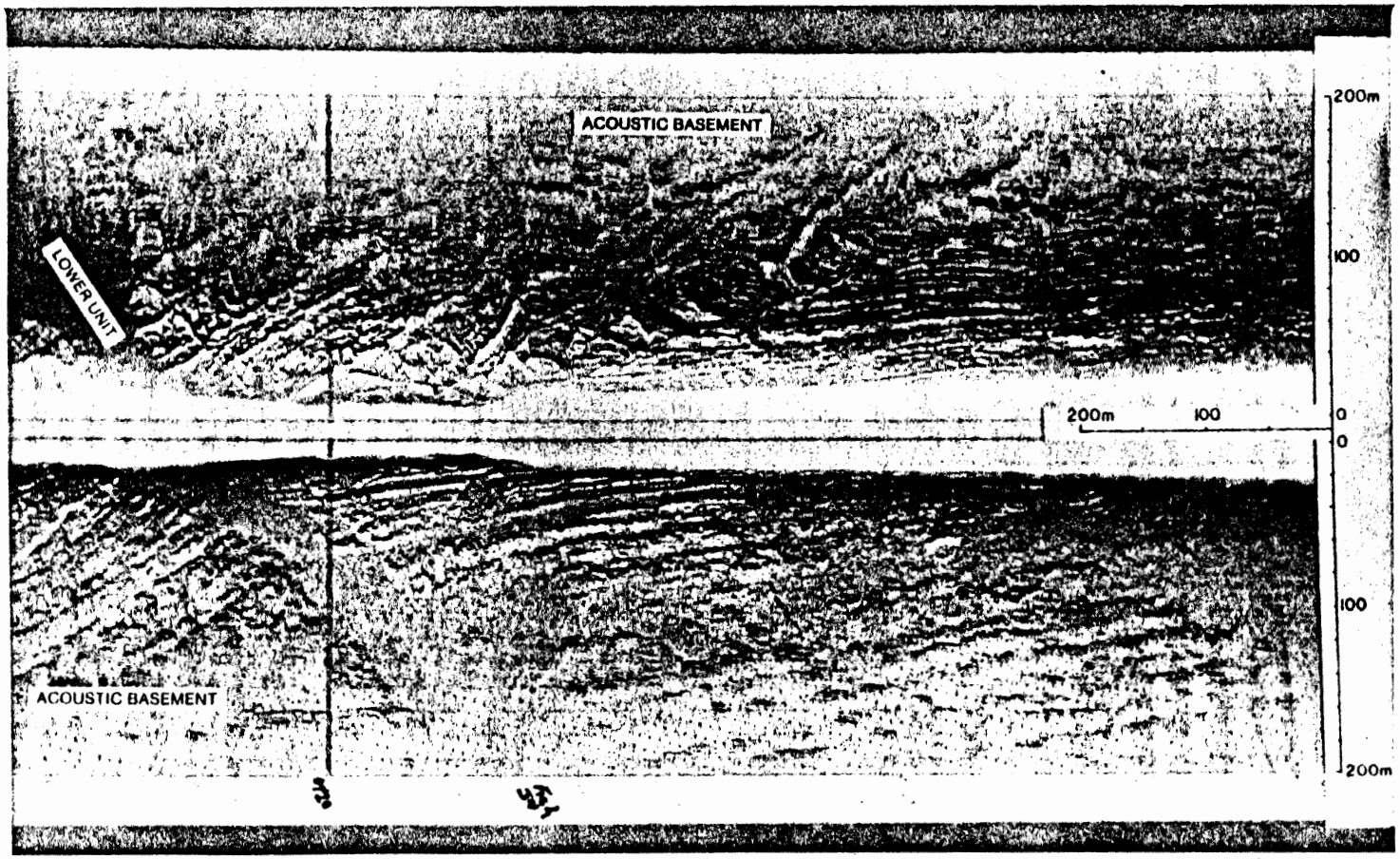

Figure 3.2. Bedrock outcrop with well developed tight fold and possible axial planar fault.

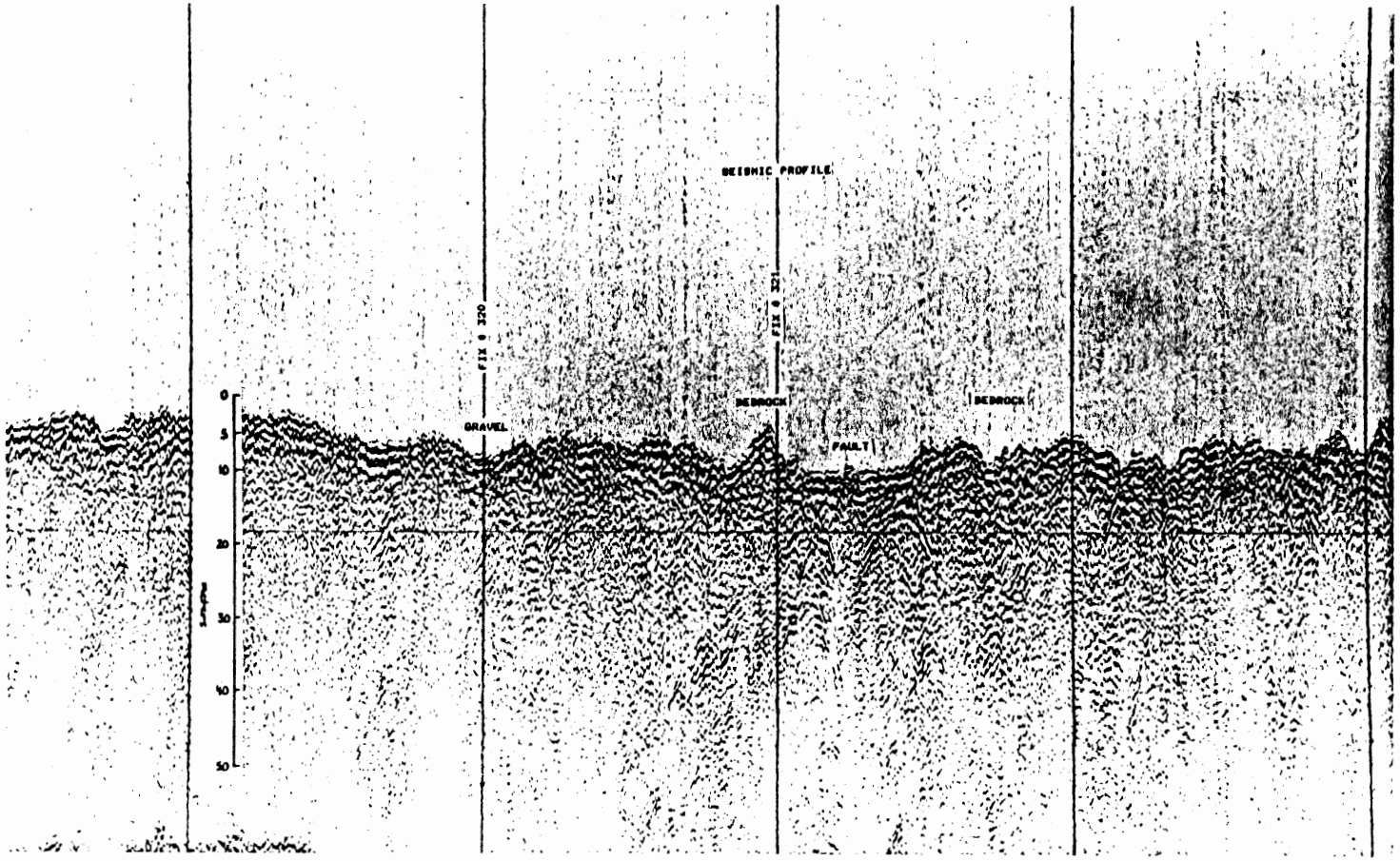

Figure 3.3. Bedrock outcrop with serrated initial arrival abundant, point hyperbolics and cross hyperbolics. Distance between fixes is approximately 600 m.

Video and Photos

Bedrock can be completely to partially masked by benthic vegetation and encrusting organisms. Where visible, bedrock outcrops show excellent bedding, jointing and microfolding of quartz (?) veins. Outcrops are very angular blocks rather than smooth polished surfaces.

3.2.2 Glacial Till

Side Scan

Outcrops of till on sonographs appear as acoustically dark areas with abundant boulder shadowing. Boulders act as shields against the acoustic beam emitted from the side scan fish so that the seabed behind the boulders appears white on sonographs. Figure 3.5 shows a till outcrop with boulder shadowing (white patches) and boulders (dark patches). These can best be seen in the middle of the figure. Till outcrops in water depths greater than 35 m, are characterized by elongate positive bathymetric features which are till ridges. These till ridges produce a hummocky seabed topography. The distance between individual hummocks differs but is generally 200 m to 300 m. Ridges are traceable from parallel and orthogonal tracklines. Figure 3.4 shows examples of till ridges right of fix mark 328. These ridges strike approximately north-northeast (in the sense of the figure). Figure 3.6 is a rose diagram showing the consistent northwest trend of these features throughout the study area. Till ridges have not been reported on the inner shelf by other workers. These features may be: a) glacial depositional, or b) erosional features. The coarse gravel composition (80% boulders which would be very difficult to move) and orientation

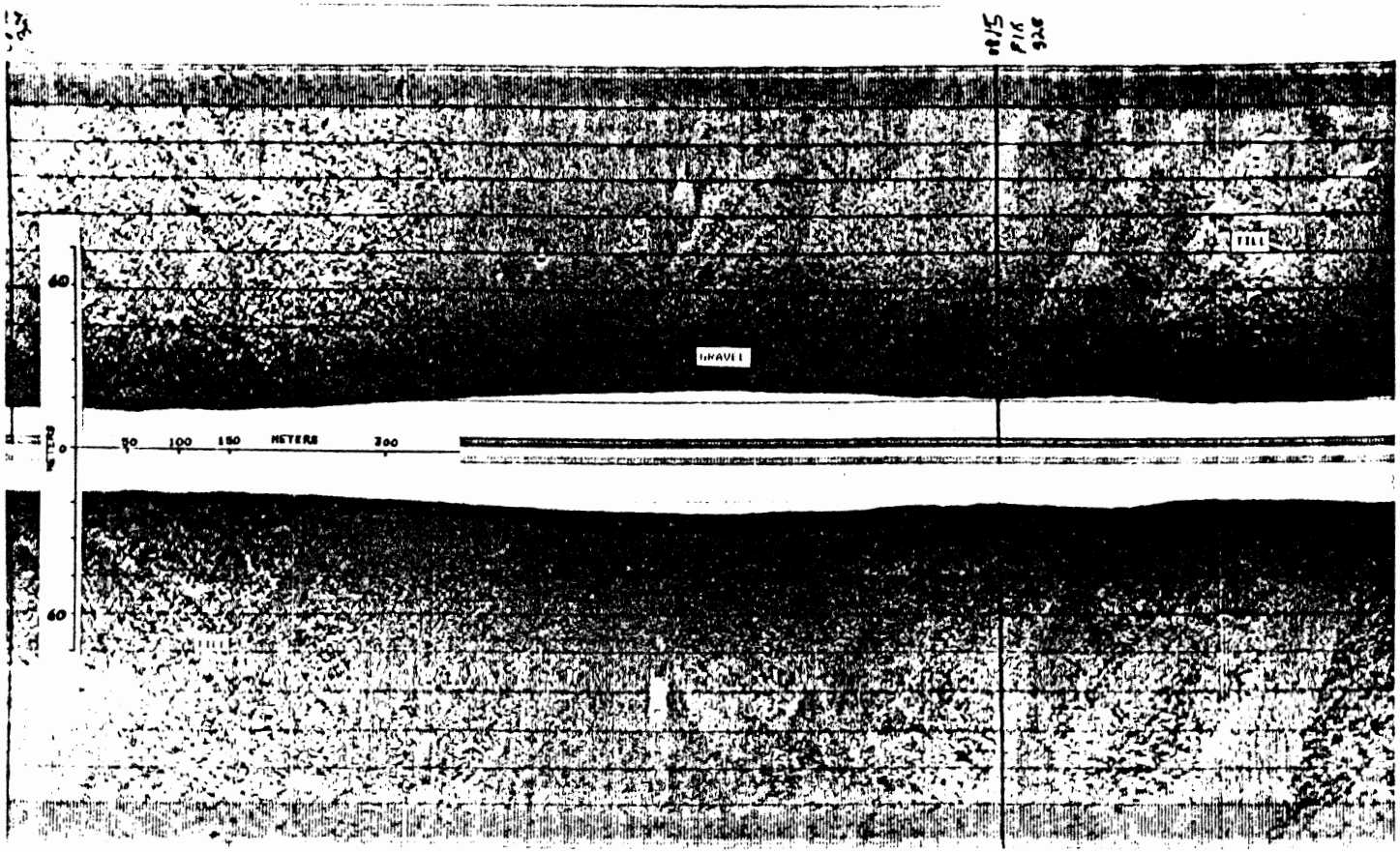

Figure 3.4: Till ridges are shown left of fix mark 328. SFGG occurs in the center of the figure and is flanked by till outcrops.

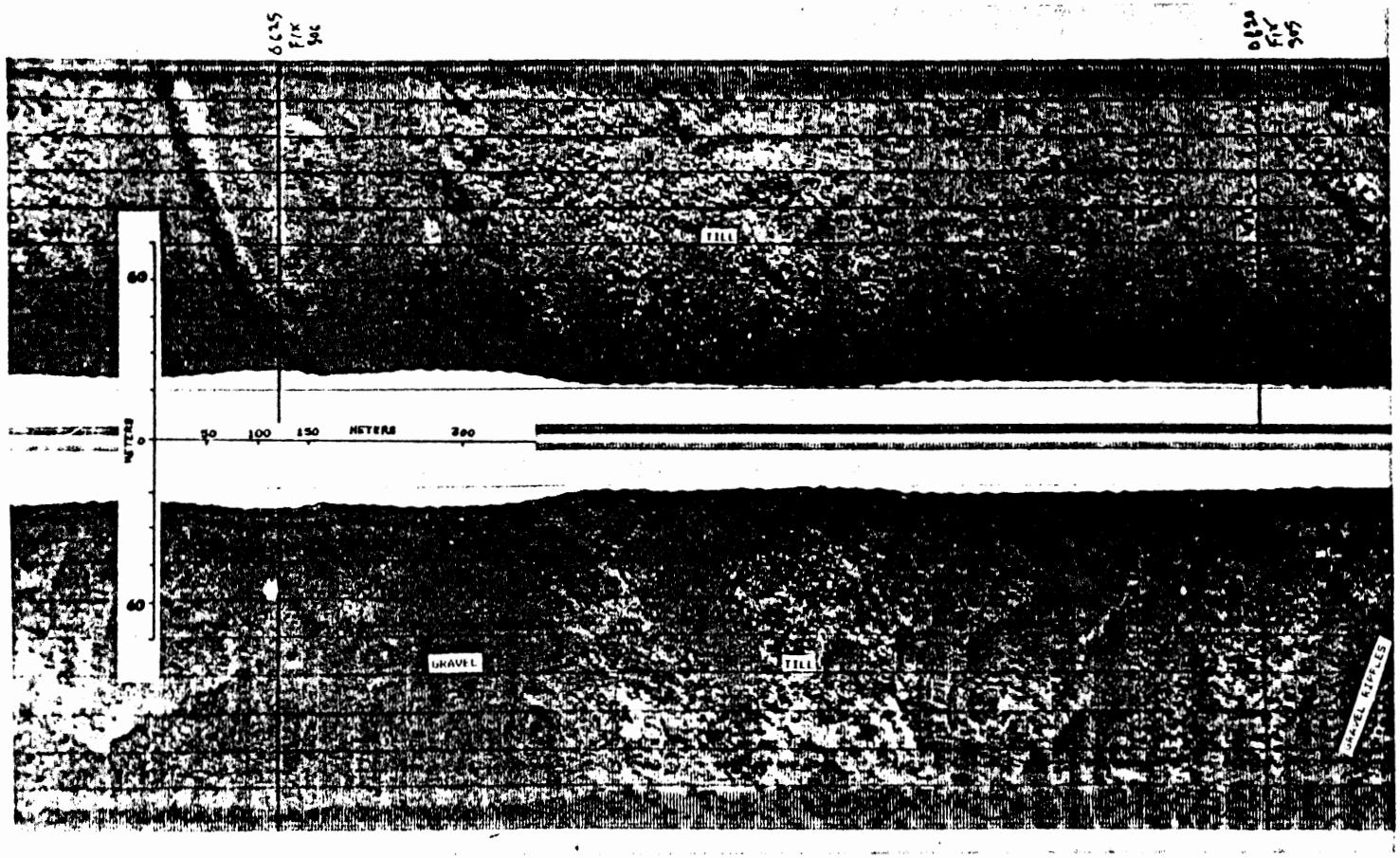

Figure 3.5; A Side Scan Sonograph showing a till outcrop halfway between fix 305 and fix 306. SFGG with occasional boulders can be seen right of fix 305 and left of fix 306. Note that the till occurs as a bathymetric high.

TILL RIDGE ORIENTATION FIGURE 3.6

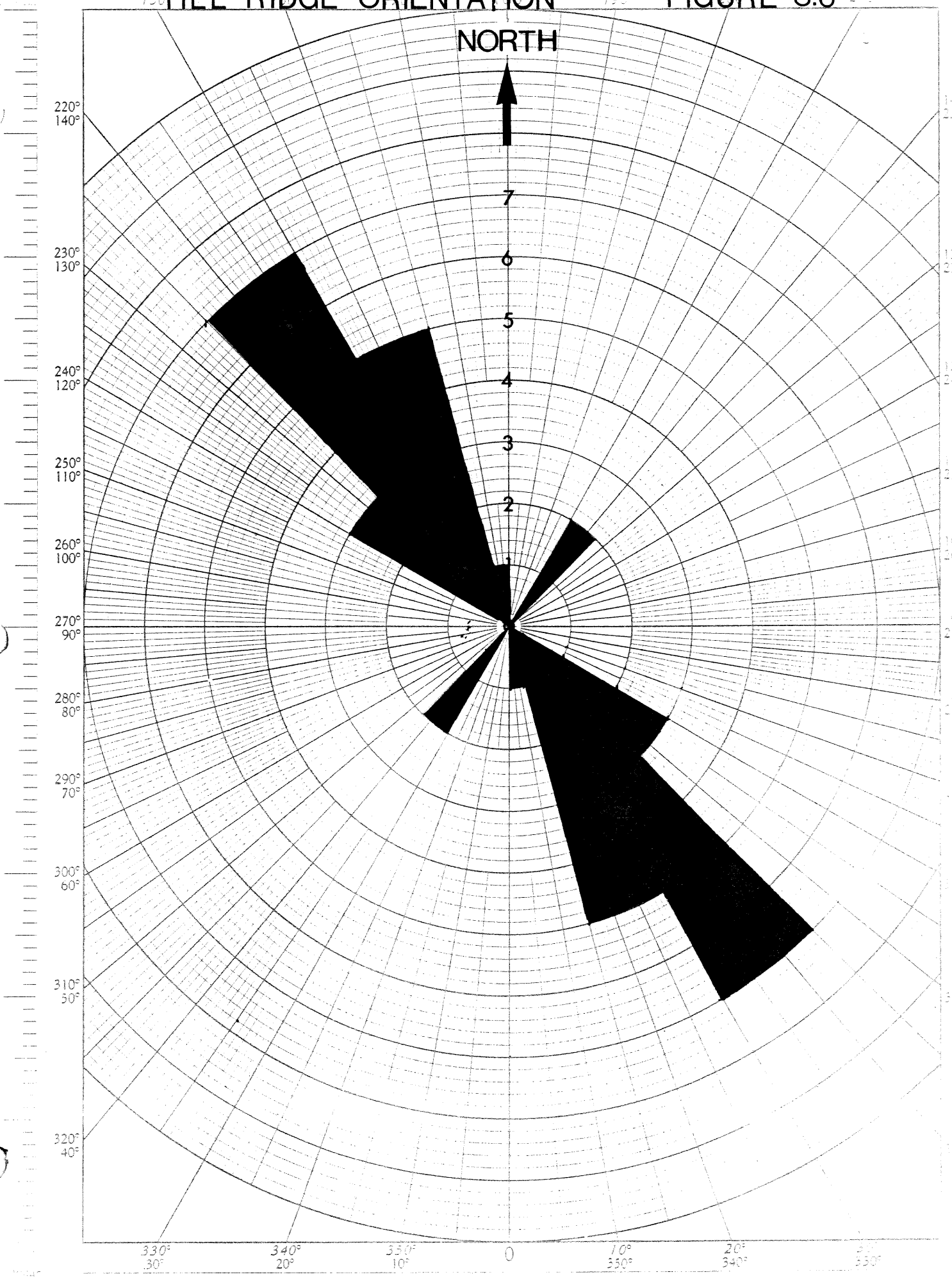

TILL RIDGE ORIENTATION FIGURE 3.6

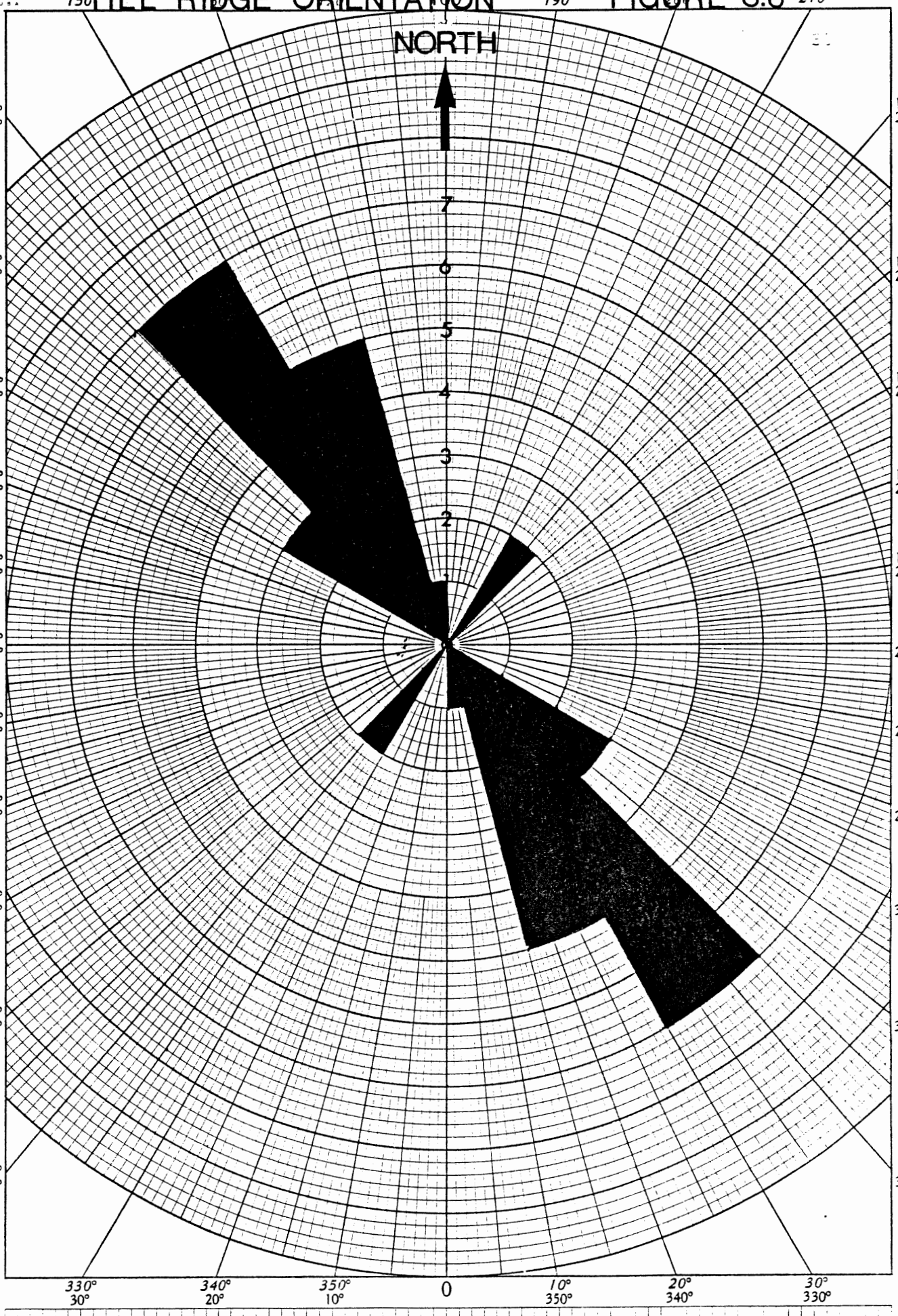

Polar
Co-ordinate

(approximately parallel to the direction of ice sheet advance and retreat) are lines of evidence for the former.

Seismic

Till can generally be distingushed from bedrock by a smoother surface expression, and from other environments by the hummocky or channelized upper reflection surface, the general lack of coherent internal reflectors, the occasional multiplicity of units and (except where obscured by multiples in shallow water) the presence of bedrock beneath it. Figure 3.7 and Figure 3.9 are raw and interpreted seismic reflection profiles showing an example of a thick (30 m) sequence of till infilling a bedrock valley. Table 3.1 is the legend for the interpreted profiles. Note the lack of coherent reflectors within the till and the channels cut into the upper surface to the left of fix mark 306 and at fix 305. Till outcrops midway between fix 305 and 306 and appears to have a hummocky surface expression. The interval between fix 305 and fix 306 corresponds to Figure 3.9. Till thicknesses range from 5 m in water depth less than 25 m up to 30 m in water depth greater than 25 m.

Video, Photos, and Grab Samples

The seabed composition of till consists of approximately 80% coarse gravel (cobbles and boulders) and 20% fine gravel (granules to pebbles) and sand. Figure 3.8 is a bottom photograph of till showing the abundance of boulders and the lack of finer grained sediments. The cobbles are composed predominantly of quartzites and slates with a few

TABLE 3.1

LEGEND FOR INTERPRETED SEISMIC REFLECTION PROFILES

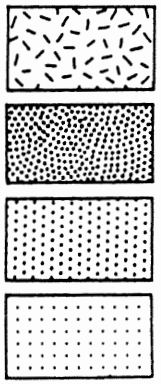

BEDROCK

GLACIAL TILL

SAND AND FINE GRAINED GRAVEL

SAND

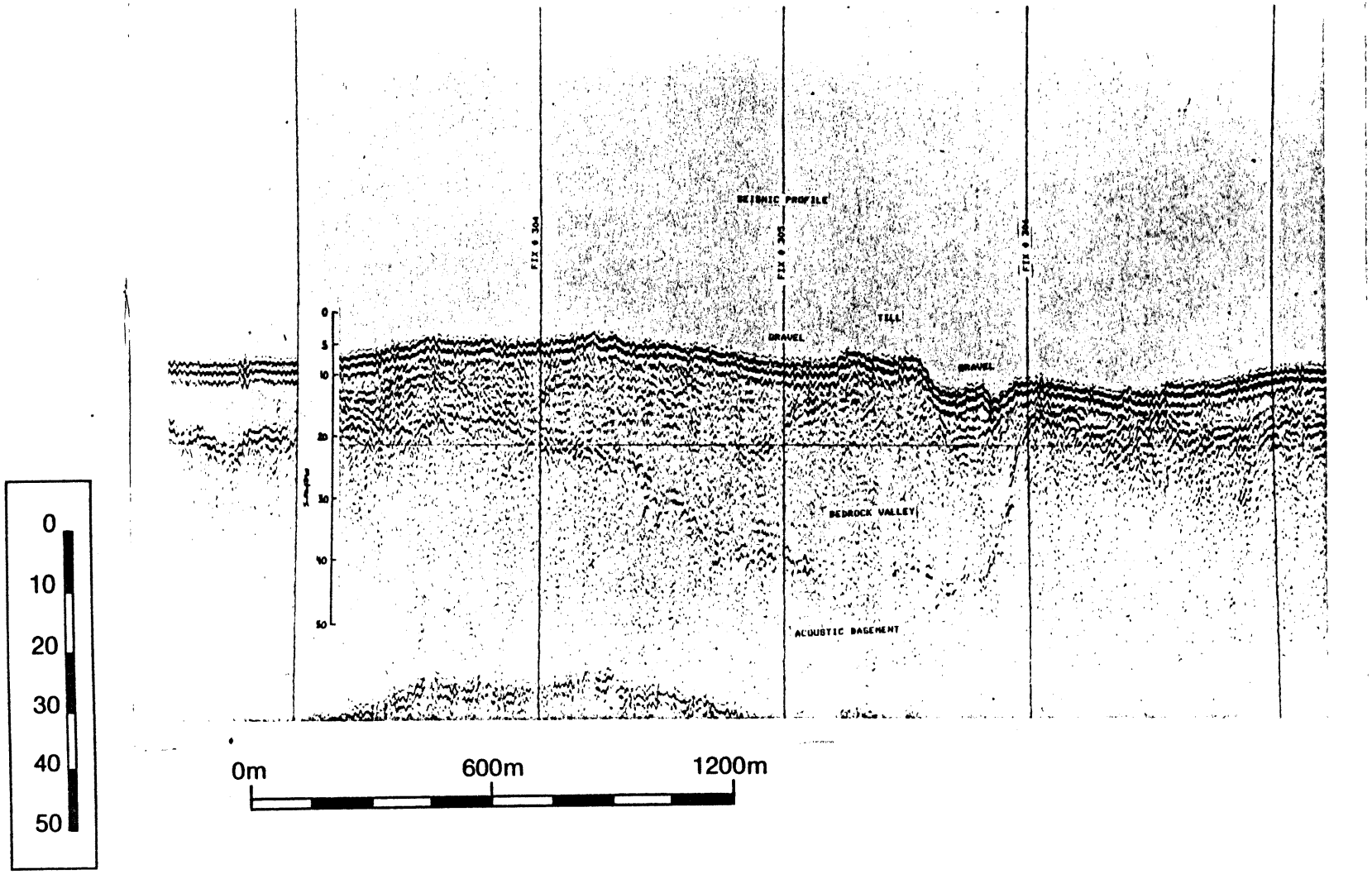

Figure 3.7: A raw seismic profile across a broad deep (30 m) bedrock valley. Note the coherent internal reflectors within the till and the planar reflectors within the sand and gravel left of fix 306. Bedrock shows good cross hyperbolies right of fix 306. The vertical scale is in metres.

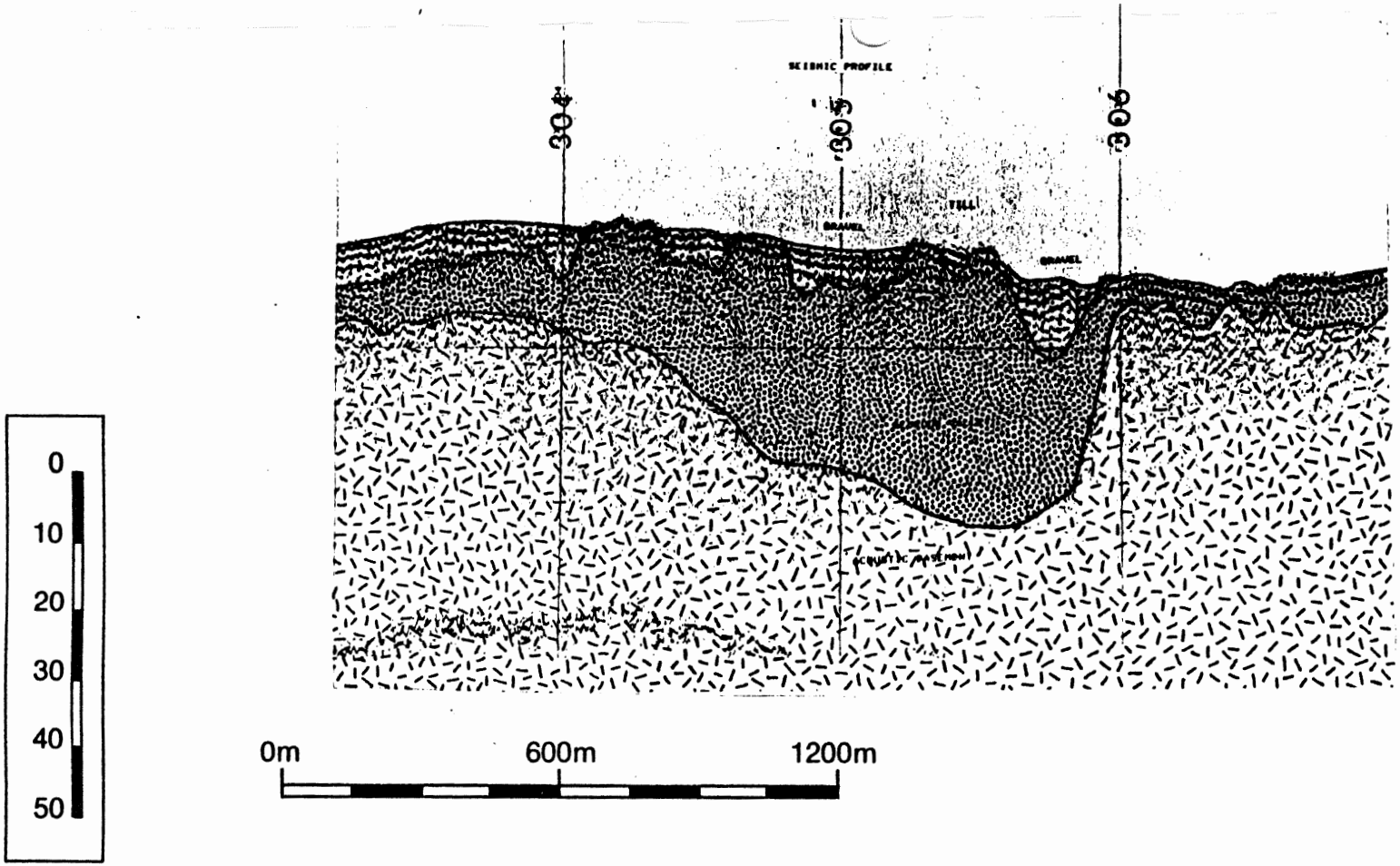

Figure 3.9: Interpreted seismic profile showing a thick sequence of till (30 m) infilling a bedrock valley. The upper surface of the tillis channeled. Channels are filled with sand and fine-grained gravel. Vertical scale is in metres.

Figure 3.8. Sea bed expression of till showing abundant boulders. Field of view approximately 2.3 m.

scattered granitic members. The cobbles are subangular to subrounded with carbonate (encrusting algae) and vegetation growing on one side. This indicates that the cobbles underwent some mechanical erosion previous to the growth of the organic material. Because of their size, movement by wave generated currents is highly unlikely. It is assumed then that this facies had been deposited in place and not transported to its present position. Smoothing of the gravel could have occurred through impact of smaller sized gravel and sand. The amount of organic material growing on the rocks would indicate that this facies has been relict for some time (Hall, unpublished data, 1984).

Sand and Fine-Grained Gravel (SFGG)

Side Scan

Like till, SFGG is acoustically dark but differs in that it lacks abundant boulder shadowing and occurs in bathymetric lows. Bathymetry can be seen from the sonographs since the fish height above the seabed is given adjacent to the ships track line. Figure 3.4 shows an excellent example of SFGG in a bathymetric depression between two till outcrops. Note that in the centre of the figure the surface is furthest from the horizontal track line. This indicates the SFGG occurs in a bathymetric depression. SFGG in this figure appears as a uniform dark acoustic signature with occasional boulder shadowing (as shown in the middle upper section of the figure along the fifth swath line from the ships track). Note also the relatively smooth surface expression of the SFGG in comparison to the adjacent till outcrops.

Seismic

SFGG have a more regular initial arrival than till and a smoother surface expression. Figure 3.7 shows sand and gravel outcropping at fix 305. Note the planar surface expression and the coherent planar reflectors within the SFGG at depth. Figure 3.9 is an interpreted section of the profile presented as Figure 3.7. From this the unconformity between the SFGG facies and the underlying till is apparent. The channeled nature of this facies indicates it is an erosional cut and fill sequence.

Figure 3.10 is a sonograph showing the SFGG facies flanking the till facies. SFGG appears to the left of fix mark 315 while till appears to the right of fix mark 315. The coarse grained megaripples (CGM) identified left of fix mark 315 are discussed in detail in Chapter 4. CGM are most abundant in this environment. Figure 3.11 is the seismic profile which corresponds to the side scan image of Figure 3.10 and shows the planar surface expression of the SFGG facies in contrast to the hummocky surface expression of the till facies. SFGG outcrops from fix mark 315 to midway between fix mark 315 and 316. Figure 3.12 is an interpreted seismic section of the same profile. From this the SFGG can be easily seen channeling through the till and the way to the bedrock. Near the base of the channelized unit coherent planar reflectors dipping toward the right are present within the SFGG facies. This may be a depositional feature of this facies. Coherent planar reflectors characterize the SFGG facies on seismic reflection profiles.

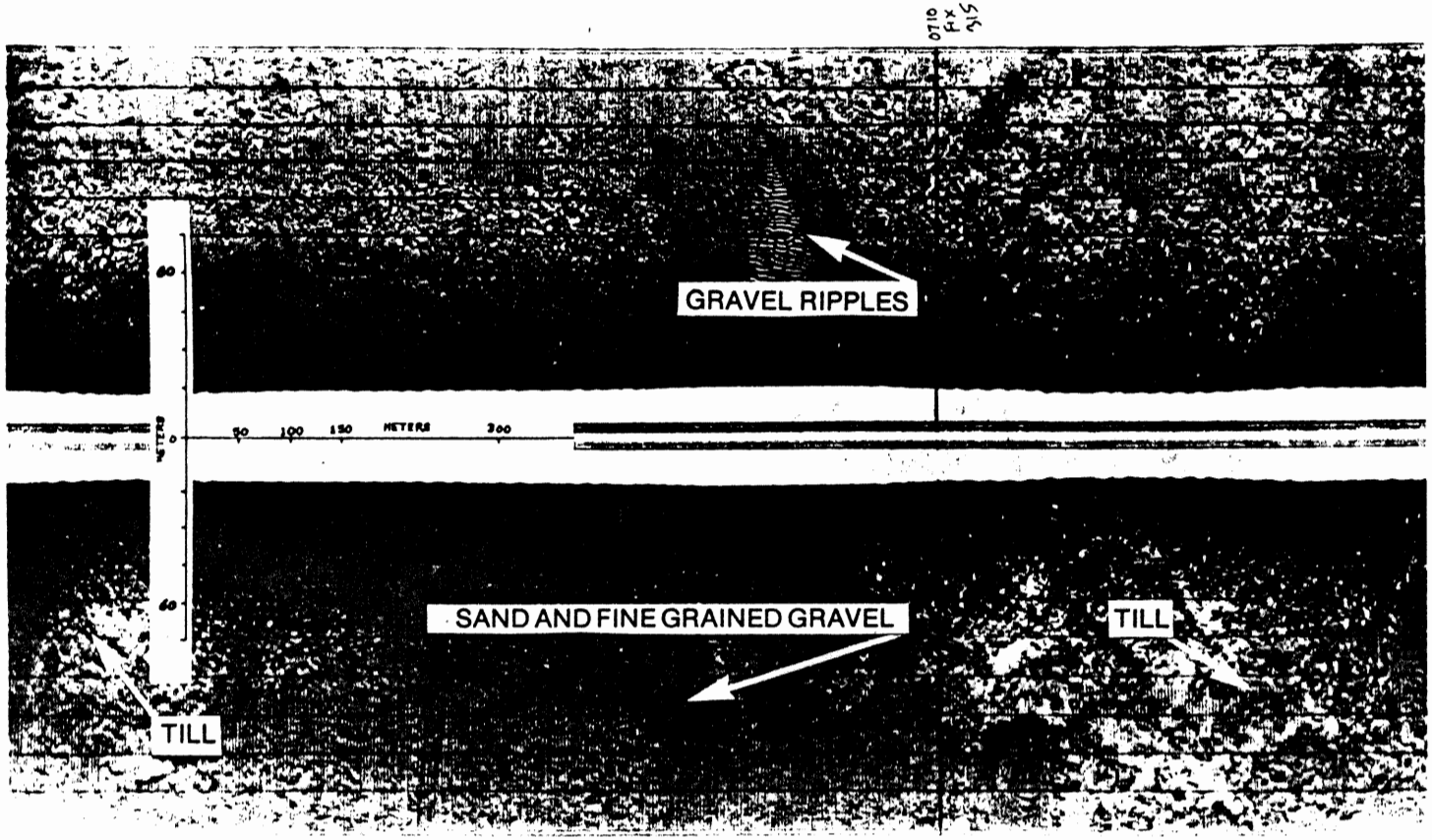

Figure 3.10. Side Scan Sonograph showing an example of a teardrop shaped CGM patch left of fix mark 315.

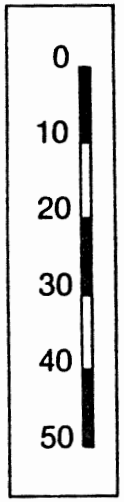

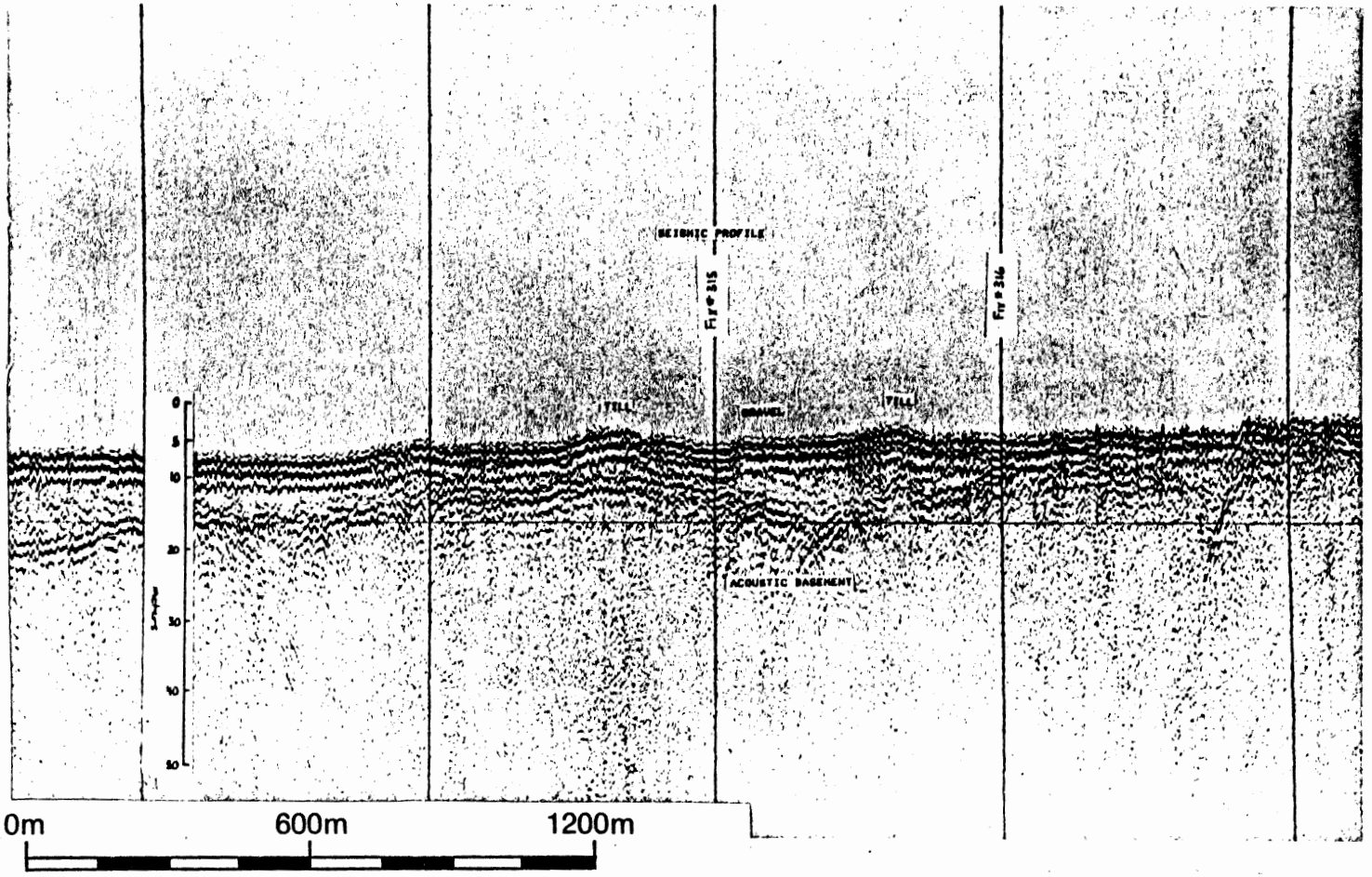

Figure 3.11: A raw seismic profile showing three characteristics of bedrock A) a point hyperbolic at fix 317; B) a cross hyperbolic between fix 315 and fix 316 and C) a serrated initial reflector. Note the planar dipping reflectors within the SFGG right of fix 315 and left of fix 313. Vertical scale is in metres.

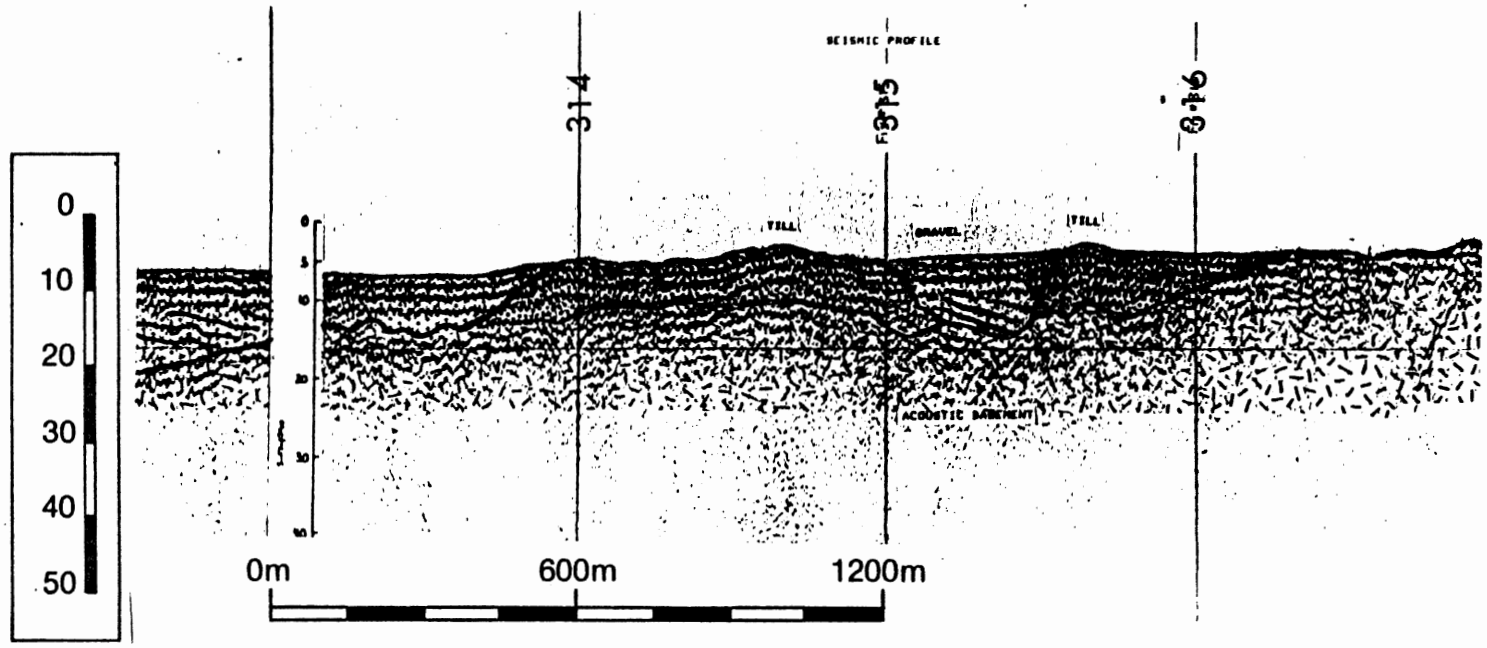

Figure 3.12: An interpreted seismic profile showing shallow bedrock covered with till on bedrock highs (between fix 314 and fix 315) and adjacent to bedrock highs (left of fix 316). The till appears to be channeled and filled with SFGG. Vertical scale is in metres.

Video, Photos, and Grab Samples

This facies is composed of poorly sorted, polymodal fine gravel and sand. The sand fraction ranges from fine to coarse. Grain surfaces range from angular with conchoidal fracturing to rounded with frosted surfaces. The gravels are subangular to rounded with polished surfaces. Offshore, in water depths greater than 30 metres, the gravels have a carbonate growth covering from 5 to 100 per cent of the pebble surface area (Hall, unpublished data). The SFGG facies consists of a homogeneous mixture of sand and gravel or isolated patches of sand and patches of gravel. SFGG usually flanks till outcrops and becomes progressively finer grained away from these outcrops. Boulders are occasionally present in this environment but probably make up less than 10% of the total sediment volume. Figure 3.13 shows a typical example of the surface expression of this facies. Field of view is approximately 2.5 m

3.2.4 Sand

Side Scan

This environment has very low acoustic reflectivity and hence appears white on side scan sonographs. The very low acoustic reflectivity is due to the lack of hard surfaces which can reflect sound and the lack of elevation variability in this environment. Sand occurs in bathymetric lows and has a planar surface expression. Figure 3.14 is a sonograph over a sandbody at the mouth of Three

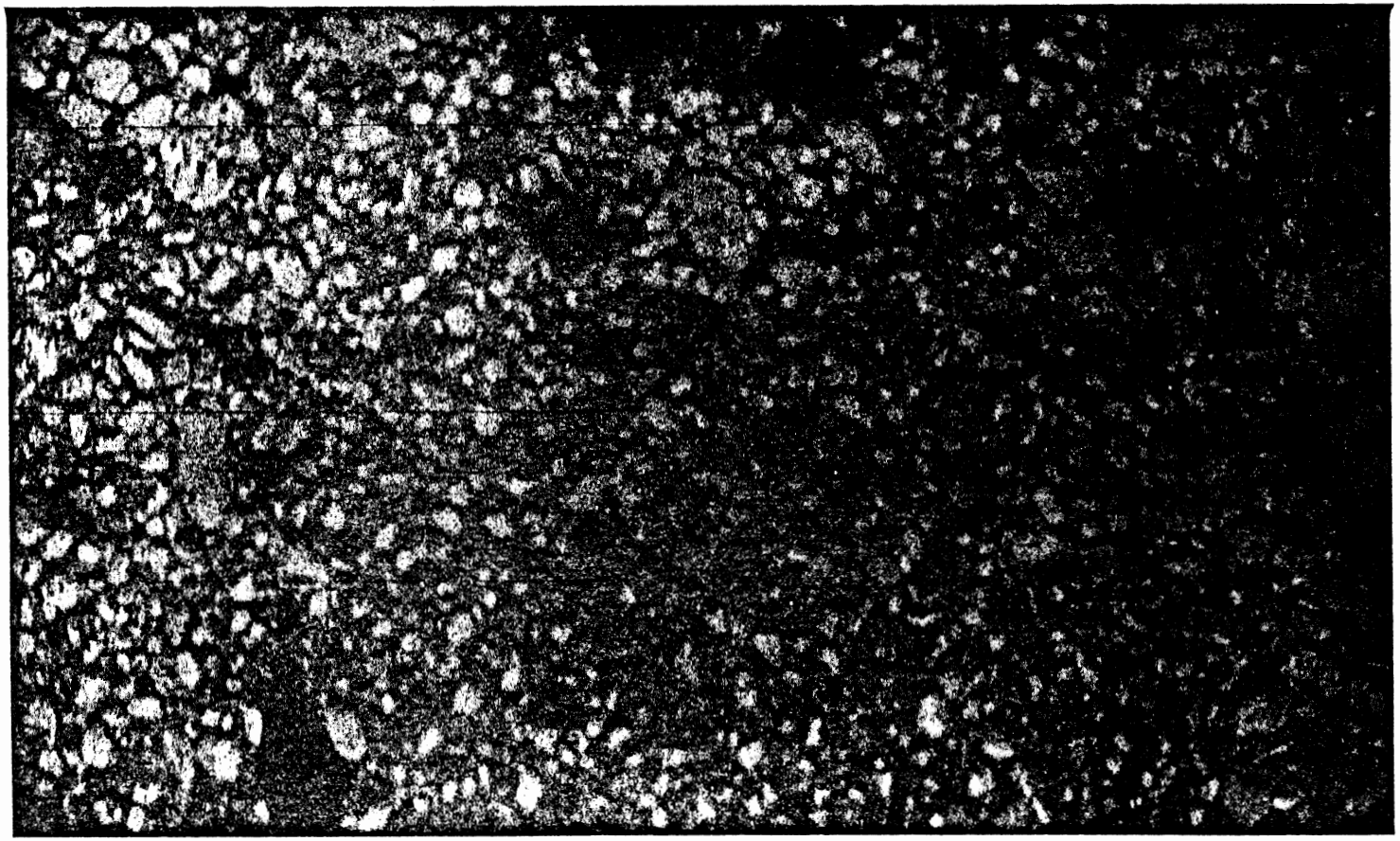

Figure 3.13. Bottom photograph showing the surface expression of the SFGG facies.

Fathom Harbour. The sand is the large white body with irregular boundaries which trend approximately vertically in the figure. Adjacent to the ship's track line in the center of the figure the sandbodies planar surface expression can be seen from the first arrival. By comparing the level of the bedrock outcrop (on the far left of the figure) to the level of the sand (in the center of the figure) the surface of the sand is seen to occupy a shallow valley. The grey spotty pattern adjacent to the horizontal track line is noise from surface waves due to shallow water depth. The vertical striped pattern at fix mark 366 (1000) is noise from the sparker.

Seismic

Low acoustic impedence results in a considerable drop in the grey level of the first arrival over sand bodies.

Sand is exposed at the seabed over bedrock valleys where till is at depth or absent. Sand appears in the subsurface as sequences without internal reflectors infilling channels cut into till or blanketing shallow valleys in the bedrock. Figure 3.15 is the seismic profile which corresponds to the side scan sonograph shown in Figure 3.14. Fix mark 349 on the seismic profile corresponds to fix mark 1000 on the sonograph. In the upper portion of the figure is a bedrock valley infilled by a 5-10 m thick section of till. The till is channelized and filled by a 5 m to 10 m sequence of acoustically transparent sediments. The surface expression of this sediment is sand with minor SFGG components. Figure 3.16 is an interpretation of the seismic profile given in Figure 3.15.

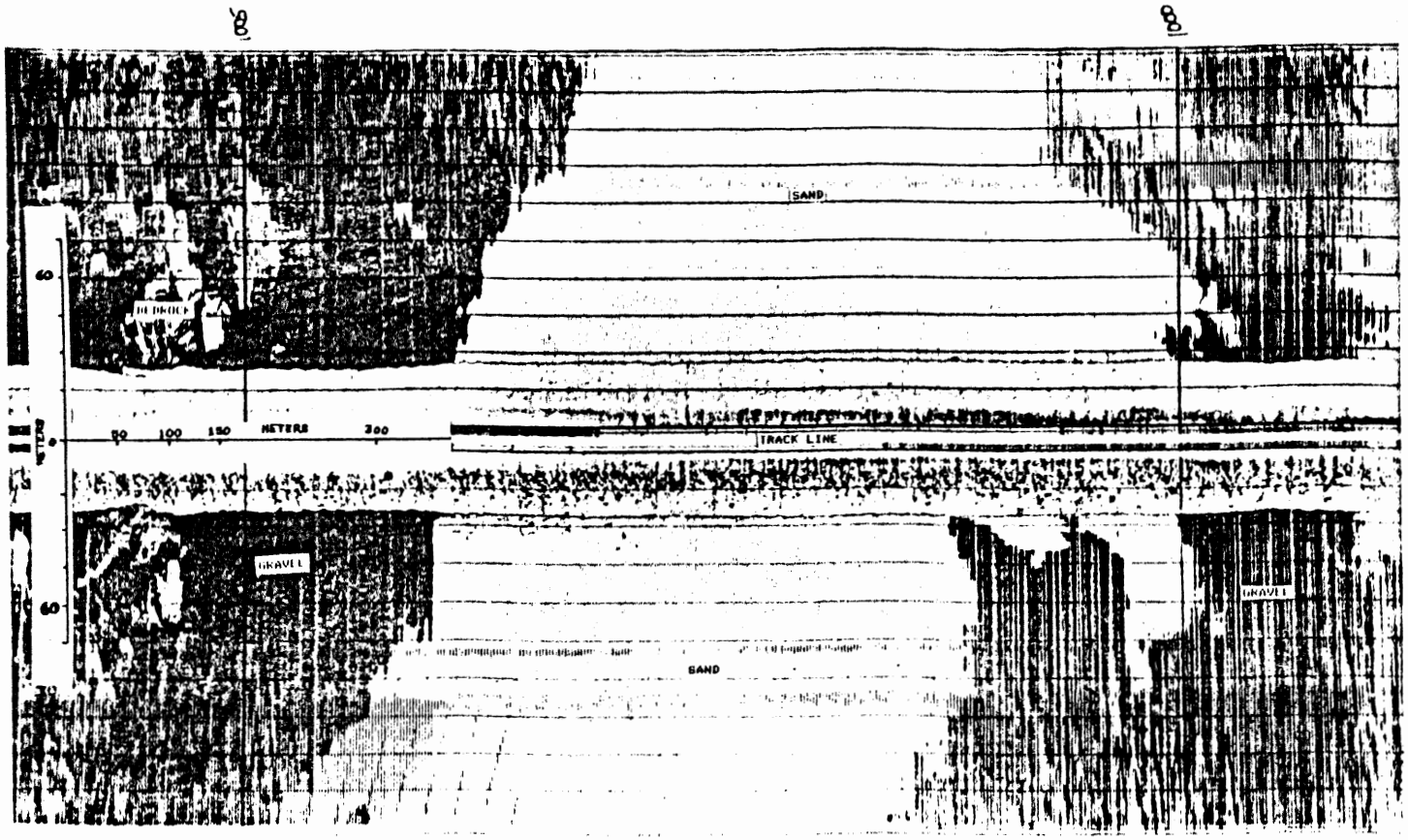

Figure 3.14: A Side Scan Sonograph across a sandbody extending from the mouth of Three Fathom Harbour is shown here. Sand appears white (no reflection) and has a planar surface expression. Sand appears in a depression as can be seen from the level of bedrock left of 1005.

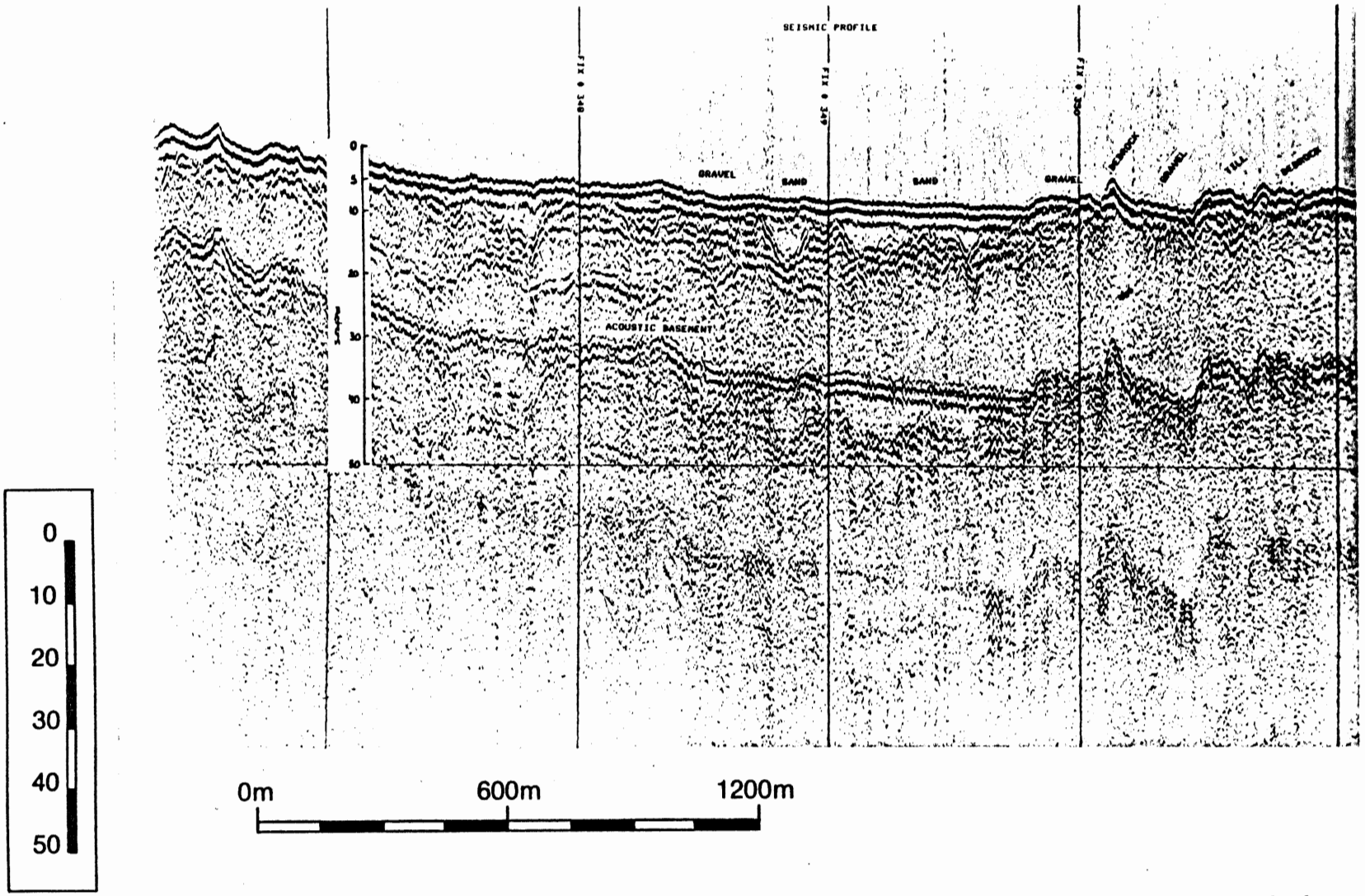

Figure 3.15: A raw seismic profile over a sandbody extending from the mouth of Three Fathom Harbour. The sand appears acoustically transparent and has a planar initial arrival. Note the well developed first order surface multiple (FOSM) to the right where bedrock is at the surface (fix 350) and the poorly developed FOSM where bedrock is at depth (fix 348). Vertical scale is in metres.

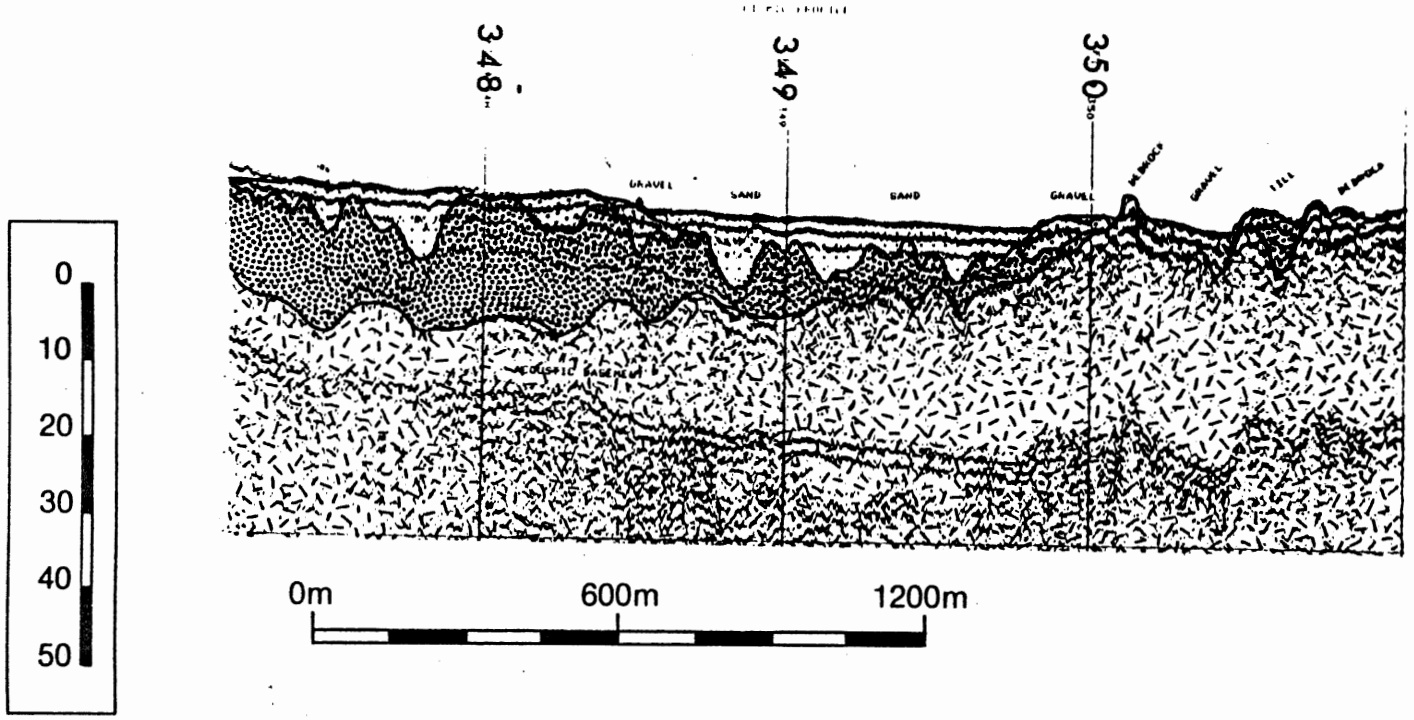

Figure 3.16: An interpreted seismic profile showing a broad shallow bedrock valley infilled with till. The upper surface of the till shows abundant channeling of variable depth. The channels are infilled with sand. Vertical scale is in metres.

Video, Photos, and Grab Samples

Offshore, the sand is medium to fine-grained, moderately well-sorted, and subangular to subrounded. It contains some benthic foraminifera, shell fragments and spicules. Nearshore, the sand is medium to fine-grained, moderately to well-sorted, angular to rounded and contains very few carbonate (shell) fragments. The lower shoreface is a fine-grained, moderately well-sorted bimodal sand, which becomes coarser and moderately sorted just before grading into the sand and gravel of the gravel facies (Hall, unpublished data).

Straight-crested, shore-parallel, two-dimensional, small-scale (wavelength 5 - 20 cm), ripples are widespread in the sand facies, where bioturbation is minimal. In areas of bioturbation rippled surfaces have undergone various degrees of reworking. Sand dollars (echinoderms) appear to be the main bioturbating organism. Extremely bioturbated areas indicate that sediment transport has been less active (static conditions) while rippled nonbioturbated areas indicate recent sediment mobilization on the seabed (dynamic conditions). Figure 3.16 is a bottom photograph of the sand environment showing clean sand with 20 straight crested ripples.

3.3 Facies Distribution

Bedrock

Bedrock occurs in scattered outcrops throughout the study area (see Side Scan Mosaic). These bedrock outcrops form the base of the highs seen along the Eastern Shore inner shelf. Bedrock highs extend seaward from the coastal headlands forming bedrock shoals. The

Figure 3.16. Bottom photograph showing the typical sand facies. Note the 2D straight crested ripples. This bedform is widespread in the sand facies. Approximate field of view 2.0 m.

bedrock shoals extending off of Story Head, Petpeswick Head,Flying Point and Jeddore Head extend to water depths of 30 metres. Outcrops seaward of Osborne Head and Graham's Head are limited to water depths of less than 40 m. Outcrops extend offshore much farther than they extend along shore. Outcrops are typically less than 3 km wide (off of Graham's Head outcrops are up to 5 km wide) and extend offshore from 2 to 10 km with most averaging about 7 km (See Bedrock Depth Map).

Bedrock outcrops are separated by bedrock valleys oriented approximately perpendicular to the shoreline. Bedrock valleys also extend offshore for about 7 km. Individual valleys are 600 m to 1.5 km wide and 5 m to 30 m deep (See B.D. Map).

East of Story Head a major change in bedrock valley orientation occurs. Valleys trending north-south are abruptly cut by an east-northeast trending valley in approximately 35 m water depth. This valley separates the shore normal valley systems from a large area (approximately 60 km^2) of bedrock outcrop. This valley also marks the seaward limit of the glacial till east of Story Head. East of Story Head bedrock outcrops are laterally more extensive and extend into deeper water. A broad (3 to 4 km) valley system separates the bedrock shoals off Osborne Head from the bedrock shoals off Graham's Head (see B.D. Map).

The east/northeast trending valley system intersects the Cole Harbour and Chezzetcook Inlet valley systems in about 45 m water depth but these shore-normal systems are not redirected and continue to at least 60 metres water depth (See B.D. Map).

Piper et al (in press) described an inner shelf valley system along the South Shore of Nova Scotia as a high sinuosity drainage system where channels shallowed toward the outer shelf. Piper used this evidence to explain the origin of these valleys as an ice drainage pattern known as rinnentaler.

Contrary to the situation on the South Shore, the Eastern Shore bedrock valleys are broad and shallow in the nearshore and deepen toward the outer shelf and are low sinuosity systems (See B.D. Map). Glacial scouring appears to be a more important factor than drainage patterns in the development of bedrock valleys.

Till

Till is eroded from topographic highs, forming boulder retreat shoals, and forms thick sequences in bedrock valleys. This facies surface expression is composed primarily of coarse cobbles and boulders. It is found throughout the study area adjacent to, and covering, the flanks of bedrock outcrops. This facies extends seaward from coastal headlands in a south-southeast direction. The main concentration of this facies is in the areas between Osborne Head and Story Head. The inner shelf west of Story Head is characterized by till extending out to the 60 m isobath. This is in contrast to the area east of Story Head which has virtually no till in water depth greater than 30 meters. In the nearshore, in water depths less than 30 metres, till outcrops can be traced from adjacent shore parallel lines for a distance of 4 km. Most till outcrops are between 0.5 and 2.5 km wide. The single area of greatest till accumulation is located 6 km to 9 km seaward of

Chezzetcook Inlet. About 12 square kilometers of till outcrop can be seen at this location (see Side Scan Mosaic).

Sand and Fine-Grained Gravel (SFGG)

As seen in the side scan mosaic, the sand and fine-grained gravel facies occupies the topographically low areas on the inner shelf. This facies begins at the base of the sand facies and extends seaward comprising most of the surficial sediment covering the study area. Most till outcrops are surrounded by SFGG. Boundaries are transitional and less than 50 m wide. SFGG outcrops can be correlated from adjacent lines off Cole Harbour for 9 km. They consistently maintain a width of 0.5 to 1.5 km and a north-south orientation. SFGG outcrops can be similarily traced off Petpeswick Inlet for 5 km. SFGG is found in all water depths but is most abundant east of Story Head. In this area in water depths greater than 30 m SFGG infills cracks in the bedrock. SFGG occurs in the shallower areas (30 - 15 m) in the eastern parts of the study area, overlying till in shore normal bedrock valleys. This unit is usually channeled into the till and is usually less than 5 m thick.

Sand

From the side scan mosaic for the Eastern Shore it can be seen that sand accumulates in the topographically low areas offshore, and extends seaward from the mouths of present day estuaries onto the inner shelf to water depths of 30 m. Sand bodies between 100 m and 800 m wide can be correlated from adjacent lines off present day estuaries up to 4 km

offshore. Seaward of the mouth of Cole Harbour a 10 m thick, 3 km wide sand body forms a thin blanket over a broad bedrock valley and can be traced for over 2.5 kilometers seaward of the estuary mouth. An isolated sand body 500 m long (shore parallel) and at least 150 m wide (shore perpendicular) was mapped in the outermost part of the survey area in a water depth of approximately 65 m. It is possible that this sand body is a relict beach. If this is the case, sea level would have had to have been at least 65 m below present sea level during its formation, presumably in Holocene times.

Sand bodies in water depths of less than 30 m are underlain by a channel cut and fill sequence and have been interpreted as Holocene transgressive sand overlying channelized estuarine fill (Boyd, et al., in press).

CHAPTER 4

4.1 Introduction

Coarse-Grained Megaripples (CGM) are limited to the continental shelf and may be important paleoshoreline, paleocurrent and paleoenvironmental indicators. Detailed description and quantitative analysis of these bedforms is lacking in the literature. Description of the morphology and explanation of the possible origin of these bedforms may be valuable aids to interpreting ancient shelf siliclastic sequences in which CGM appear. Side scan sonar, video and underwater photography were used to investigate the morphology, distribution, orientation, texture, and possible modes of generation of the CGM observed on the inner shelf.

4.2 Ripple Dimensions, Crest Morphology and Plan Shape

Ripple wavelengths were accurately measured for approximately 110 examples of CGM on side scan sonographs. CGM have wavelengths ranging from 133 to 300 cm and are found in water depths from 15 to 60 metres. Ripple crests may be straight, sinuous, digitate or branching. Figure 4.1 is a side scan sonograph showing three varieties of ripple crest morphology. The CGM unit located in the lower right hand corner of the sandbody has straight crests. The patch to the left has branching and digitate ripple crests (these varieties usually occur together). The CGM patch in the upper right hand corner of the sandbody has sinuous crests. Figure 3.10 shows CGM which are branching and digitate. Figure 4.2 shows GCM with crests that are sinuous,

branching, and digitate. As can be seen from these examples crest morphology can be highly variable. Scale may control this variation since large ripples have fewer bifurcations per unit area (Boyd, pers. comm.).

The plan shape of CGM occurrences is classifiable into three modes. These are CGM patches, CGM bands and CGM fields. CGM patches may be lensoid, rectilinear or teardrop shaped. In Figure 4.1 the CGM occurrences in the upper right and lower left are rectilinear, while the example in the lower left is lensoid. Figure 3.10 shows an example of a teardrop shaped CGM occurrence . CGM patches have variable width but are always less than 150 m wide. CGM patches occur in the SFGG facies in areas where bedrock is at depth, in SFGG-floored bedrock cracks and in areas of extensive sand facies. Figure 3.1 shows a gravel ripple patch approximately 50 m wide and 10 m long (left of fix mark 321) within a SFGG floored bedrock cracks. Figure 3.10 shows an example of a CGM patch in the SFGG facies where bedrock is 10 metres below the surface (from reflection profile shown in Figure 3.11). Figure 4.1 shows examples of CGM patches associated with sand. CGM bands are shown in Figure 4.2 to be less than 100 metres in width (x-axis, parallel to ships track) and greater than 300 metres in length (y-axis, perpendicular to ships track). CGM bands occur over shore-perpendicular bedrock valleys in channels cut into the till and can be correlated north-south on adjacent east-west lines up to 3 km without significant change in width. Examples of this can be seen on the side scan mosaic off Martinique beach and off

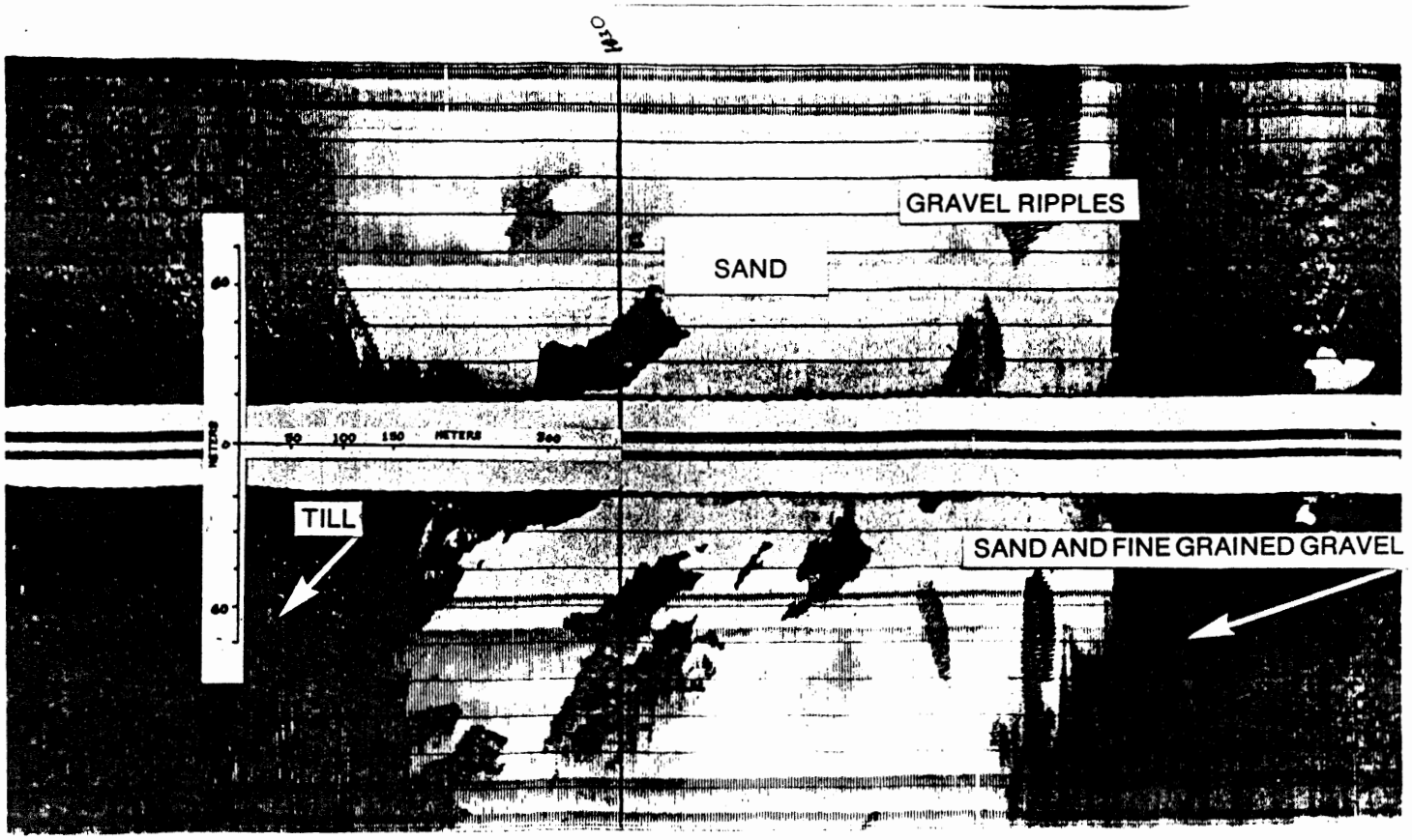

Figure 4.1 . Side Scan Sonograph showing four CGM occurrences. All units are classified as patches. Note that the CGM patch in the upper right corner of the sandbody has a smaller wavelength on the left margin than the rest of the patch. Patches in the same area may have different wavelengths.

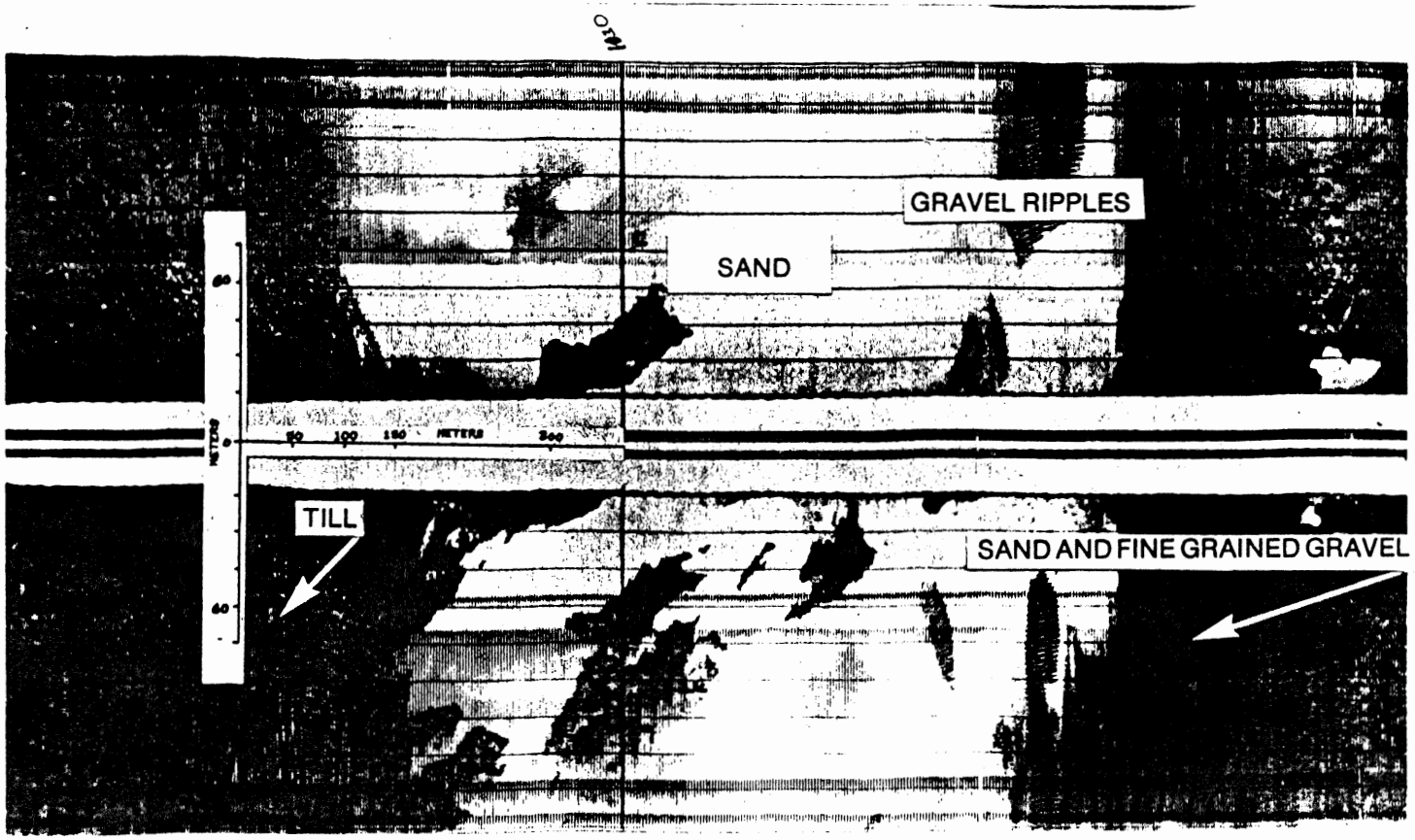

Figure 2. Side Scan Sonograph showing four CGM occurrences. All units are classified as patches. Note that the CGM patch in the upper right corner of the sandbody has a smaller wavelength on the left margin than the rest of the patch. Patches in the same area may have different wavelengths.

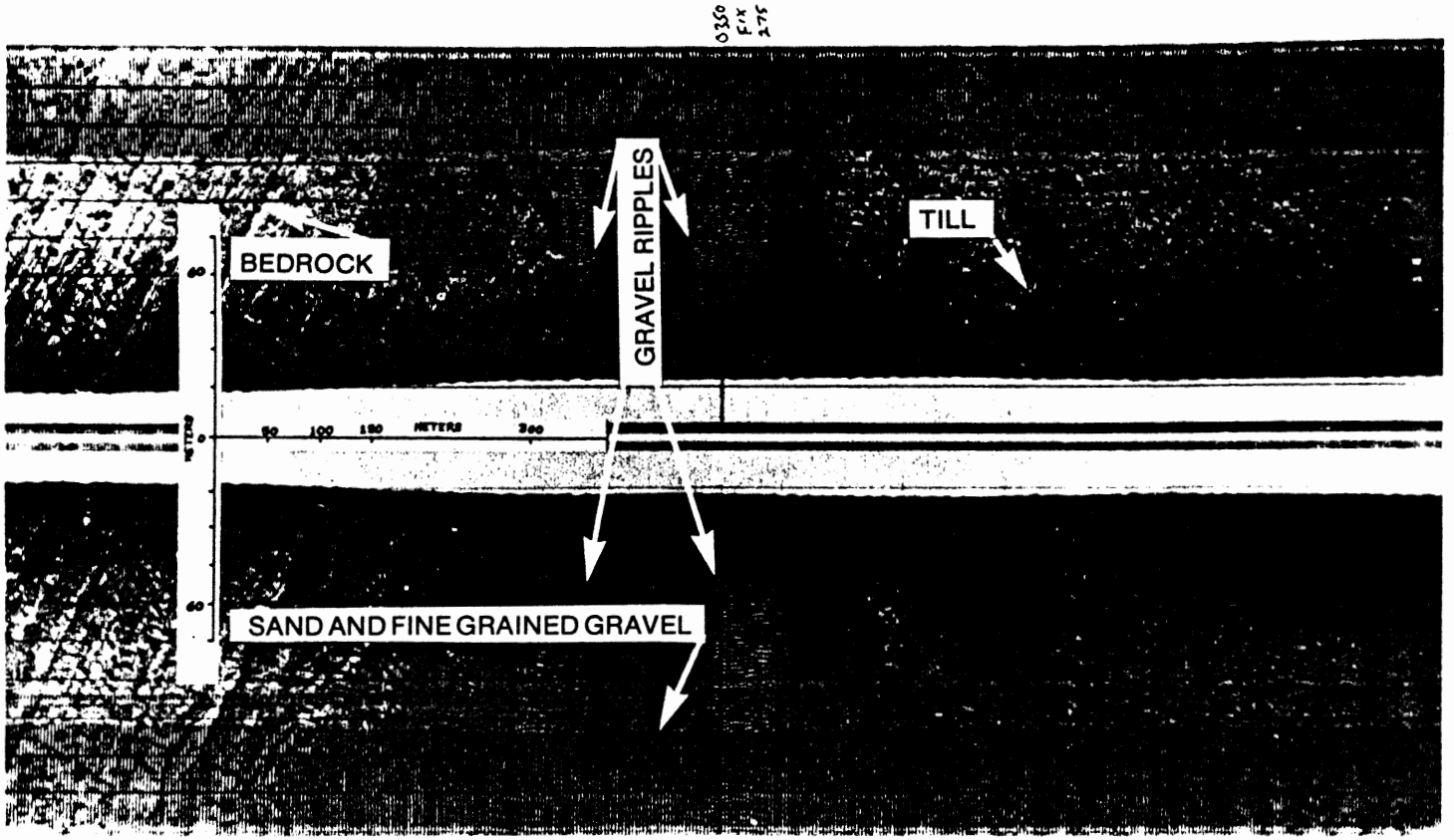

Figure 4.2 . Side Scan Sonograph showing two CGM bands oriented perpendicular to the ships track line.

Lawrencetown beach. CGM bands are associated with the SFGG and sand facies.

CGM fields are similar to CGM bands differing only in the width which ranges from 150 m to 400 m in the fields. From the side scan mosaic CGM fields can be seen to form bands off Martinique beach by tapering offshore. Bands and fields of CGM are limited to water depths of less than 30 m. Patches are the most common type of CGM in water depths of greater than 30 m.

Table 4.1 summarizes the classes, dimensions, plan shapes and associated facies for coarse-grained megaripples on the Eastern Shore inner shelf.

Table 4.1

Class	Dimension		Plan Shape	Associated Facies
CGM Field	width length	100 m 150 m	Rectilinear to Equant	SFGG Sand
CGM Bands	width length	100 m 300 m	Rectilinear	SFGG
CGM Patches	width length	150 m 150 m	Lensoid Rectilinear Teardrop	Sand SFGG Till

4.3 Ripple Symmetry and Grain Size

CGM are symmetrical and asymmetrical with sharply peaked or rounded crests and flat to gently concave troughs. Ripple symmetry was established by visually studying the underwater video and photography. On the basis of this, ripples appear to be mostly symmetrical flat though some appear slightly asymmetric. Inman (1957) classifies

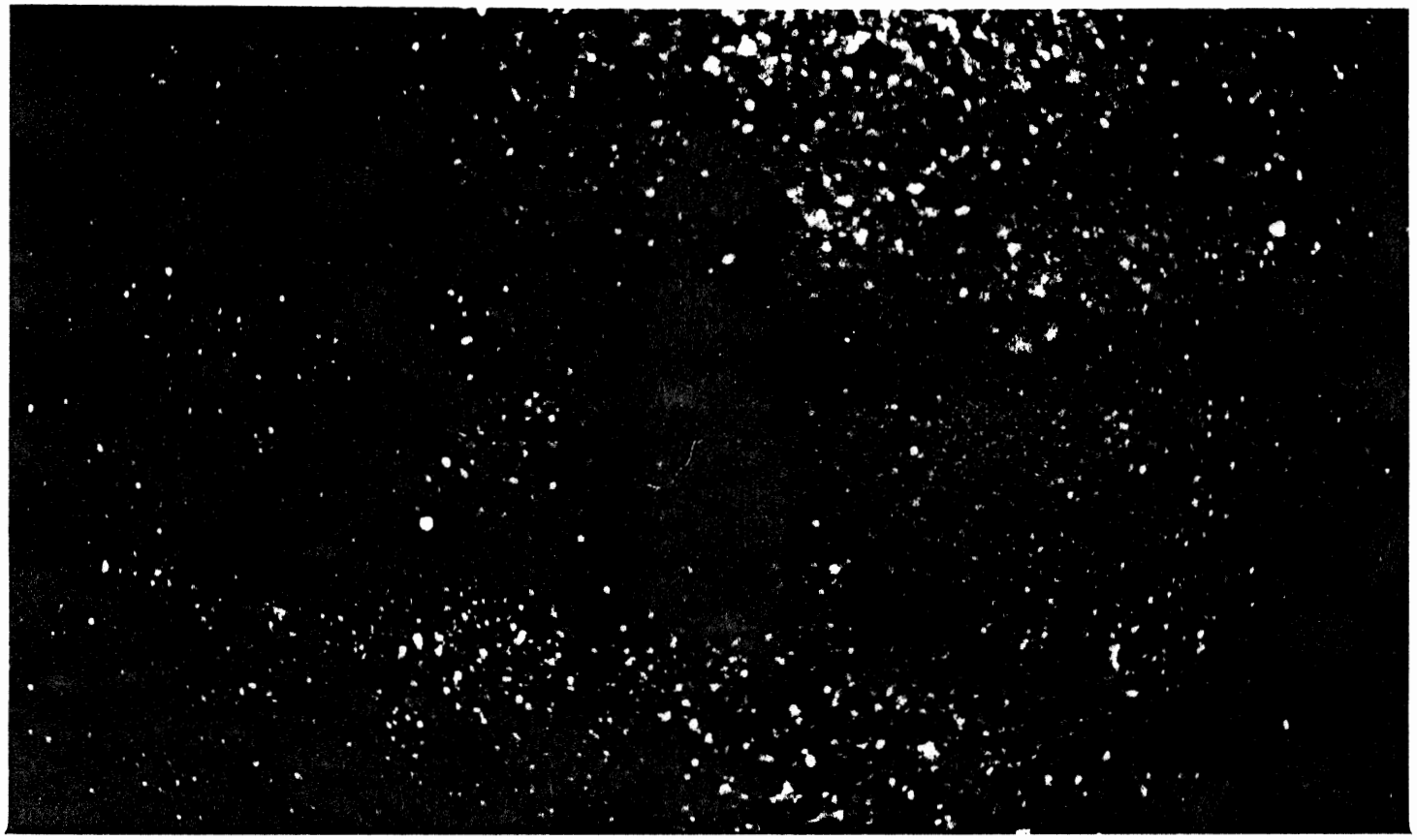

Figure 4.3. Bottom photograph of CGM with cobbles to small boulders in the troughs and sand to pebbles on the crest. The crest appears slightly asymmetric.

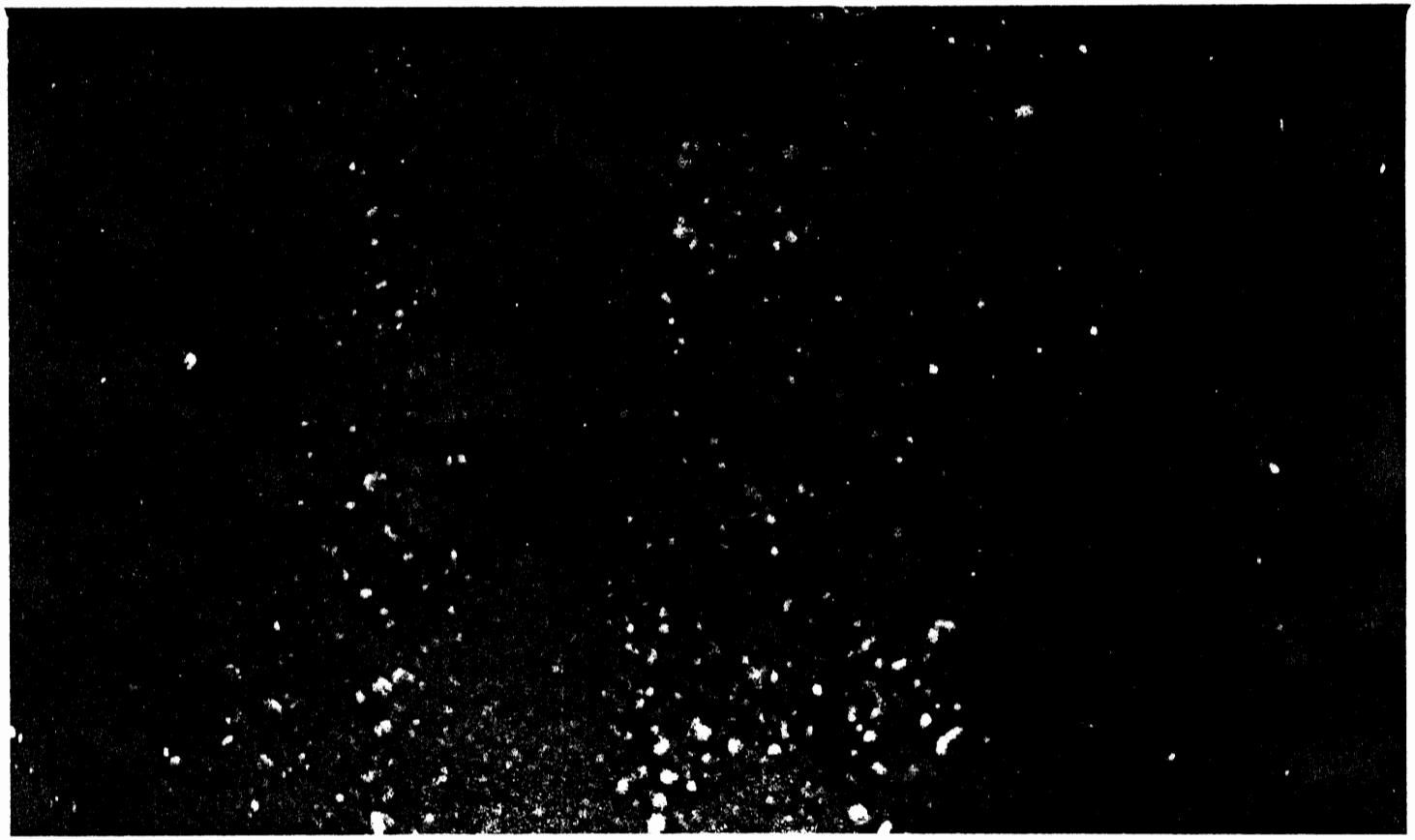

Figure 4.4. Bottom photograph of a CGM associated with the SFGG facies.

flat trough ripples as solitary ripples and ripples with concave troughs as trochoidal.

Figure 4.3 is a bottom photograph of a typical CGM, associated with the till facies, on the Eastern Shore inner shelf. The approximate field of view in the photograph is 2.0 metres. The crest is composed of fine sand to fine gravel (granules to pebbles) and a coarse carbonate shell hash. These are the least dense materials. The densest materials, coarse-grained gravel and coarsest (cobbles to small boulders) remain in the troughs. Gravel up to 10 cm in diameter can be seen in the trough of the ripple in figure 4.3. Figure 4.4 is a bottom photograph of a typical CGM associated with the SFGG facies. In this case boulder-sized grains are not found in the troughs. The field of view is approximately 2.5 metres.

Yorath et al (1979) reported coarse pebbles, cobbles, and some boulders localized in the troughs of large scale (wavelength 30 to 100 cm) "oscillation ripples" on the Northeast Pacific Continental Shelf. The coarse grained nature of the troughs was interpreted by Yorath et al (1979) as representing lag deposits underlying the coarse-grained megaripples. This interpretation is probably also valid for the coarse-grained megaripples on the Eastern Shore inner shelf.

4.4 CGM Orientation

CGM crest orientations were obtained from 59 occurrences. The acute angle between the ships track line and the individual CGM crests was measured for each occurrence. This angle was then corrected for distortion by applying a velocity-paper feed speed distortion ratio

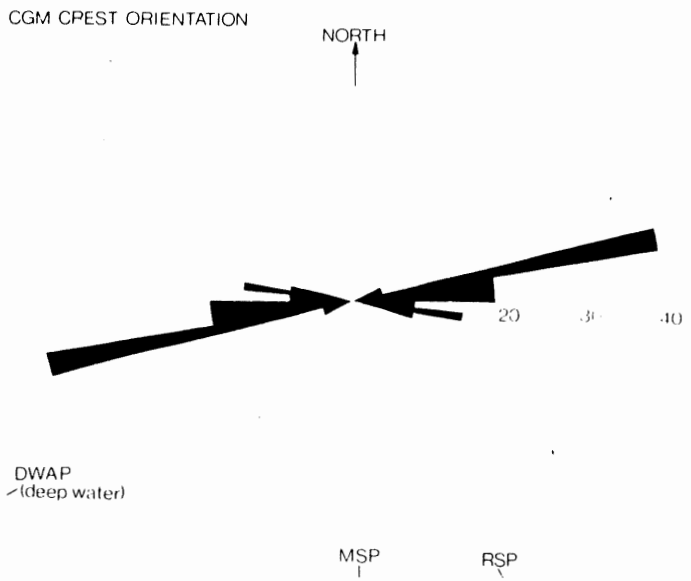

Figure 4.5. Rose diagram showing the strongly bipolar nature of CGM crests on the Eastern Shore inner shelf.

correction. Flemming et al (1982) developed distortion ellipses which were used in this study to make the appropriate corrections graphically. Once corrected for distortion, this angle represents the true angle between the CGM crests and the ships track line. Because the azimuth of the track line is known at each point along the ships track, the angle between the CGM crests and the ships track can be manipulated (added or subtracted accordingly) to obtain the azimuth of the CGM crest. Figure 4.5 is a rose diagram showing the orientation of CGM crests for the entire study area. Crests are strongly bimodal and parallel/subparallel to the regional bathymetry of the Eastern Shore (Figure 1.1). The normals to the Martinique beach shoreline (MSP), Eastern Shore regional shoreline (RSP); and dominant wave approach direction (DWAP) are plotted on the same rose diagram. Regional shoreline trend and local shoreline trend are highly conformable with crest orientation. Dominant wave approach direction, however, is strongly oblique to the CGM crest orientations. Oscillatory bedforms are generated with crests parallel to the crests of the waves generating them. If these bedforms are in fact formed by oscillatory current generated by onshore propagating waves, they should be parallel to the wave approach direction. There appear to be at least four possible explanations for these observations: (1) these bedforms are not oscillatory, (2) dominant wave approach direction as measured in deep water is not representative of the Eastern Shore inner shelf, because wave refraction may operate to redirect the wave fronts into a shore-parallel orientation as water shallows, (3) these bedforms are generated by waves which do not approach from the

dominant wave approach direction but rather from the south or south-southeast or (4) the orientations measured are an artifact of the ships track line orientation (i.e. the side scan beams may reflect from the bedform crests; and if these crests are not parallel to the side scan beam, reflection may not occur). The latter is considered to be unlikely since CGM crests at high angles to the ships track line were observed at line changes.

4.5 Wave Generation Hypothesis

4.5.1 Wave Climate Character

Wave climate for the Scotian Shelf shows a predominant ground swell superimposed with locally derived wind generated waves. The highest wave energies are experienced during winter months but may also occur in the late summer and early fall with the passing of hurricanes. The most frequent waves seen along the Eastern Shore are 0.6 to 0.9 metres high with an 8 to 9 second period (Boyd and Penland, 1984). Modal waves are 1.2 to 1.5 metres high with a 9 to 10 second period. Storm waves may reach heights of 5 m with a period of 10 to 15 seconds (Boyd and Bowen, 1983). The highest frequency of storm activity is from the south-southwest (Hall, unpublished data).

4.5.2 Parameters Effecting Ripple Generation

Ripples are generated by shear stresses between the water and the sediment at the seabed. Shear stresses are generated by the oscillation of the water column as surface waves propagate forward. These oscillations are circular at the sea surface but decay into oblate

ellipses with increased water depth and at the seabed are reduced to linear oscillations. The diameter of the oscillations (orbital diameter) decreases with increased water depth, and increases with increases in the height and wavelength of the surface waves.

For simple sinusoidal waves generated in laboratory waveflumes, the orbital diameter (d_o) can be determined from linear Airy wave theory with

$$d_o = \sinh \frac{H}{\frac{(2\pi \cdot h)}{L}} = \frac{U_o \cdot T}{\pi}$$

where H is the wave height, L is the wavelength, h is the water depth, U_o is the maximum orbital velocity of the near-bottom orbital motions, and T is the wave period (Miller and Komar, 1980). Wave period is related to wavelength by:

$$L = \frac{g \cdot T^2}{2\pi}$$

where T, L are the same as above and g is acceleration due to gravity (Lynby, 1974). For this study, errors in theoretical calculations are less than the error in field measurements (water depth and ripple wavelength). Inman (1957) showed that at a low value of orbital diameter, (d_o) the ripple spacing (λ), in coarse-grained sand, is given by $\lambda = 0.80\ d_o$. With increased grain size and orbital diameter, ripple spacing may increase to a maximum of $\lambda = 1.0\ d_o$ (Inman, 1957).

4.5.3 Genesis of Coarse Grained Megaripples

There are at least two possible mechanisms thought to be responsible for the generation of CGM. Cook (1982), Morang and

McMaster, (1980); Morang and McMaster (1982) and Tabat (1979) postulate that the elongate, shore-perpendicular morphology of CGM bands, indicates formation of these bedforms by rip currents. These authors suggest that subsequent reworking by oscillatory currents under normal wave conditions destroys any evidence of unidirectional flow (namely ripple assymmetry) and creates a symmetric ripple profile indicative of oscillatory flow. During a detailed study of Martinique beach, shoreward of the largest CGM field, no evidence was found for rip currents strong enough to influence the seabed more than 200 m from the coastline (Nair, pers. comm.). Rip currents which could generate CGM fields off Martinique beach (see side scan mosaic) would have to be strong enough to maintain a flow 400 m wide over 1.5 km from the shoreline. This field tapers seaward to form CGM bands which extend up to 4 km from the coastline. Rip currents which could generate features of this scale would probably produce an observable erosional feature at the shoreline. Thus, rip currents seem to be an unlikely mechanism for generation of CGM, on the Eastern Shore inner shelf.

Oscillatory currents generated by storms waves have been recognized by Komar et al (1972), Yorath et al (1979) and Swift et al (1979) as an alternate mechanism for the generation of CGM.

Testing the wave generation hypothesis requires comparison of observed ripple parameters (wavelength and water depth) to theoretical ripple parameters which can be determined given the wave climate of the field area and the sediment grain size.

In order to quantify observed parameters (water depth and

corresponding ripple wavelengths) bathymetric measurements obtained from fathometer records and concurrent side scan sonographs were used. Draft and tidal corrections were made to the raw bathymetry. A 4.5 m draft correction was found to be appropriate for CSS Dawson. Tidal corrections were made by applying a sinusoidal function with a six hour period and 90 cm amplitude. Tidal amplitude and period were obtained from CHS tidal tables for the Halifax wave station. Water depth and corresponding ripple wavelengths are given in Table 4.2.

CGM wavelengths were measured from side scan sonographs. Range distortions due to changes in fish height produced less than 2% error and thus did not warrant correction. Measurements of CGM wavelength required use of a Gärber Variable Scale calibrated to the swath width of the sonograph. Measurements were confined to mid channel thus eliminating the effects of beam spreading (as discussed in Flemming, 1982).

The theoretical ripple parameters (water depth and ripple wavelength) can be established from linear Airy Theory if the wave climate and grain size are known. The wave climate for the study area is easily established since wave observations have been made in the immediate vicinity of the observed ripples. At Osborne Head, on the western margin of the study area, wave heights are recorded for a 5 minute period every 3 hours by a waverider buoy located in 53 m of water. Grain sizes of sand-SFGG were established from bottom photographs, video and grab samples.

Table 4.2. Measured CGM wavelength and water depth. Note same format for water depth and wavelength.

Water Depth (m)

59.8	60.8	61.8	59.5	58.5
21.3	24.7	24.7	24.7	13.6
13.6	19.1	19.1	19.1	19.1
25.2	25.2	25.2	25.2	16.2
22.5	22.5	22.5	22.4	22.4
29.5	32.6	32.6	30.0	30.0
32.0	35.0	35.0	35.0	35.0
35.1	35.1	28.3	28.3	27.3
27.3	27.3	27.3	27.3	27.3
27.3	27.3	27.3	30.3	42.8
42.8	35.7	35.7	36.5	36.5
35.3	36.1	35.9	34.9	34.9
34.9	33.8	33.8	20.8	27.7
47.6	47.6	54.7	49.4	49.4
40.2	40.2	40.3	40.3	42.3
48.3	55.1	55.1	55.0	57.0
57.9	54.8	54.8	53.7	53.6
59.7	59.7	19.6	19.6	22.6
23.6	23.6	22.6	22.6	22.6
12.6	17.4	17.4	17.4	17.4
20.4	19.5	19.5	19.5	29.7
29.7	29.7	28.8	28.8	29.8
29.8	29.8	29.8	30.9	32.0
31.0	31.0			

Ripple Wavelength (m)

1.97	2.72	2.08	2.50	2.14
1.36	2.05	2.30	2.50	2.10
1.67	2.14	1.66	1.66	1.66
1.76	2.04	2.33	2.30	1.67
2.30	2.10	2.22	2.04	2.14
2.14	2.00	2.14	2.14	1.94
1.89	1.87	1.83	1.71	1.78
1.54	1.60	2.30	1.92	2.27
2.50	1.66	1.66	1.80	1.50
1.75	1.73	1.72	1.63	1.89
1.85	1.67	1.67	1.85	1.74
1.70	1.60	2.20	1.43	2.18
1.33	1.57	1.30	2.05	1.87
1.87	1.67	1.87	1.87	2.04
1.50	1.76	1.60	1.46	1.50
1.50	2.30	2.30	2.30	3.00
2.00	2.50	2.14	2.50	2.50
2.00	1.87	1.87	2.20	1.60
1.50	1.40	2.30	1.87	1.50
1.80	2.30	2.40	2.40	2.50
2.10	2.40	2.10	1.50	2.00
1.90	2.00	1.50	1.76	1.60
1.87	1.60	1.87	1.80	2.00
1.87	1.87			

The relationship between observed water depth and observed ripple wavelength is shown in Figures 4.6 a to c and 4.7. Note that ripple wavelength increases with decreasing water depth from approximately 40 to 15 metres. In water depth between approximately 40 and 60 m, ripple wavelength increases with increasing water depth. Increasing ripple wavelength with decreasing water depth would be expected if these bedforms were generated in an oscillatory flow regime, since the orbital diameter at the seabed is greater in shallower water (Miller and Komar (1980)).

Waverider buoy records for a period of four months prior to the data collection cruise were investigated for storm waves (large amplitude, long period waves) which could produce large enough orbital diameters to account for the wavelength and water depth of the observed ripples. Wave parameters picked from major storms have been used to define orbital diameters in water depth of 15 to 60 m. Figure 4.8 shows the relevant wave data for May, June, July, and August (Marine Environmental Data Service, Department of Fisheries and Oceans). As previously stated, the most frequent waves seen on the Eastern Shore are 0.6 to 0.9 m high with an 8 to 9 second period (Boyd and Bowen, 1983). Waves with heights greater than 2.0 m and periods greater than 9 seconds were designated as storm waves.

Characteristic wave height, wave period, water depth, orbital diameter, orbital velocity and ripple wavelength (based on $\lambda = 0.8\ d_o$), calculated from Airy theory, for these various storms are given in Table 4.3. Storm waves on 06/26/2100, 06/02/1500 and 05/19/0300 show the best

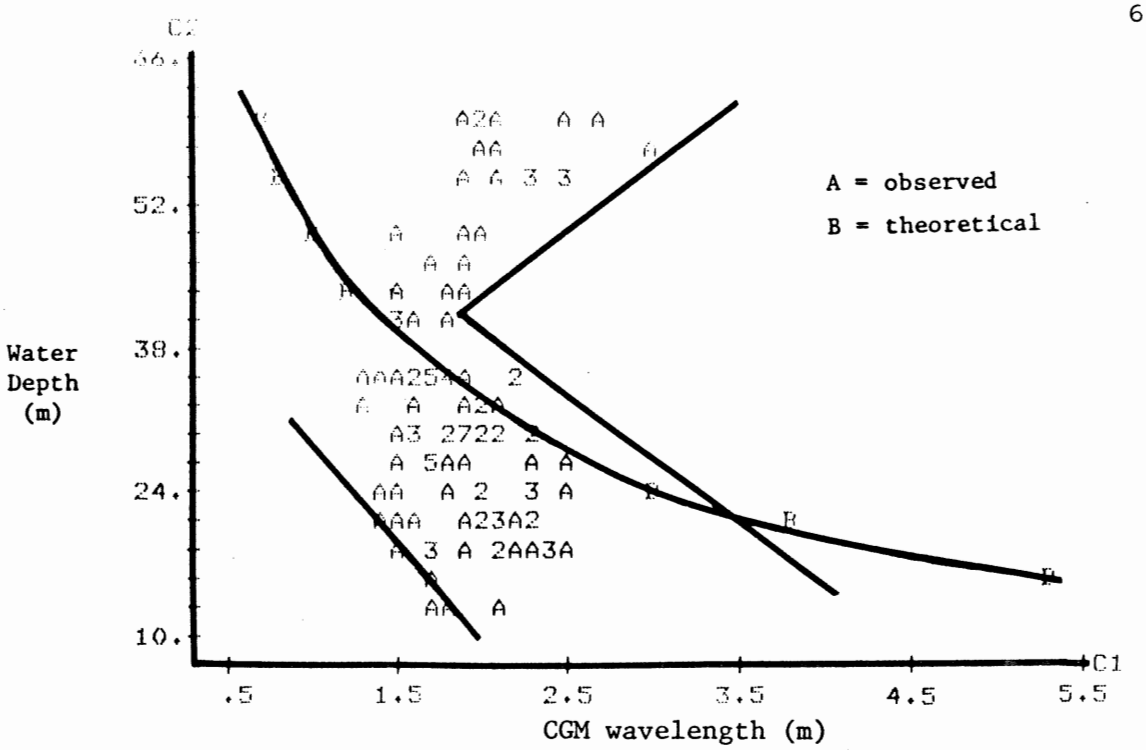

Figure 4.6a. Plot of observed ripple wavelength versus water depth and theoretical ripple wavelength versus water depth for the storm which occurred on 06/02/1500.

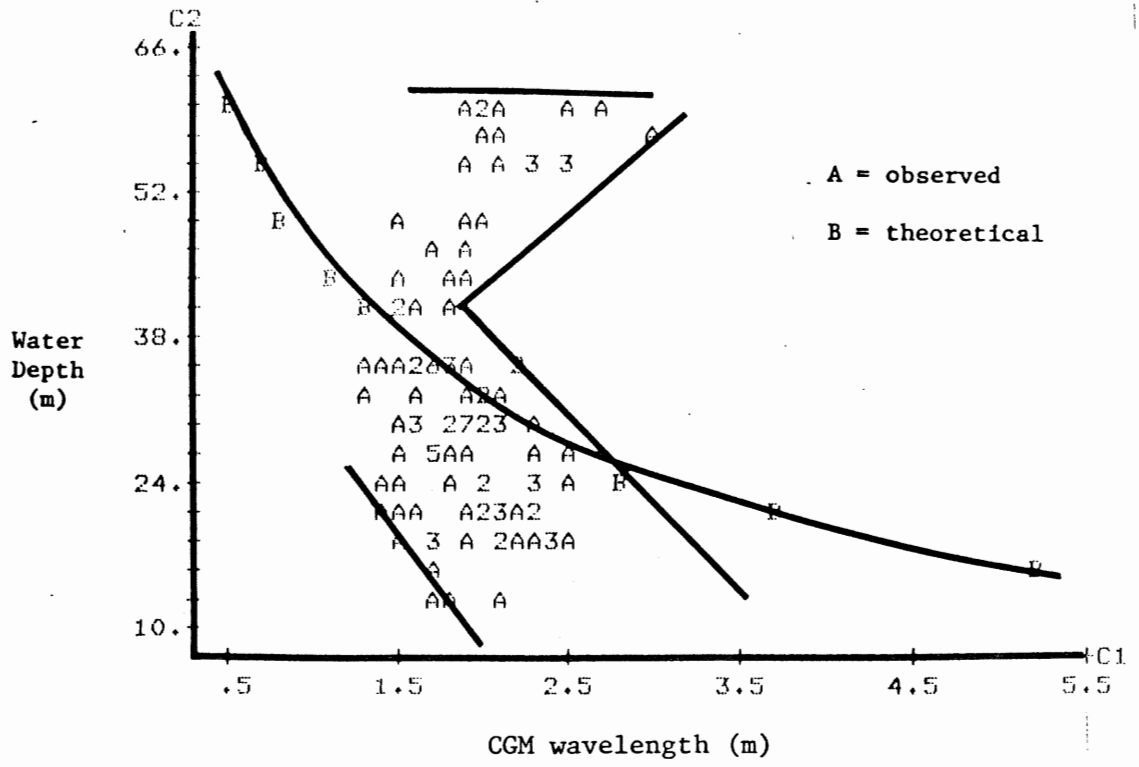

Figure 4.6b. Plot of observed ripple wavelength versus water depth and theoretical ripple wavelength versus water depth for the storm which occurred on 06/26/2100.

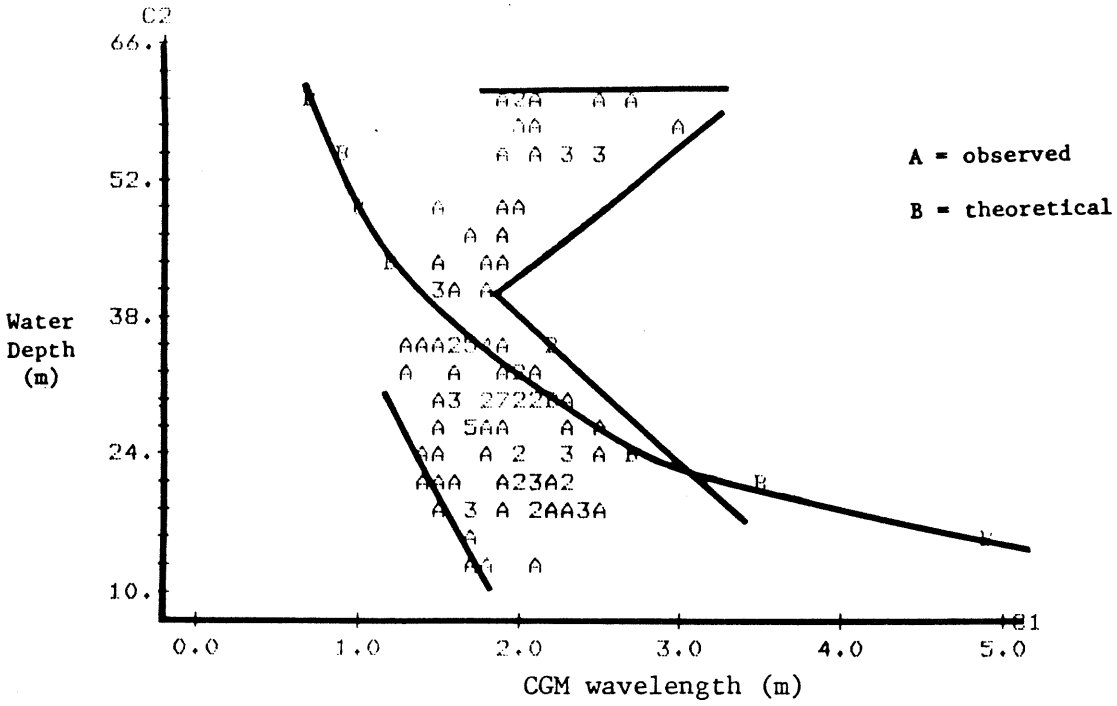

Figure 4.6c. Plot of observed ripple wavelength versus water depth and theoretical ripple wavelength versus water depth for the storm which occurred on 05/19/0300.

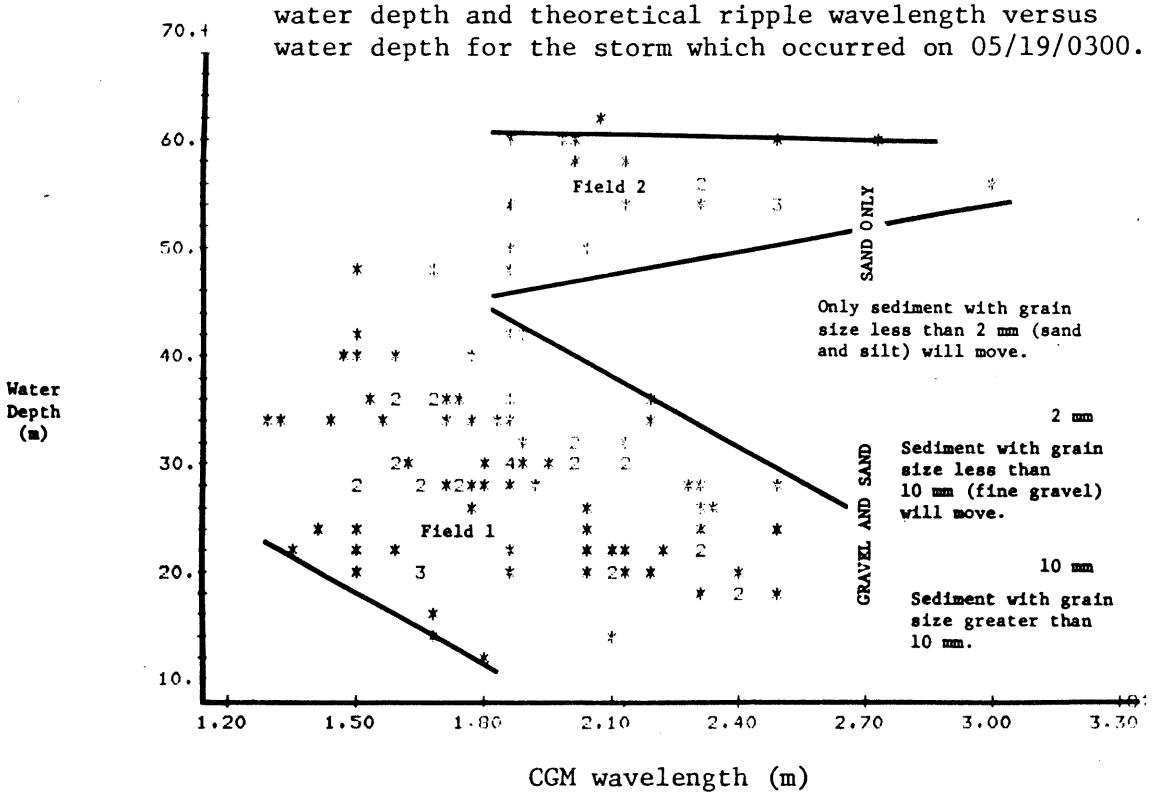

Figure 4.7. The relationship between water depth, CGM wavelength and grain size is shown here. Note that gravel cannot be transported in water depth greater than 40 m when the wave period is less than or equal to 10 seconds.

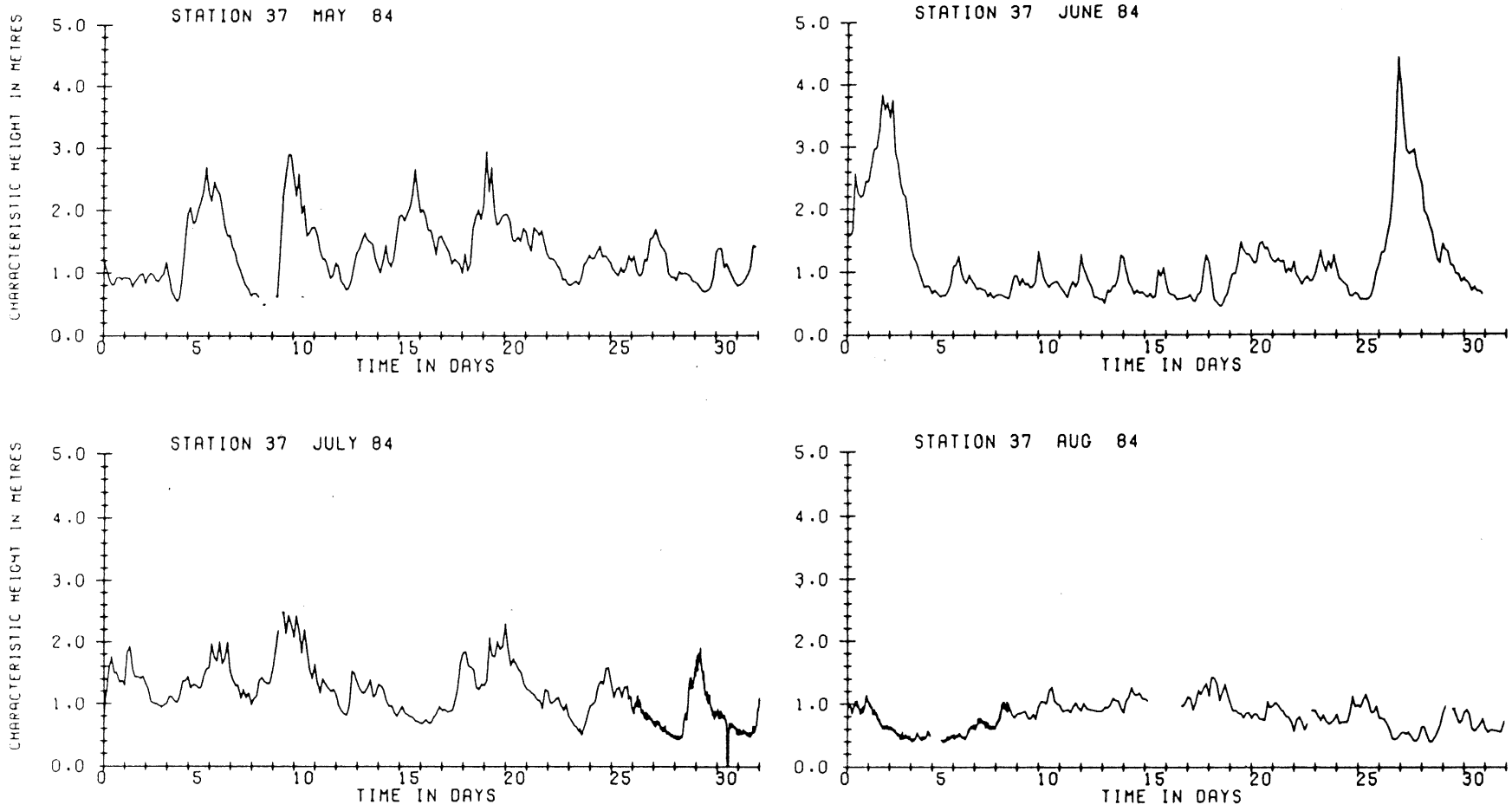

Figure 4.8. Characteristic wave heights for the months of May, June, July and August.

(From Marine Environmental Data Service, 1984)

Table 4.3

MAY

DATE: 05/19/0300

CHARACTERISTIC WAVE HEIGHT (M)	WAVE PERIOD (SEC)	WATER DEPTH (M)	ORBITAL DIAM. (M)	ORBITAL VELOCITY (M/SEC)	RIPPLE WAVELENGTH (M)
2.95	11.38	15	6.09	1.68	4.87
2.95	11.38	20	4.45	1.22	3.56
2.95	11.38	25	3.43	0.94	2.74
2.95	11.38	30	2.74	0.75	2.19
2.95	11.38	35	2.24	0.61	1.79
2.95	11.38	40	1.85	0.51	1.48
2.95	11.38	45	1.54	0.42	1.23
2.95	11.38	50	1.30	0.36	1.04
2.95	11.38	55	1.10	0.30	0.88
2.95	11.38	60	0.93	0.25	0.74
2.95	11.38	65	0.79	0.21	0.63
2.95	11.38	70	0.67	0.18	0.54

MAY

DATE: 05/15/1800

CHARACTERISTIC WAVE HEIGHT (M)	WAVE PERIOD (SEC)	WATER DEPTH (M)	ORBITAL DIAM. (M)	ORBITAL VELOCITY (M/SEC)	RIPPLE WAVELENGTH (M)
2.67	9.1	15	3.35	1.15	2.68
2.67	9.1	20	2.35	0.81	1.88
2.67	9.1	25	1.73	0.59	1.38
2.67	9.1	30	1.31	0.45	1.04
2.67	9.1	35	1.00	0.34	0.80
2.67	9.1	40	0.77	0.26	0.62
2.67	9.1	45	0.60	0.20	0.48
2.67	9.1	50	0.47	0.16	0.37
2.67	9.1	55	0.36	0.12	0.29
2.67	9.1	60	0.28	0.09	0.23
2.67	9.1	65	0.22	0.07	0.18
2.67	9.1	70	0.17	0.06	0.14

JUNE

DATE: 06/26/2100

CHARACTERISTIC WAVE HEIGHT (M)	WAVE PERIOD (SEC)	WATER DEPTH (M)	ORBITAL DIAM. (M)	ORBITAL VELOCITY (M/SEC)	RIPPLE WAVELENGTH (M)
4.4	9.75	15	6.47	2.08	5.18
4.4	9.75	20	4.61	1.48	3.69
4.4	9.75	25	3.46	1.11	2.77
4.4	9.75	30	2.67	0.86	2.14
4.4	9.75	35	2.10	0.67	1.68
4.4	9.75	40	1.67	0.53	1.33
4.4	9.75	45	1.33	0.43	1.06
4.4	9.75	50	1.07	0.34	0.85
4.4	9.75	55	0.86	0.27	0.69
4.4	9.75	60	0.69	0.22	0.55
4.4	9.75	65	0.56	0.18	0.45
4.4	9.75	70	0.45	0.14	0.36

JUNE

DATE: 06/02/1500

CHARACTERISTIC WAVE HEIGHT (M)	WAVE PERIOD (SEC)	WATER DEPTH (M)	ORBITAL DIAM. (M)	ORBITAL VELOCITY (M/SEC)	RIPPLE WAVELENGTH (M)
3.84	10.5	15	6.66	1.99	5.33
3.84	10.5	20	4.81	1.44	3.85
3.84	10.5	25	3.67	1.09	2.93
3.84	10.5	30	2.88	0.86	2.31
3.84	10.5	35	2.31	0.69	1.85
3.84	10.5	40	1.88	0.56	1.50
3.84	10.5	45	1.54	0.46	1.23
3.84	10.5	50	1.26	0.37	1.01
3.84	10.5	55	1.04	0.31	0.83
3.84	10.5	60	0.86	0.25	0.69
3.84	10.5	65	0.72	0.21	0.57
3.84	10.5	70	0.59	0.17	0.47

JULY

DATE: 07/09/1800

CHARACTERISTIC WAVE HEIGHT (M)	WAVE PERIOD (SEC)	WATER DEPTH (M)	ORBITAL DIAM. (M)	ORBITAL VELOCITY (M/SEC)	RIPPLE WAVELENGTH (M)
2.43	10.5	15	4.22	1.26	3.37
2.43	10.5	20	3.04	0.91	2.43
2.43	10.5	25	2.32	0.69	1.85
2.43	10.5	30	1.82	0.54	1.46
2.43	10.5	35	1.46	0.43	1.17
2.43	10.5	40	1.19	0.35	0.95
2.43	10.5	45	0.97	0.29	0.78
2.43	10.5	50	0.80	0.24	0.64
2.43	10.5	55	0.66	0.19	0.53
2.43	10.5	60	0.54	0.16	0.43
2.43	10.5	65	0.45	0.13	0.36
2.43	10.5	70	0.37	0.11	0.30

JULY

DATE: 07/09/1200

CHARACTERISTIC WAVE HEIGHT (M)	WAVE PERIOD (SEC)	WATER DEPTH (M)	ORBITAL DIAM. (M)	ORBITAL VELOCITY (M/SEC)	RIPPLE WAVELENGTH (M)
2.47	9.1	15	3.10	1.07	2.48
2.47	9.1	20	2.17	0.75	1.74
2.47	9.1	25	1.60	0.55	1.28
2.47	9.1	30	1.21	0.41	0.97
2.47	9.1	35	0.93	0.32	0.74
2.47	9.1	40	0.72	0.24	0.57
2.47	9.1	45	0.56	0.19	0.44
2.47	9.1	50	0.43	0.15	0.34
2.47	9.1	55	0.34	0.11	0.27
2.47	9.1	60	0.26	0.09	0.21
2.47	9.1	65	0.20	0.07	0.16
2.47	9.1	70	0.16	0.05	0.13

correlation of theoretical wavelength and water depth with observed ripple wavelength and water depth. These storm waves have an appropriate combination of wave height and/or wave period large enough to generate orbital diameters that could account for the observed ripple wavelengths.

From Figures 4.6 a to c and Figure 4.7, it can be seen that the theoretical depths and ripple wavelengths (threshold values) which correspond with the observed depths and wavelength (15 m to 40 m water depth and 1.3 to 3.0 m wavelength) define the maximum depth of the field observed in shallow water (<35 m). This may indicate that the observed CGM are formed in the waning phase(s) of the storm event(s). Since observed, CGM wavelengths correspond to orbital diameters which are generated when orbital velocities were below threshold values, most CGM must have been formed after the peak storm period had ended.

Based on relationships between threshold orbital velocity, grain diameter and wave period, discussed by Komar and Miller (1975a) the maximum depth at which particular grain sizes can move has been established.

From Figure 4.7 the maximum depth at which sediment, with grain size greater than 2 mm (gravel), can be moved by oscillatory flow is approximately 40 m. This depth is the approximate maximum limit to which the theoretical and observed wavelength and water depth relationship (discussed above) applies.

This probably indicates that the CGM observed in water depth greater than 40 m could not have been generated during the same storm

event(s) which generated the CGM in water depths of less than 40 m. Appropriate velocities may be generated in water depths greater than 40 m under hurricane conditions. Wave heights of 5 m and wave periods as high as 15 seconds are known to occur on the Eastern Shore (Boyd and Bowen, 1983) under such conditions. Note in Figures 4.6 a to c and 4.7 that the observed ripple wavelengths do not increase as significantly in shallow water as Airy theory would predict. This may be due to the dispersive nature of wave groups in shallow water (Yorath, et al., 1979).

Waves with periods between about 10 seconds and 12 seconds and maximum wave heights of about 3 metres to 5 metres, are probably optimal for the construction of the observed ripples in water depth shallower than 40 m. Yorath et al., 1979 concluded that the optimal wave conditions for the generation of coarse-grained "oscillation ripples" on the Northeast Pacific Continental Shelf occurred with wave periods between 12 and 14 seconds and wave heights between 4.5 and 9.0 metres. Oscillation ripples studied by Yorath et al (1979) occur in water depth between 80 and 105 metres and have wavelengths from 30 to 100 cm. These bedforms occur in considerably deeper water and are smaller scale than those described in this study. Similarily, Komar et al (1972) described oscillation marks on the Oregon continental shelf in water up to 204 m deep. The Eastern Shore example of coarse-grained oscillation megaripples may be unique among reported cases in the fact that these bedforms occur in very shallow water (60 to 15 m) and are relatively large scale features (130 to 300 cm). Wave data, analysed for the

period 1970 through 1981 show that optimal wave conditions are present on the Eastern Shore approximately 5 days/year (Boyd, pers. comm.) Therefore CGM, observed in water depths of less than 40 m, could be generated by storm waves 5 days a year. CGM in water depth greater than 40 m are probably not capable of forming more often than 1 day/year.

CHAPTER 5

A conceptual model proposing an explanation for the surficial sediment distribution and seismic stratigraphy of the Eastern Shore inner shelf, is presented here. Table 1 is a legend to the seismic stratigraphic units recognized in Figures 5.1 to 5.4.

Stage 1

During Stage 1 the last glacial advance occurs scouring bedrock and depositing glacial till (Figure 5.1). Scouring of bedrock produces bedrock valleys and shoals in water depths less than 30 m below present sea level (b.p.s.l.) and broad basins and ridges in water depths greater than 30 m. Map 2 confirms this glacially scoured bedrock topography. Glacial till, predominantly Goldenville Formation quartzite lodgement till, may have been deposited in bedrock lows in this stage forming sequences up to 30 m thick as shown in Figures 3.7 and 3.8. Here raw and interpreted shore-parallel seismic profiles show a 30 m thick sequence of till infilling a broad (approximately 1.2 km) valley about 10 km seaward of the mouth of Cole Harbour in 60 m of water. Till is also widespread west of Storey Head where bedrock is at depth, and is absent east of Storey Head. This may be explained by: 1) the mode of deposition of the till (lodgement till is deposited preferentially in bedrock lows) or, 2) the much higher preservation potential of till deposited in topographic lows compared to topographic highs. Till ridges are formed during this stage as a glaciodepositional feature parallel to the direction of ice advance.

Table 5.1

LEGEND

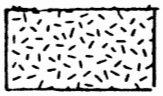

Bedrock

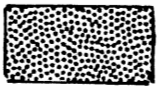

Lodgement Till

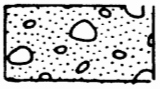

Drumlin Till

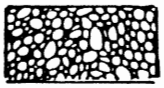

Boulder Retreat Shoal

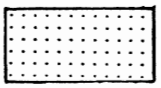

Barrier Beach Sediment

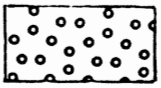

Sand and Gravel

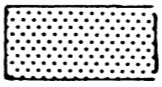

Estuarine Fill

Figure 5.1

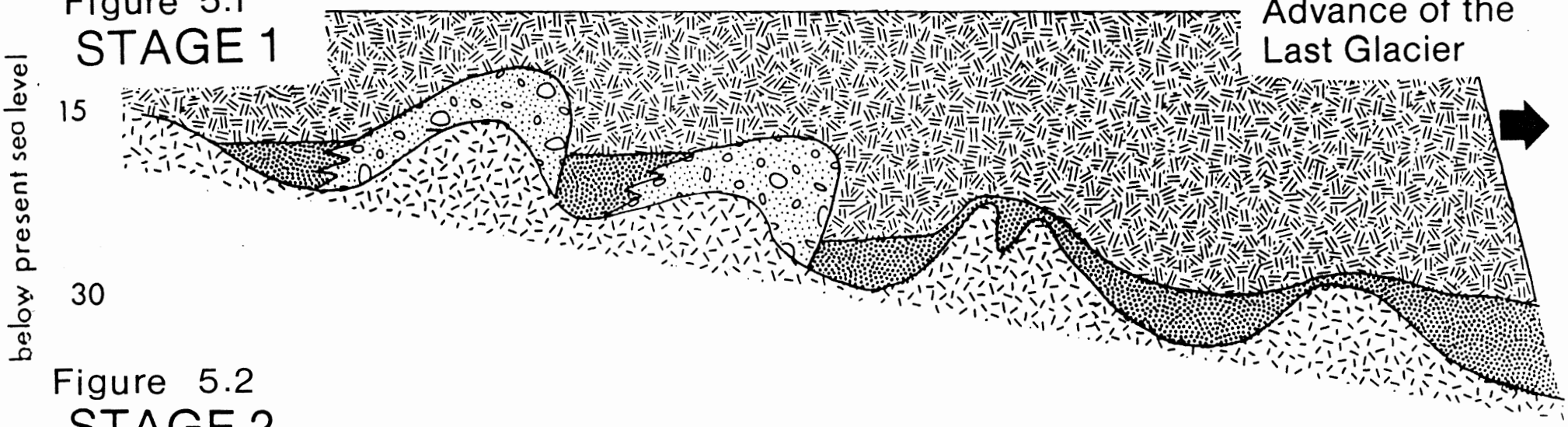

Figure 5.2

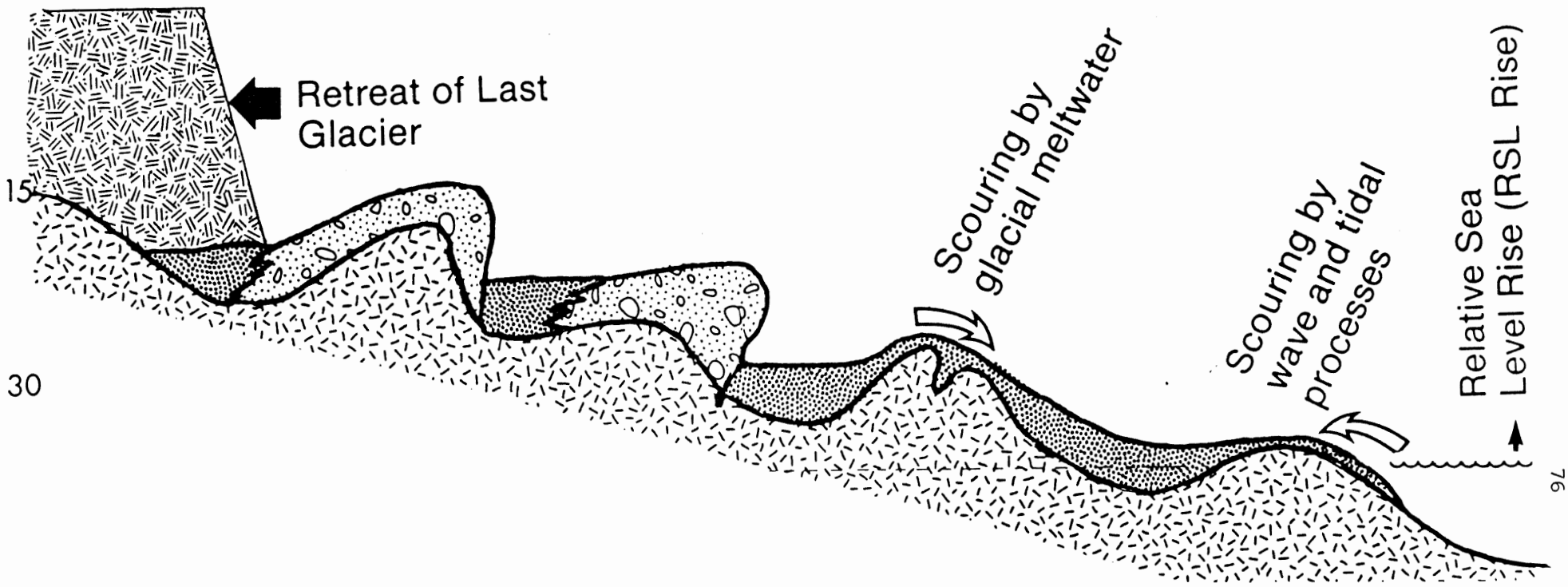

The Lawrencetown drumlin till was deposited during this stage at locations presently in water depth less than 30 m. The significance of drumlins as a sediment source for barrier systems on the present coastline of the Eastern Shore (Boyd and Bowen, 1983) leads to speculation that the absence of sand on the inner shelf (except for one location) seaward of the 30 m isobath may be due to the absence of drumlins beyond this depth.

Stage 2

Stage 2 begins with retreat of the ice sheet and RSL rise, from at least 65 m (b.p.s.l.) due to isostatic and eustatic changes in sea level (Figure 5.2). The presence of a possible submerged barrier beach mapped in this study, in a water depth of 65 m, would require Holocene sea level to have been at least 65 m (b.p.s.l.). Channels in the lodgement till were cut and filled during this stage. At least two possible modes of channeling and filling could have occurred; these are: 1) subaerial, and 2) sub-ice. The first scenario would have developed if glacier retreat was more rapid than relative sea level rise. The presence of glaciofluvial sediments at Petpeswick Inlet, along the coastline of the study area (Figure 1.1) confirms that subaerial glaciofluvial processes were active during deglaciation (Stea and Fowler, 1979). In this case, a broad glacial meltwater plain would have been present between the base of the glacier and the coastline. In contrast, if relative sea level rise kept up with the pace of glacier retreat, the melt water runoff would have been sub-ice. Either of these mechanisms could explain the development of deep

(5 m to 10 m) channels cut into the till. These features can be seen in Figure 3.7and Figure 3.15, which are shore-parallel seismic profiles. On the basis of side scan (Figure 3.5), these channels appear to be infilled by sand and fine-grained gravel. This sediment may have been derived from within the icesheet or from reworking of the lodgement till.

Stage 3

Stage 3 begins approximately 7000 y.b.p. when RSL was 30 m b.p.s.l. (Figure 5.3) (Scott and Medioli, 1982). Drumlins located in water depth less than 30 m b.p.s.l. occur on bedrock highs, separated by bedrock valleys oriented perpendicular to the coastline. Erosion of these drumlins by wave processes causes transport of fine-grained sediments longshore into adjacent bedrock valleys and formation of boulder retreat shoals at the site of the former drumlins. The transported sediments establish a barrier beach system within the bedrock valley. Tidal channels may cut through the barrier and deposit fine-grained sand behind the barrier as estuarine sediment. Figure 5.3 illustrates the erosion of drumlins at the 30 m isobath and the development of boulder retreat shoals. Figure 1.3 (Stage 3) best illustrates barrier system establishment in bedrock valleys adjacent to bedrock highs. Boulder retreat shoals can be seen on the side scan mosaic seaward of present day drumlin headlands.

Stage 4

As sea level continues to rise additional drumlins are eroded

Figure 5.3

STAGE 3

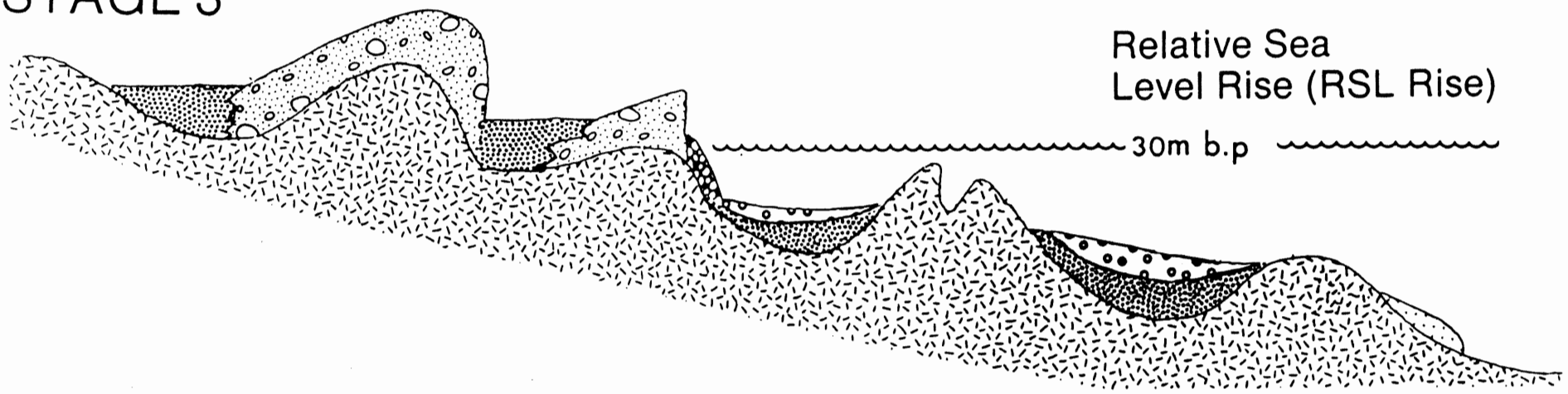

Figure 5.4

STAGE 4

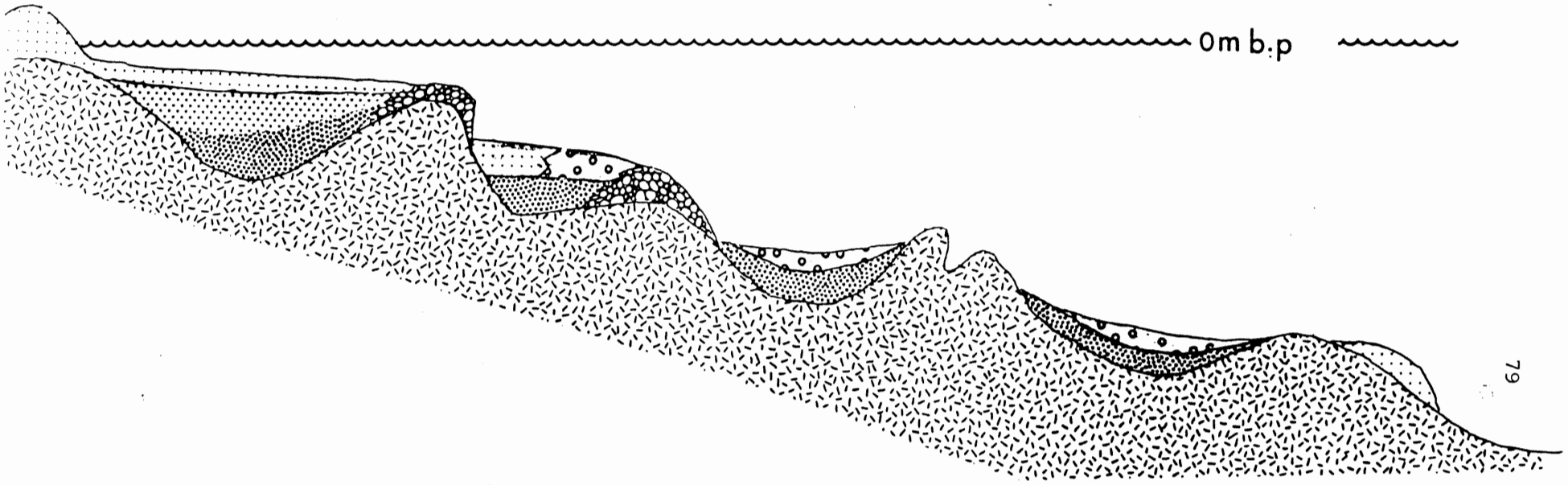

forming boulder retreat shoals on their seaward side. Erosion of these drumlins continues to add sand to the barrier sediment supply. Irregular spacing of drumlins relative to the shoreline may mean that during certain periods of sea level rise, individual barrier beaches will lose their adjacent sediment supply and thus be unable to keep up with rising sea level. At these times, barrier beaches become unstable and retreat into the valleys. Barrier beach retreat and destruction is best illustrated in Figure 1.3, (Stages 4 and 5). Retreat into the estuary occurs through washover events and tidal channels. Sequences of sand, generally 5 m to 10 m thick, located in bathymetric lows in water depths less than 30 m probably represent barrier sediment (estuarine fill sequences) which were transgressed as the barriers retreated landward into the valley. Examples of this can be seen on the side scan mosaic seaward of Cole Harbour, Lawrencetown Lake, Porters Lake, Three Fathom Harbour, Chezzetcook Inlet, Petpeswick Inlet, and Musquodoboit Harbour (Martinique Beach). Sand bodies intertongue with the SFGG facies at the 25 m isobath. Figures 3.15 and 3.16 are raw and interpreted seismic profiles across the sand body which extends out of the mouth of Three Fathom Harbour (see side scan mosaic and note that fix mark 348 corresponds to fix time 1000). The broad (approximately 2 km), shallow (approximately 15 m) bedrock valley is infilled with till which has subsequently been channeled, infilled with estuarine sediments, and submerged. Comparing Figures 3.15 and 3.16 with Figures 3.7 and 3.9, channels incised into the till appear with much greater abundance and variability in the shallower

water section. The till channels in the deeper water section are probably one generation of glaciofluvial channels while the till channels in the shallower water may be either glaciofluvial or highly sinuous estuarine tidal channels. Figure 1.3, stage 5 illustrates the high sinuosity of estuarine tidal channels. Figure 5.4 illustrates the seismic stratigraphy on the inner shelf by the end of stage 4 (present day).

Discussion

Bedrock topography controls the deposition of lodgement till so that thick sequences of till were deposited and preserved in bedrock valleys and thin sequences of till were deposited but not preserved on bedrock highs.

Glaciofluvial processes have distributed SFGG in channels till in areas of thick till accumulation, west of Story Head. Wave processes have reduced whatever till was deposited on bedrock highs to a thin veneer of SFGG in bedrock cracks. Large areas of the seafloor east of Story Head and seaward of the 30 m isobath consist of an irregular bedrock surface with abundant cracks, scarps and occasional banks (Yankee Bank and Darby Bank, See Bedrock Distribution Map).

Development of Holocene barrier systems in less than 30 m water depth appears to be controlled by the restriction of the Lawrencetown drumlin till to this inner shelf zone. Scoured bedrock topography and RSL rise also contribute to confining the sand supply to the area landward of the 30 m isobath.

The till outcrops which extend in linear belts seaward of Osborne

Head, Lawrencetown Head, Half Island Point, Grahams Head, Rudey Head, Sellars Head, Gaetz Head, Story Head, Petpeswick Head, Flying Point, and Jeddore Cape, are probably retreat shoals marking the sites of former drumlins (see side scan mosaic). The presence of drumlins at these headlands along the present-day Eastern Shore coastline is strong evidence in support of this notion (Figure 1.3).

CONCLUSIONS

This project compared the distribution of environments and processes on the Eastern Shore inner shelf to those on the present day coastline.

Four environments have been distinguished on the Eastern shore inner shelf. These are: (1) sand, (2) sand and fine-grained gravel, (3) glacial till and (4) Paleozoic bedrock. From the surficial and subsurface distribution of these environments two broad provinces have been identified. The first province, located in water depth shallower than 30 m, has a lateral and vertical distribution of environments which are closely related to the distribution of environments on the present day coastline. Present day coastal processes can be used to explain the distribution of environments on this part of the inner shelf.

Sandbodies connected to estuary-barrier systems on the present day coastline extend offshore to form broad (200 m to 3 km), thin (5 m to 10 m) and long (up to 5.8 km) inner shelf sandbodies. Topographic highs flanking barrier systems on the coast extend onto the inner shelf for an average of 7 km, forming bedrock shoals. Coastal headlands along the Eastern shore mark the sites of drumlins. Sites of former drumlins are traceable offshore of the coastal headlands for approximately 5 km.

In the nearshore province the combination of favourable bedrock topography and an additional sediment supply (drumlin till) led to the

development of barrier systems. Inefficient barrier retreat with RSL rise has left large volumes of sandy sediment seaward of present day barrier systems forming inner shelf sandbodies. Three types of CGM have been identified on the inner shelf and include: (1) CGM bands, (2) CGM patches, and (3) CGM fields.

A second province is located in water depth greater than 30 m and has a lateral and vertical distribution of environments which appear to be dissimilar to present day coastal environments. Large areas of bedrock outcrop (up to 60 km^2), broad bedrock valleys (up to 7 km along bathymetric strike) and absence of extensive sandbodies characterize this part of the inner shelf.

The deposition and preservation of glacial till, (which was controlled by bedrock topography) has had a key role in determining the distribution of environments in the offshore province. Thick sequences of till are widespread in bedrock valleys but are absent on bedrock highs. Glaciofluvial and wave processes appear to have channeled and reworked the till, generating the SFGG environment in bedrock cracks and infilling till channels.

Oscillatory currents generated by onshore propagating swells offer the most likely explanation for the generation of these bedforms on the Eastern Shore inner shelf, in water depth less than 40 m, around 5 days/year while those in deeper water probably require hurricanes. Waves with periods between 10 seconds and 12 seconds and heights between 3 and 5 m appear to produce the most optimum wave conditions for the construction of CGM in water depths shallower than 40 m.

Based on the crest orientation of CGM and regional shoreline trend, it is apparent that these bedforms provide an excellent indication of shoreline orientation throughout the Eastern Shore inner shelf.

Till ridges may be glaciodepositional features formed parallel/subparallel to the direction of ice flow.

REFERENCES

BOYD, R., and PENLAND, S., 1984. Shoreface Translation and the Holocene Stratigraphic Record: Examples from Nova Scotia, the Mississippi Delta and Eastern Australia, Marine Geology, 60, p. 391-412.

BOYD, R., and BOWEN, A.J., 1983. The Eastern Shore Beaches: Final Report to N.S. Dept. of Lands and Forests, 71 p.

BOWEN, A.J. and EDMOND, D.P., PIPER, D.J.W., and WELSH, D.A., 1975. The maintenance of beaches. Technical Report, Institute of Environmental Studies, Dalhousie University, Halifax, 582 p.

BOYD, R., BOWEN, A.J., and HALL, R.K., (in press). An evolutionary model for transgressive sedimentation on the Eastern Shore of Nova Scotia. Glaciated Coasts, Fitzgerald and Rosen (ed.), Academic Press.

COOK, D.O., 1982. Nearshore Bedform patterns along Rhode Island from side scan sonar surveys - discussion: Jour. Sed. Protrology, v. 52, pp. 677-679.

FARIBAULT, E.R., 1906. Structural Geology Map of the Eastern Shore Nova Scotia, Osborne Head to Flying Point, Lawrencetown, Sheet No. 53 (1:63,360) Geological Survey of Canada.

FARIBAULT, E.R., 1897. Structural Geology Map of the Eastern Shore, Jeddore Head to Ship Harbour. Ship Harbour, Sheet Nos. 51 (and 52) (1:63,360) Geological Survey of Canada.

FLEMMING, B.W., KLEIN, M., DENBIGH, P.N., 1982. Recent Developments in Side Scan Sonar Techniques. Cape Town, Russell-Cargill, South Africa, 141 p.

GRANT, D.R., 1963. Pebble lithology of tills of southeast Nova Scotia, unpublished M.Sc. thesis, Dalhousie University, Halifax, N.S., 114 p.

HARRIS, J.M. and SCHENK, P.E., 1975. The Meguma Group IN Harris, I.M., (editor), Ancient Sediments of Nova Scotia. 1975 Field Trip Eastern Section Soc. Eco. Paleo. Min., pp. 17-38.

HOSKIN, S., 1983. Coastal sedimentation at Lawrencetown Beach, Eastern Shore, Nova Scotia; unpublished B.Sc. thesis, Dalhousie University, Halifax, N.S., 46 p.

INMAN, D.L., 1957. Wave-generated ripples in nearshore sands: U.S. Army, Corps of Engineers, Beach Erosion Bd., Tech. Memo 100, 42 p.

KEPPIE, M.J., 1979. (Principle Compiler). Geological Map of Nova Scotia (1:500,000). Nova Scotia Department of Mines and Energy.

KING, L.H., and FADER, G.G., 1984. Wisconsinan Glaciation of Continental Shelf Southeast Atlantic Canada. Geological Survey of Canada, Open File Report, 112 p.

KING, L.H., 1980. Aspects of regional surficial geology related to site investigation requirements - Eastern Canadian shelf: in Ardus, D.A., (ed.) Offshore Site Investigation (London), pp. 1-34.

KNEBEL, H.J., NEEDELL, S.W. and O'HARA, C.J., 1982. Modern Sedimentary Environments on the Rhode Island inner shelf, off the eastern United States. Mar. Geol., 49: pp. 241-256.

KOMAR, P.D., 1976. Beach Processes and sedimentation. Englewood Cliffs, New Jersey, Prentice-Hall, 429 p.

KOMAR, P.D., and MILLER, M.C., 1975. The initiation of oscillatory ripple marks and the development of plane-bed at high shear stresses under waves. Jour. Sed. Petrology, v. 45, pp. 697-703.

KOMAR, P.D. and MILLER, M.C., 1974. Oscillatory ripple marks and the evaluation of ancient wave conditions and environments. Jour. Sed. Petrology, v. 44, pp. 169-180.

KOMAR, P.D., NEUDECK, R.H. and KULM, L.D., 1972. Observations and significance of deep water oscillatory marks on the Oregon continental shelf. In: D.J.P. Swift, D.B. Durma and O.H. Pilkey (Editors), Shelf Sediment Transport, Process and Pattern. Dowden, Hutchinson and Ross, Stroudsburg, pp. 601-619.

KRANCK, K., 1972. Geomorphological development and post-pleistocene sea level change, Northumberland Strait, Maritime Provinces. Can. J. Earth Sci., 9, pp. 835-844.

LYNBY, P.N., 1977. Sinusoidal and cnoidal gravity waves formulae and tables. Inst. of hydrodynamic and hydraulic engineering, Technical University of Denmark, pp. 1-4.

LORING, D.H., 1970. Marine Geology of the Gulf of St. Lawrence; 1, Bedrock Geology; 2, Glacial and post-glacial geology (abstr): Mar. Sediments, v. 6, No. 3, pp. 140.

Marine Environmental Data Service, 1984. Waves recorded off the Osborne Head, N.S., Stn. 37., May 1, 1984 to August 31, 1984. Environment Canada, Fisheries and Marine Service.

McQUILLIN, R., and ARDUS, D.A., 1977. Exploring the Geology of Shelf Seas: London, Graham and Trotman, 218 p.

MILLER, M.C., and KOMAR, P.D., 1980. Oscillation ripple marks generated by laboratory apparatus: Journal Sed. Petrology, v. 50, pp. 171-182.

MORANG, A., McMASTER, R.L., 1982. Nearshore Bedform Patterns along Rhode Island from Side Scan Sonar - Reply to David O. Cook, Jour. Sed. Petrology, v. 52, pp. 680-681.

MORANG, A., and MACMASTER, R.L., 1980. Nearshore bedform patterns along Rhode Island and from side scan sonar surveys: Jour. Sed. Petrology, v. 50, pp. 831-840.

PARROTT, D.R., DODDS, D.J., KING, L.H., and SIMPKIN P.G., 1980. Measurement and evaluation of the Acoustic reflectivity of the sea floor. Can. J. Earth Sci. 17, pp. 722-737.

PIPER, D.J.W., MUDIE, P.J., LETSON, J.R.J., BARNES, N.G., IULIUCCI, R.J., (in preparation). The marine geology of the Inner Scotian Shelf of the South Shore, Nova Scotia. G.S.C. Paper

QUINLAN, G. and BEAUMONT, C., 1981. A comparison of observed and theoretical postglacial relative sea level in Atlantic Canada; Can. J. Earth Sci. v. 18, pp. 1146-1163.

SCOTT, D.B. and MEDIOLI, F.S., 1982. Micropaleontological documentation for early Holocene fall of relative sea level on the Atlantic coast of Nova Scotia: Geology v. 10, pp. 278-281.

SENGBUSH, R.L., 1983. Seismic Exploration Methods, International Human Resources Development Corporation, Boston, 297 pp.

SONNICHSON, G., 1984. The Relationship of Coastal Drumlins to Barrier Beach Formation along the Eastern Shore, Nova Scotia, unpublished B.Sc. thesis, Dalhousie University, N.S., 66 p.

STEA, R. and FOWLER, J., 1979. Minor and trace element variations in Wisconsinan tills, Eastern Shore region, Nova Scotia. Nova Scotia Dept. of Mines and Energy Paper 79-4.

SWIFT, D.J.P., FREELAND, G.L., and YOUNG, R.A., 1979. Time and space distribution of megaripples and associated bedforms, Middle Atlantic Bight, North American Atlantic Shelf. Sedimentology, v. 26, pp. 389-406.

TABAT, W. 1979. Sedimentologische Verteilungsmuster in der Nordsee: Meyniuna, v. 31, pp. 83-124.

WALKER, R.G.,1984. Facies Models, Second Editon, Geoscience Canada, Reprint Series 1, pp. 141-170.

YORATH, C.J., BORNHOLD, C.D., THOMSON, R.E., 1979. Oscillation ripples on the Northeast Pacific Continental Shelf. Mar. Geol., 31, pp. 45-58.

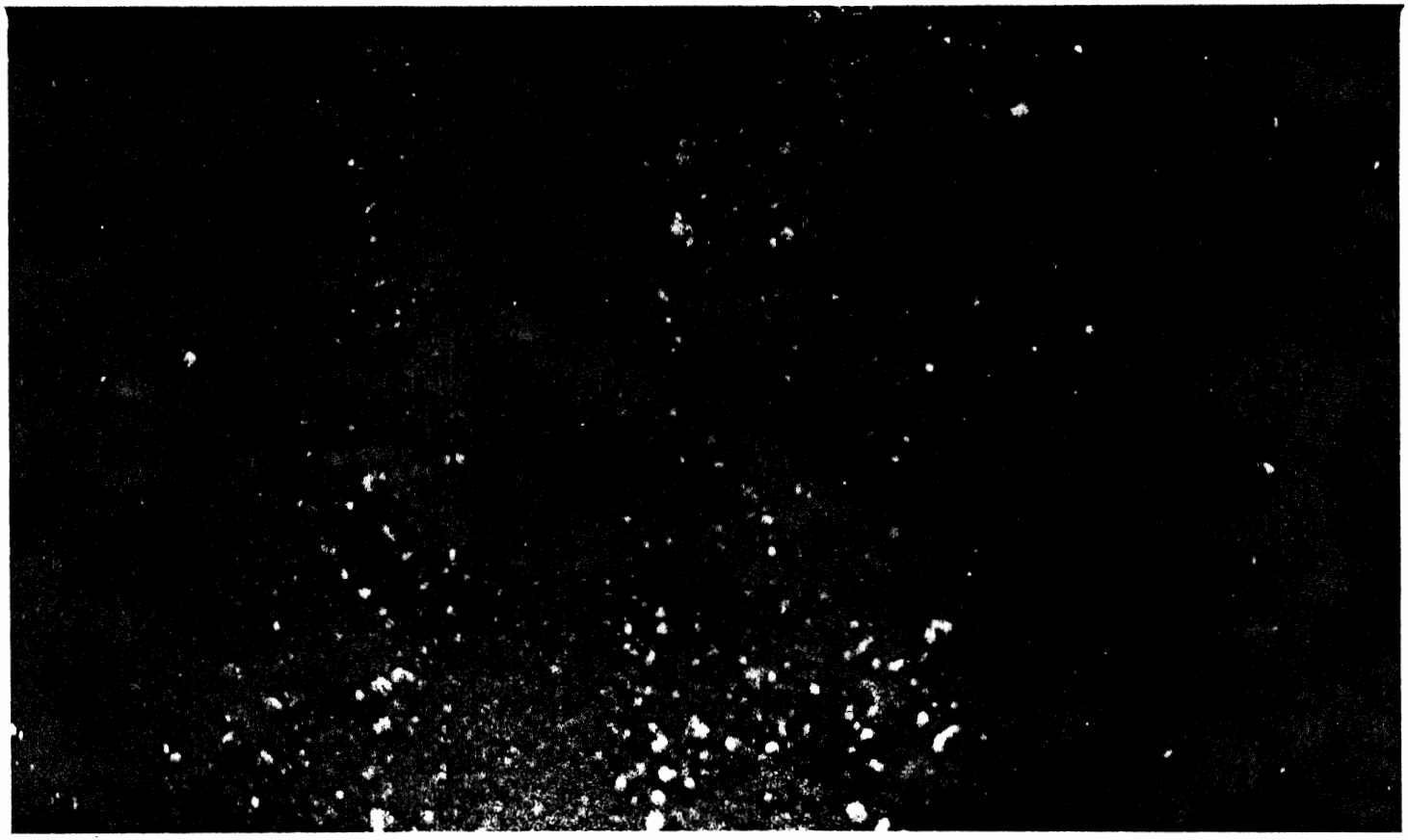

Figure 6 . Bottom photograph of a CGM associated with the SFGG facies.

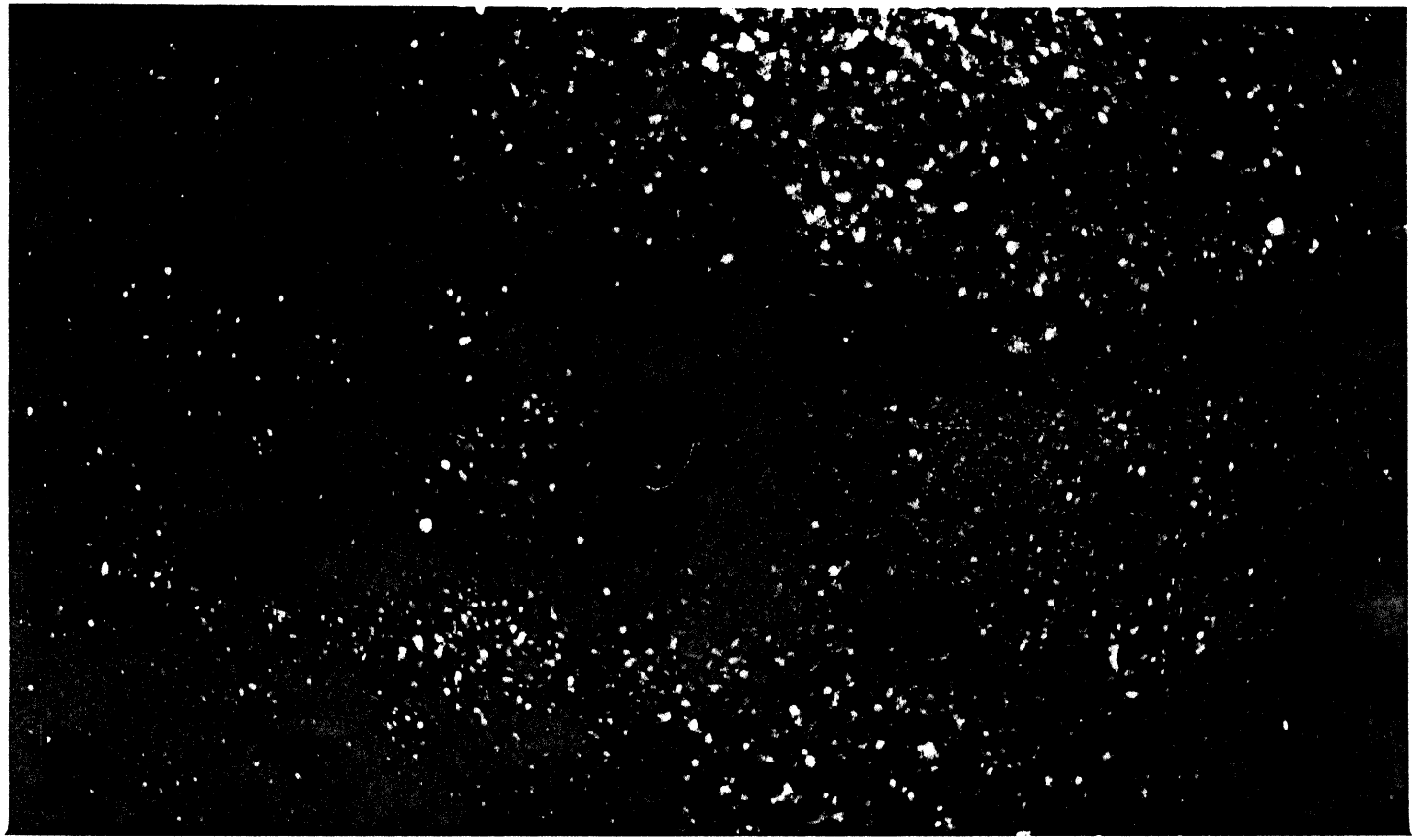

Figure 5 . Bottom photograph of CGM with cobbles to small boulders in the troughs and sand to pebbles on the crest. The crest appears slightly asymmetric.

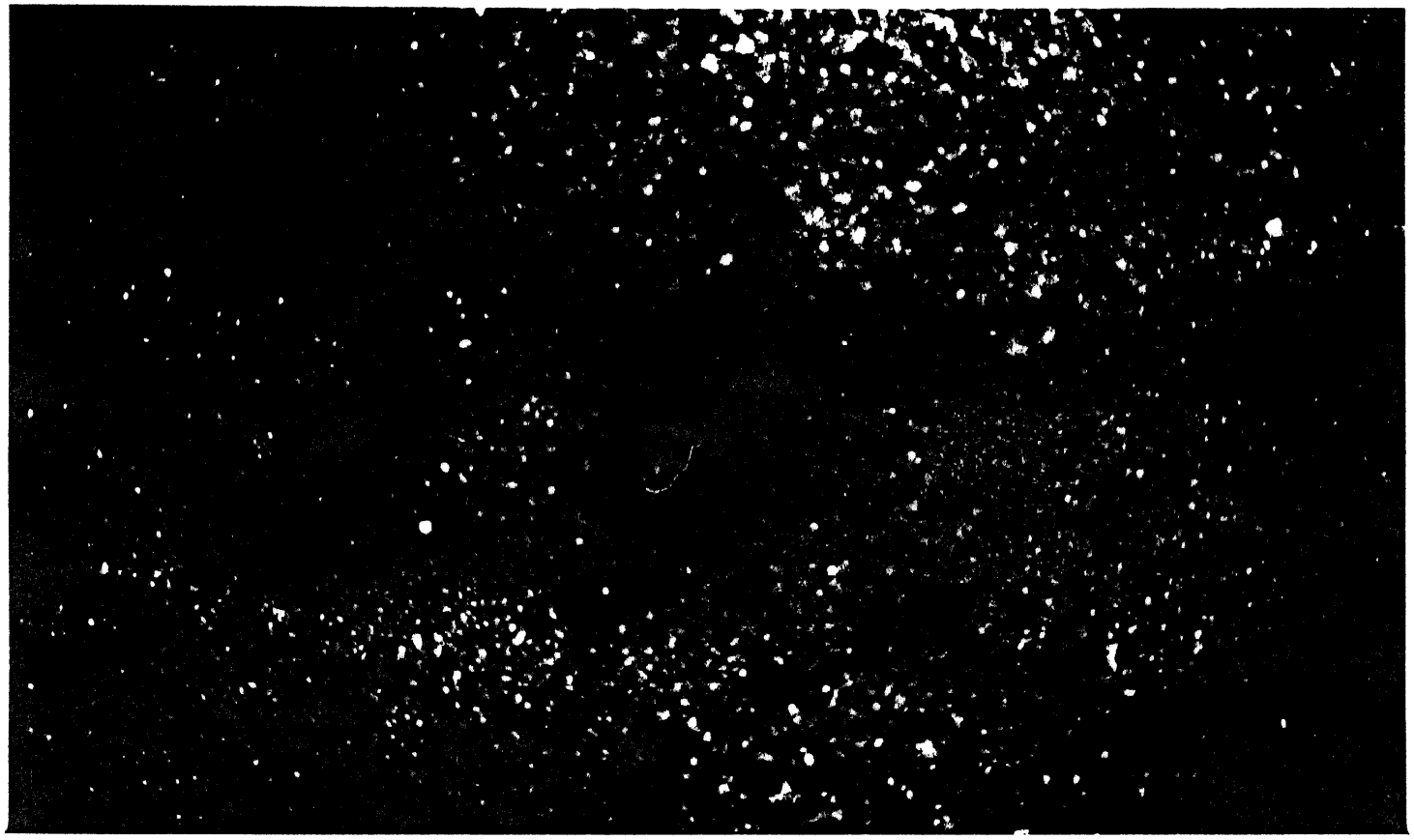

Figure 5 . Bottom photograph of CGM with cobbles to small boulders in the troughs and sand to pebbles on the crest. The crest appears slightly asymmetric.

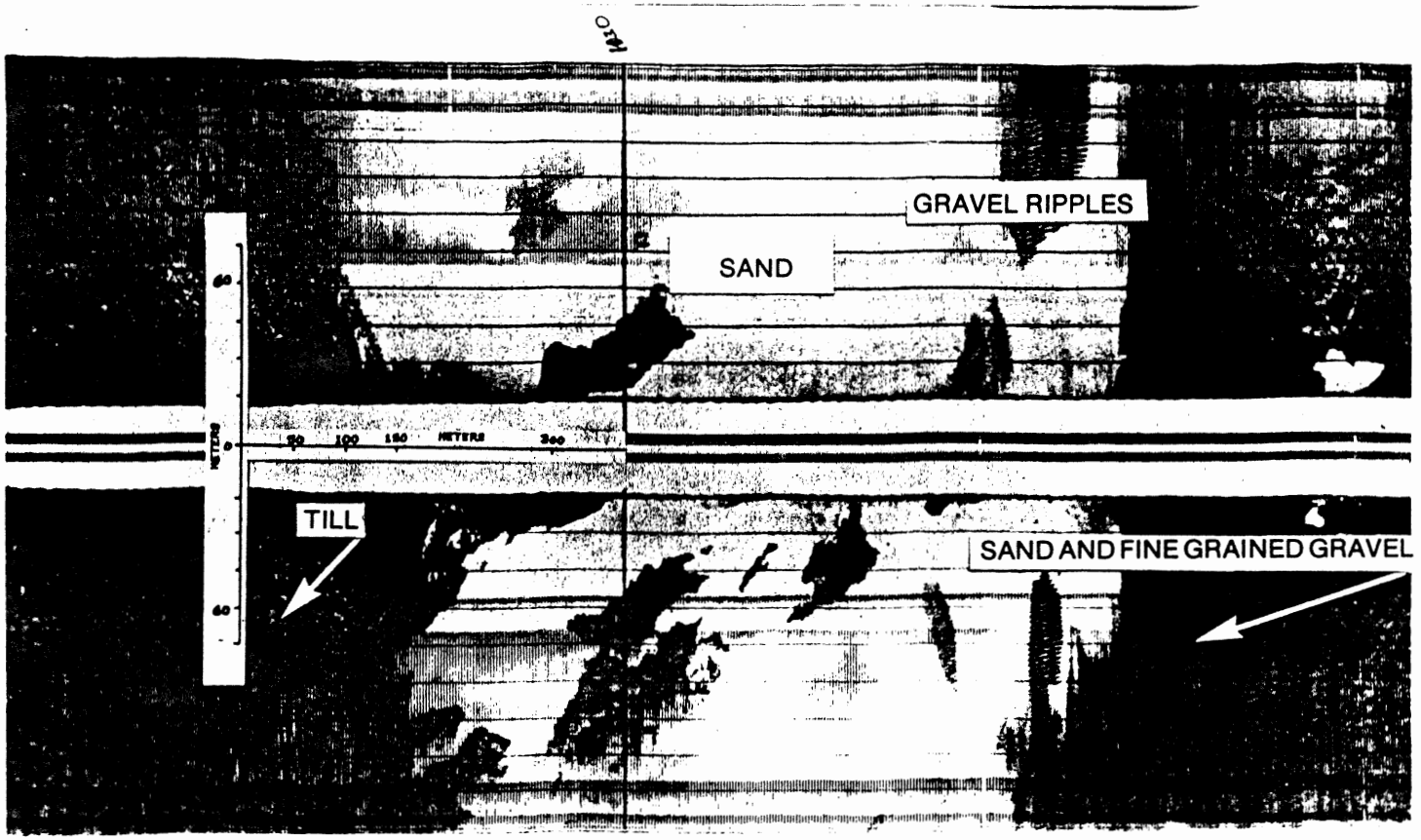

Figure 2. Side Scan Sonograph showing four CGM occurrences. All units are classified as patches. Note that the CGM patch in the upper right corner of the sandbody has a smaller wavelength on the left margin than the rest of the patch. Patches in the same area may have different wavelengths.